การประยุกต์ใช้ตัวเร่งปฏิกิริยาโคบอลต์-แมกนีเซียมออกไซด์บนตัวรองรับไทเทเนียมไดออกไซด์

ในปฏิกิริยาซีเลคทีฟออกซิเดชันของแอลกอฮอล์

นางสาวหนึ่งฤทัย ไชยสิทธิ์

APPLICATION OF Co-Mg-O/TiO$_2$ CATALYST ON SELECTIVE
OXIDATION OF ALCOHOLS

Miss Nungruetai Chaiyasit

A Thesis Submitted in Partial Fulfillment of the Requirements
for the Degree of Master of Engineering in Chemical Engineering
Department of Chemical Engineering
Faculty of Engineering
Chulalongkorn University
Academic Year 2000
ISBN xxx-xxx-xxx-x

Thesis Title   Application of Co-Mg-O/TiO$_2$ catalyst on selective
                         oxidation of alcohols
By   Miss Nungruetai Chaiyasit
Field of study   Chemical Engineering
Thesis Advisor   Assistant Professor Tharathon Mongkhonsi, Ph.D.
Thesis Co-advisor   Professor Piyasan Praserthdam, Dr.Ing.

_____

   Accepted by the Faculty of Engineering, Chulalongkorn University in Partial
Fulfillment of the Requirements for the Master's Degree

     ....……………….Dean of Faculty of Engineering
     (Professor Somsak Panyakeow, Dr.Eng.)

Thesis Committee

     ....Chairman
     (Associate Professor Ura Pancharoen, D.Eng.Sc)

     ....Thesis Advisor
     (Assistant Professor Tharathon Mongkhonsi, Ph.D.)

     ....Thesis Co-advisor
     (Professor Piyasan Praserthdam, Dr.Ing.)

     ....Member
     (Assistant Professor Prasert Pavasant, Ph.D.)

หนึ่งฤทัย ไชยสิทธิ์ : การประยุกต์ใช้ตัวเร่งปฏิกิริยาโคบอลต์-แมกนีเซียมออกไซด์บนตัวรองรับไทเทเนียมไดออกไซด์ในปฏิกิริยาซีเลคทีฟออกซิเดชันของแอลกอฮอล์(APPLICATION OF Co-Mg-O/TiO$_2$ CATALYST ON SELECTIVE OXIDATION OF ALCOHOLS) อ. ที่ปรึกษา : ผศ. ดร. ธราธร มงคลศรี, อ. ที่ปรึกษาร่วม : ศ. ดร. ปิยะสาร ประเสริฐธรรม, 106 หน้า.

การศึกษาสมบัติออกซิเดชันของตัวเร่งปฏิกิริยาโคบอลต์-แมกนีเซียมออกไซด์บนตัวรองรับไทเทเนียมไดออกไซด์ โดยใช้ปฏิกิริยาออกซิเดชันบางส่วนของสารประกอบ 1-โพรพานอล และ 2-โพรพานอล เป็นปฏิกิริยาทดสอบ พบว่าสมบัติการทำปฏิกิริยาของตัวเร่งปฏิกิริยาจะขึ้นอยู่กับชนิดของสารตั้งต้นที่เข้าทำปฏิกิริยา ผลิตภัณฑ์หลักที่ได้จากปฏิกิริยาออกซิเดชันของ 1-โพรพานอล คือ โพรพิโอนาลดีไฮด์ โดยจะให้ค่าการเลือกเกิดโพรพิโอนาลดีไฮด์สูงสุด ร้อยละ 57 สำหรับในกรณีของปฏิกิริยาออกซิเดชันของ 2-โพรพานอล ตัวเร่งปฏิกิริยาจะมีความว่องไวในการทำปฏิกิริยาสูง ผลิตภัณฑ์หลักในช่วงอุณหภูมิการทำปฏิกิริยาต่ำคือโพรพิลีน เมื่ออุณหภูมิการทำปฏิกิริยาสูงขึ้นพบว่าผลิตภัณฑ์หลักที่ได้คือโพรพิลีนและโพรพิโอนาลดีไฮด์ ซึ่งจากการศึกษาปฏิกิริยาออกซิเดชันของโพรพิลีนทำให้ทราบว่าโพรพิโอนาลดีไฮด์ที่เกิดขึ้นในปฏิกิริยาออกซิเดชันของ 2-โพรพานอล เกิดจากการออกซิเดชันโดยตรงของโพรพิลีนไปเป็นโพรพิโอนาลดีไฮด์ นอกจากนี้ยังพบว่าโครงสร้างและสมบัติในการทำปฏิกิริยาของตัวเร่งปฏิกิริยาไม่ขึ้นอยู่กับลำดับการเติมโคบอลต์และแมกนีเซียม   ส่วนชนิดของตัวรองรับมีผลต่อค่าการเลือกเกิดของตัวเร่งปฏิกิริยา

ภาควิชา......วิศวกรรมเคมี...............   ลายมือชื่อนิสิต...

สาขาวิชา......วิศวกรรมเคมี.............   ลายมือชื่ออาจารย์ที่ปรึกษา.............................

ปีการศึกษา......2543....................   ลายมือชื่ออาจารย์ที่ปรึกษาร่วม........................

NUNGRUETAI CHAIYASIT : APPLICATION OF Co-Mg-O/TiO$_2$ CATALYST ON SELECTIVE OXIDATION OF ALCOHOLS. THESIS ADVISOR: ASSIST.PROF. THARATHON MONGKHONSI, Ph.D. THESIS CO-ADVISOR : PROF. PIYASAN PRASERTHDAM, Dr.Ing. 106 pp. ISBN 974-13-0423-4.

The oxidation property of the Co-Mg-O/TiO$_2$ (8wt%Co, 1wt%Mg) catalyst was investigated by using the selective oxidation reaction of 1-propanol and 2-propanol as test reactions. It was found that the oxidation property of Co-Mg-O/TiO$_2$ catalyst depended on type of the reactants. For the oxidation of 1-propanol, Co-Mg-O/TiO$_2$ catalyst provided the maximum propionaldehyde yield ca. 57%. In case of 2-propanol oxidation reaction, it was found that Co-Mg-O/TiO$_2$ catalyst was an active catalyst for selective oxidation reaction. The main product at low reaction temperature was propylene while at high reaction temperature the main reaction products were propylene and propionaldehyde. From the result of propylene oxidation, it indicated that propionaldehyde was produced directly from propylene. In addition, the sequence of cobalt and magnesium loading had no effect on the structure and catalytic performance of this catalyst, while the type of support affected the selectivity of supported cobalt catalyst.

Department …Chemical Engineering…   Student's signature......................................

Field of study... Chemical Engineering ...   Advisor's signature...................................

Academic year............2000...................   Co-advisor's signature................................

ACKNOWLEDGEMENT

CONTENTS

LIST OF TABLES

LIST OF FIGURES

CHAPTER I

INTRODUCTION

Selective oxidation of organic compounds is generally used in numerous industries to produce organic oxides, aldehydes, organic acids and anhydrides. The supported transition metal oxides are used as the catalyst in this reaction. Since total oxidation evolves the heat of reaction more than selective oxidation, without a proper control, the reactant can be completely oxidized to CO_2 and H_2O rather than a selective oxidation product. Therefore, the development of a catalyst having high selectivity to produce the value of product is necessary.

Several previous studies discovered that the property of the catalyst, in several cases, depended on the support. A suitable support not only improves the catalytic activity and selectivity of catalyst but also increases the thermal stability and life time of the catalyst.

Among oxide catalysts, cobalt oxide (Co_3O_4) shows very high catalytic activity when compared with other transition metal oxide. Therefore it is widely used as the catalyst in total oxidation reaction of hydrocarbon compounds, diesel soot, carbonmonoxide, and ammonia. It is interesting whether the oxidation power of this oxide can be attenuated, to produce a new selective oxidation catalyst.

MgO is a basic support ever used as the support of V_2O_5 in oxidative dehydrogenation reactions. There is a formation of complex metal oxides between V_2O_5 and MgO (V-Mg-O) and then the oxidation ability of V_2O_5 is changed.

In addition, it has been reported that V-Mg-O/TiO_2 catalyst is suitable catalyst for the oxidation of propane, propylene, 1-propanol and CO_2. [Leklertsunthorn (1998)]. Therefore, the idea have been brought to the loading of Co_3O_4 on MgO, Co-Mg-O, to

decrease the oxidation ability of Co_3O_4. It was found that Co-Mg-O is the new catalyst applied to use in the oxidative coupling of methane, the catalytic decomposition of N_2O, the oxidation of methane to synthesis gas, the oxidative dehydrogenation of propane, propylene, 1-propanol, and CO [Youngwanishsate (1998)], and the selective oxidation of alcohols [Kittikerdkulchai (1999)]

Many research have been studied the property of various supported cobalt catalysts such as Co/MgO, Co/TiO$_2$, and Co/Al$_2$O$_3$, nevertheless the property of Co-Mg-O/TiO$_2$ have not been studied before. From the reason above, MgO can reduce the oxidation ability of Co_3O_4 and TiO$_2$ is the suitable support for selective oxidation reaction. Therefore, there is idea to study about the cobalt-magnesium oxide system supported on TiO$_2$.

In this research cobalt-magnesium oxide supported on TiO$_2$ is used as catalysts for selective oxidation of 1-propanol and 2-propanol.

In this study Co-Mg-O/TiO$_2$ catalyst have been used to investigated:

1. The oxidation property of Co-Mg-O/TiO$_2$ catalyst for 1-propanol and 2-propanol
2. The effect of the different order of cobalt and magnesium loading to the oxidation property of supported cobalt-magnesium oxide catalyst.
3. The influence of other support such as Al$_2$O$_3$ to oxidation property in selective oxidation reaction of alcohols.

This present work is organized as follows:

Chapter II contains literature reviews of cobalt oxide and supported cobalt catalysts on various reactions

The theory of this research, studies about the oxidation reaction and its possible mechanism, reaction of alcohols, properties of cobalt oxide and supports are presented in chapter III.

Description of experimental systems and the operational procedures are described in chapter IV.

Chapter V reveals the experimental results of the characterization of Co-Mg-O/TiO_2 and Co-Mg-O/Al_2O_3 catalysts and the oxidation reaction of 1-propanol and 2-propanol over these catalysts.

Chapter VI contains the overall conclusion emerged from this research.

Finally, the sample of calculation of catalyst preparation, external and internal diffusion limitations, calibration curve from area to mole of 1-propanol, 2-propanol, formaldehyde, acetaldehyde, propionaldehyde, methane, ethylene, propylene, and CO_2, catalytic activity of blank test, and data of this experiment which has emerged from this study are included in appendices at the end of this thesis.

CHAPTER II
LITERATURE REVIEWS

Selective oxidation of organic compounds, in particular of hydrocarbons, are the basis of numerous industrial process yielding organic oxides, aldehydes, organic acids and their anhydrides. Supported cobalt catalyst have been interesting and widely used for combustion of organic compounds, CO, diesel soot, and ammonia because cobalt oxide demonstrates the highest catalytic activity compared with other transition metal oxide. From the previous studies, supported cobalt catalyst have been known for many decades as active in many reaction such as oxidation, Fischer-Tropsch synthesis, combustion, hydrogenation and hydrodesulfurization reaction. However, only a few papers have reported the selective oxidation reaction over supported cobalt catalysts.

This chapter reviews the works about cobalt oxide and supported cobalt catalysts in various reactions. In addition, the effect of support, metal concentration, catalyst preparation and metal-support interaction on the property of catalyst is also demonstrated in this section.

2.1 Literature reviews

Chan and Smith (1990) investigated a series of Co-Mg-O catalysts for the oxidative coupling of methane. The performance of the mixed oxides was found to depend on the preparation procedure and their cobalt oxide content. The catalyst prepared by co-precipitation was amorphous according to X-ray Diffraction (XRD) analysis and inactive toward the oxidative coupling of methane whereas the catalysts prepared by mixing procedure retained their crystallinity and were active toward the oxidative coupling reaction. From these results it was concluded that the crystallinity of the MgO was important in producing selective catalysts. Preparation by physically mixing the oxide led to crystalline MgO that gave active and selective cobalt magnesium

oxide catalyst, whereas, the materials prepared by co-precipitation, were amorphous and nonselective to higher hydrocarbon production.

Busca *et al*. (1990) explored the surface property of cobalt oxide by means of Fourier-transform infrared (FT-IR) spectroscopy. The IR absorption bands of Co_3O_4 were observed at 667, 580, and 385 cm^{-1}. Their pretreatment data showed that the surface of Co_3O_4, even after the slight reduction arising from evacuation at 517°C, is highly oxidized, showing only Co^{3+} centers. The surface of evaluated Co_3O_4 exposed Co^{3+} cations reacted rapidly with CO, producing Co^{2+} and probably Co^+. The surface of Co_3O_4 was very active, even with respect to stable molecules such as ammonia and methanol, which were rapidly decomposed at room temperature. This agreed with the very high catalytic activity of cobalt oxide towards methanol, ammonia, and hydrocarbon combustion, and was probably related to the instability of Co^{3+} ions that tended to be reduced to Co^{2+}, or even lower oxidation states.

Garbowski *et al*. (1990) reported that cobalt oxide (Co_3O_4) deposited on alumina-based supports active for the oxidation of methane to CO_2 and water within 500°C. Alumina was found not to be a good support because at reaction temperature higher than 500°C, reaction between Co_3O_4 and alumina support occurring which resulted in the formation of $CoAl_2O_4$, which was an inactive compound, then deactivation of the catalyst took place. This is because alumina support had a spinel structure with octahedral and tetrahedral vacancies and Co(II) ions had a strong affinity, therefore leading to $CoAl_2O_4$ formation. In addition, for a good catalytic oxidation, Co(II) and Co(III) ions must be presented at the catalyst surface is possible. At low temperature the kinetics of this reaction were slow. At high temperature and in the presence of water, the formation of the cobalt aluminate phase was thermodynamically and kinetically favored. During the catalytic activity measurement deactivation was often observed. The main causes have been suggested to be (i) sintering of the active phase and (ii) reaction of the support with an active phase leading to an inactive phase.

Wang and Chen (1991) investigated a series of cobalt oxide/alumina with various metal loadings prepared by incipient-wetness impregnation. The reducibility of cobalt oxide in these samples was investigated by TPR technique. TPR result indicated that the nature of cobalt species varied with the cobalt loading. For low cobalt loadings the cobalt phase was present primarily as $CoAl_2O_4$. For catalysts having high cobalt contents, bulk Co_3O_4 was observed. CO hydrogenation activity measurement was carried out on these catalysts. The catalytic activity was increased with increasing cobalt loading. Nevertheless, if the comparison was based on cobalt metal, there was an optimum activity at 12wt%$CoAl_2O_4$. They suggested that might be due to different causes. First, the introduction of cobalt onto alumina led to a decrease in the pores of alumina during the preparation process. Second, the dispersion of the active phase was changed with the cobalt content. Higher cobalt loading favored large particles gave a low activity when expressed per gram of cobalt introduced.

Okamoto and co-workers (1991) investigated the effects of the starting cobalt salt on the cobalt-alumina interaction modes and cobalt dispersion in Co/Al_2O_3 catalysts. The catalysts were characterized by temperature-programmed reduction (TPR), X-ray photoelectron spectroscopy (XPS), and X-ray diffraction (XRD) techniques. It was found that the cobalt-alumina interaction modes depended strongly on the starting salt of cobalt. It was demonstrated that CoO/Al_2O_3 catalysts prepared from cobalt acetate showed higher cobalt dispersion than the catalysts prepared from conventional cobalt nitrate. From the intensity of TPR profiles, the total TPR areas were measured between room temperature and $650^{\circ}C$ as function of CoO content. They found that the TPR areas steadily increased with increasing cobalt oxide content. Accordingly, the easily reducible cobalt species abruptly raised.

Chang and Heinemann (1993) investigated the partial oxidation of methane to synthesis gas over Co/MgO catalysts with high Co-loading (>28wt%). These catalysts were able to initiate the reaction of methane with oxygen at temperature around $500^{\circ}C$.

High conversions of methane (~70%) and very high selectivity for hydrogen and carbon monoxide (~90%) were obtained at very high reactant gas space velocities (10^5-10^6 h^{-1}).

Santos *et al*. (1996) have studied the oxidation of methane to synthesis gas on Co(12%Co)/MgO catalysts. The XRD patterns showed that the fresh catalysts were made up of MgO and $MgCoO_2$. No cobalt oxide crystalline was detected in these patterns. Besides, the TPR thermograms did not show any well-define reduction peak up to 900°C due to the low reducibility of catalyst. This was expected that $MgCoO_2$ was more difficult to reduce than the single cobalt oxide. The oxidation of methane to synthesis gas was performed on Co/MgO catalyst. Between 400°C and 800°C, the products detected were almost exclusively CO_2 and H_2O but when the temperature was increased to 800-900°C the reaction rate increased strongly, and the product distribution shifted. At 900°C, the measured methane conversion was approximately 98% and the selectivity to CO and H_2 reached values close to thermodynamic equilibrium. The Co/MgO catalyst reached the reaction at about 800-850°C, they become partially reduced, and metallic centers were generated on their surface, with a sharp increase in the overall activity and in the selectivity for both CO and H_2 that reached values very close to equilibrium.

Sewell *et al*. (1996) studied a combined TPR/TPO technique for characterization of supported cobalt catalysts. The results show that the extent of metal reduction following hydrogen reduction at 500°C is affected considerably by the type of metal carrier. In particular, the extent of metal reduction decreased with increasing aluminium content of the support material. Decreasing extents of metal reduction could be correlated with an increase in the temperature required for reduction of the nitrate ion during TPR. Increasing the time and temperature of hydrogen reduction results in increased extents of metal reduction.

Novochinsky *et al*. (1998) studied the selective catalytic reduction of NO by methane over impregnated cobalt-containing catalysts. The active component of all the impregnated cobalt-containing catalysts was Co_3O_4. The role of O_2 seemed to maintain the surface stoichiometry of Co_3O_4. The main reason of decrease of catalytic activity of samples based on MgO, SiO_2, and Al_2O_3 in selective catalytic reduction of NO is due to oxide-oxide interaction promoted by water. All the carriers can be placed by the capability for oxide-oxide interaction in the following order: $SiO_2 \gg MgO > Al_2O_3$.

Querini *et al*. (1998) investigated the catalytic combustion of diesel soot particles on Co/MgO (12wt%Co) and potassium-promoted Co/MgO (1.5wt%K) catalysts that were calcined at different temperatures in the 300 to $700^{o}C$ range. The results of characterization and catalytic activity show a correlation between the structure of the catalyst and the calcination temperature. While the samples calcined at temperature of 300 and $400^{o}C$ show catalytic activity for soot combustion, those calcined at $500^{o}C$ or higher are practically in active. The TPR, ESR and XRD results indicated that this is due to the formation of Mg-Co mixed oxide. The promotion of these solids with potassium not only increases the sample activity, probably due to the important in surface mobility, but also enhanced stability at high temperatures.

Youngwanishsate (1998) studied the oxidation property of the Co-Mg-O catalyst in the oxidation reaction of propane, propene, 1-propanol, and CO. It was found that the oxidation property of Co-Mg-O catalysts depends upon the type of reactants. For 1-propanol oxidation, at low reaction temperature and low 1-propanol conversion Co-Mg-O catalyst behaves as a selective catalyst. While at high reaction temperature it plays role as a combustion catalyst. The cobalt composition in Co-Mg-O catalyst affected the catalytic activity and selectivity for propane oxidation. Co-Mg-O (8wt%Co) catalyst was the suitable catalyst for propane oxidation because it was active and selective for olefin production.

Kittikerdkulchai (1999) investigated the oxidation property of the Co/MgO (8wt%Co) and Co/Al2O3 (8%wtCo) catalysts by using the oxidation reaction of methanol, ethanol, 1-propanol, 2-propanol, and 1-butanol as test reactions. The nature of support affected the catalytic activity and selectivity of the catalyst for ethanol, 1-propanol, and 2-propanol oxidation. The basic support, MgO, promoted aldehyde formation for the oxidation of the ethanol and 1-propanol while the acidic supports promoted the formation of alkene instead.

Querini et $al.$ (1999)b studied the catalytic combustion of diesel soot over 12%Co and 4.5%K, supported on MgO and CeO_2 catalysts. It has been found that this reaction occurred by a redox mechanism when Co and K were deposited on any of the above-mentioned supports. On MgO-supported catalysts, CoO_x species were responsible for the supply of oxygen by a redox reaction. In this catalyst, K plays different roles, one of them being the stabilization of the CoO_x particles. XPS analysis indicated that the oxygen availability on the surface is much higher on CeO_2 than on MgO.

Chernavskii et $al.$ (2000) studied the influence of oxide-oxide interaction on the catalytic properties of cobalt in CO hydrogenation on the example of Co/Al_2O_3 catalyst. Oxide-oxide interaction was prevented by modification of the alumina surface with magnesia. It has been shown that oxide-oxide interaction affects catalytic activity and the amount of carbon deposited on the catalyst surface.

Riva et $al.$ (2000) studied the Co/support interaction and their effect on the dispersion and reducibility of cobalt in cobalt supported on silica and titania catalysts by XPS, TPR, TPD, XRD, and TEM. A significant Co/titania interaction was found, while no conclusive proof of any interaction was found for Co/silica. The degree of interaction between cobalt and the support affected not only the response of cobalt to reduction, but also its dispersion. In fact, cobalt spreads on titania during reduction and tends to sinter on silica.

Ruckenstein and Wang (2000) investigated the effect of calcination conditions on the species formed and the reduction behavior of the Co/MgO catalysts. As observed by TPR and XRD results, many factors affect the structural and chemical properties of the MgO-supported Co catalysts. The structural changes are mainly induced by the tendency to from a solid solution between CoO and MgO. The extent of solid solution formation increased as the calcination temperature and calcination time increased. A much lower calcination temperature was needed to from a solid solution in the impregnated catalysts than in the physically mixed ones. The formation of a solid solution rendered the catalyst less reducible.

2.2 Comments on previous works

From the previous studies there are many researches about cobalt oxide on various supports such as Al_2O_3, TiO_2, MgO and SiO_2 but most of reactions are total oxidation. The studies about supported cobalt catalysts on the selective oxidation are still scarce. Since MgO support can reduce the strong oxidation capability of catalyst, it is used as support for cobalt oxide catalyst to attain selective oxidation catalyst. On Co/TiO_2 the significant Co/titania interaction was found. Although the cobalt-titania and Co-Mg-O systems have been studies widely, there is no information about the combination of these two systems. Therefore, there is an idea to investigate the characteristic of Co-Mg-O/TiO_2 catalyst for selective oxidation reaction.

In this study, the oxidation properties of Co-Mg-O/TiO_2 catalyst on 1-propanol and 2-propanol are studied. Moreover, the sequence of metal loading and the effect of support to the oxidation property of catalyst are also investigated.

CHAPTER III
THEORY

Catalytic oxidation reactions involving free oxygen can be divided into complete oxidation and selective oxidation. Complete oxidation is the combustion of organic compound to the combustion products; CO_2 and H_2O. While selective oxidation is the reaction between hydrocarbon, the most used reactant, and oxygen to produce oxygenates or unsaturated hydrocarbons.

Selective oxidation of organic compounds, in particular of hydrocarbons, using air or oxygen on oxide catalysts are the basis of numerous industrial process yielding organic oxides, aldehydes, organic acids and their anhydrides. In the manufacture of organic chemicals, oxygen may be incorporated into the final product, as in the oxidation of methane to formaldehyde; or the reaction may be an oxidative dehydrogenation in which the oxygen does not appear in the desire product, as in the conversion of propane to propylene. The desire reaction may or may not involve C-C bond scission.

The ability to give and take oxygen appears to be a prime requirement for an oxidation catalyst. Elements that form relatively unstable oxides (surface or bulk compounds) which are capable of reacting with the material being oxidized but yet can be regenerated by oxygen or by an oxygen carrier under reaction conditions, are generally active catalysts.

Active sites in selective oxidation catalysts must be capable of activating a specific C-H bond in a reactant without significantly activating other C-H bonds in the reactant or product. Conventional selective oxidation catalysts discriminate between reactants and products primarily on a bond strength basis. This means that the weakest bond in a reactant or mixture of reactant and selective oxidation products is activated preferentially. The best selective oxidation catalysts are capable of discriminating in

favor of activation of a bond in a reactant provided that the bond dissociation enthalpy of the weakest C-H bond being activated ($D^oH_{C-H\ reactant}$) is not more than 30-40 kJmol^{-1} stronger than that of the weakest bond in the selective oxidation product ($D^oH_{C-H\ or\ C-C\ product}$).

Most of the selective oxidation reactions can be described by a simple kinetics scheme of the parallel-consecutive reactions:

$$RH \overset{1}{\underset{3}{\diagdown}} \quad \begin{matrix} RO \\ \downarrow 2 \\ CO_2 \end{matrix}$$
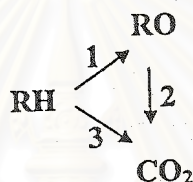
where RH is an organic substrate, RO is a selective oxidation product. A scheme of the consecutive route for oxidation reactions has been proposed by Montarnal and Germain in the form of so called "rake mechanism". It is shown in figure 3.1, where R' and RO', denoted surface complexes of substrate and intermediate products, RO_i are products of different number of oxygen atom, i, in a molecule, r_i are rates of surface reactions and r'_i and r'_{-i} are the rates of adsorption and desorption of intermediate products on or from the surface, respectively. According to this scheme the selectivity to a product RO_i will depend on the relative rate of its desorption to the rate of the surface reaction leading to RO_{i+1}. The high desorption rate will require a low heat of bonding of the product to the catalyst surface. Formally speaking one may then control the selectivity by choosing the catalyst of appropriate adsorption/desorption parameters of a desired product. The first order with respect to hydrocarbon has been observed in most cases of the selective oxidation reaction, the breaking of weakest C-H bond in a hydrocarbon molecule being considered as a rate-determining step, r.d.s. of the reaction.
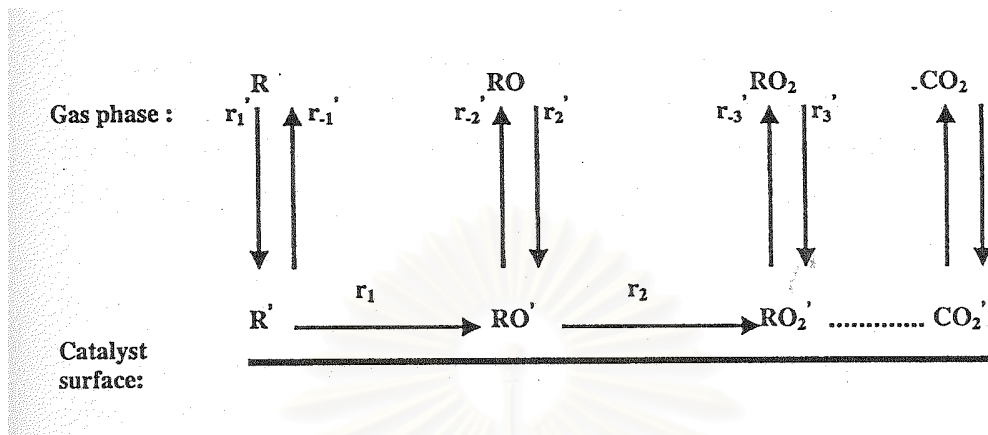
Figure 3.1 The "rake" mechanism of oxidation reactions.

3.1 Redox mechanism

The behavior of most oxidation catalysts can be interpreted within the framework of a redox mechanism. This postulates that the catalytic reaction comprises two steps [Mars van Krevelen (1954)]:

1. Reaction between catalyst in an oxidized form, Cat-O, and the hydrocarbon, R, in which the oxide becomes reduced:

$$Cat\text{-}O \ + \ R \ \longrightarrow \ RO \ + \ Cat$$
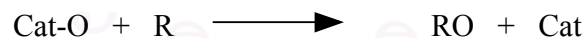
2. The reduced catalyst, Cat, becomes oxidized again by oxygen from the gas phase:

$$2Cat \ + \ O_2 \ \longrightarrow \ 2Cat \ + \ O$$
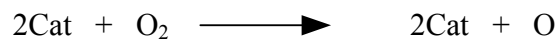
Under steady-state conditions the rates of the two steps must be the same.

3.2 Reactions of alcohols

Reactions of an alcohol can involve the breaking of either of two bonds: the C-OH bond, with removal of the -OH group; or the O-H bond, with removal of -H bond. Either kind of reaction can involve substitution, in which a group replaces the -OH or -H, or elimination, in which a double bond is formed.

3.1.1 Oxidation

The oxidation of an alcohol involves the loss of one or more hydrogens (α-hydrogens) from the carbon bearing the -OH group. The kinds of product that is formed depends upon how many of this α-hydrogens the alcohol contains, that is, upon whether the alcohol is primary, secondary, or tertiary.

A primary alcohol contains two α-hydrogens, and can either lose one of them to form an aldehyde,

$$
\begin{array}{ccc}
\underset{\displaystyle H}{\overset{\displaystyle H}{R-\underset{|}{\overset{|}{C}}-OH}} & \longrightarrow & R-\overset{\displaystyle H}{\underset{}{C}}=O
\end{array}
$$

A 1°alcohol   An aldehyde

or both of them to form a carboxylic acid.

$$
\begin{array}{ccc}
\underset{\displaystyle H}{\overset{\displaystyle H}{R-\underset{|}{\overset{|}{C}}-OH}} & \longrightarrow & R-\overset{\displaystyle OH}{\underset{}{C}}=O
\end{array}
$$

A 1° alcohol   A carboxylic acid

A secondary alcohol can lose its only α-hydrogen to form a ketone.

$$R-\underset{\underset{\displaystyle H}{|}}{\overset{\overset{\displaystyle R}{|}}{C}}-OH \longrightarrow R-\overset{\overset{\displaystyle R}{|}}{C}=O$$

A 2° alcohol   A ketone
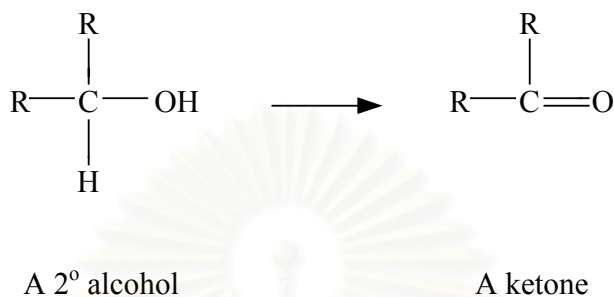
A tertiary alcohol contains no α-hydrogen and is not oxidized.   (An acidic oxidizing agent can, however, dehydrate the alcohol to an alkene and then oxidize this).

$$R-\underset{\underset{\displaystyle R}{|}}{\overset{\overset{\displaystyle R}{|}}{C}}-OH \longrightarrow \text{no oxidation}$$
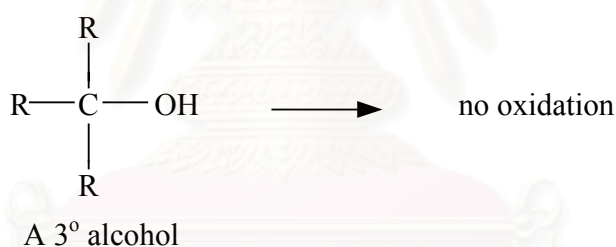
A 3° alcohol

3.1.2 Dehydration

Dehydration requires the presence of an acid and the application of heat. It is generally carried out in either of two ways: (a) by heating the alcohol with sulfuric or phosphoric acid; or (b) by passing the alcohol vapor over a catalyst, commonly alumina (Al_2O_3), at high temperature. An alcohol is converted into an alkene by dehydration (elimination of a molecule of water).

Alcohol	Alkene	Water
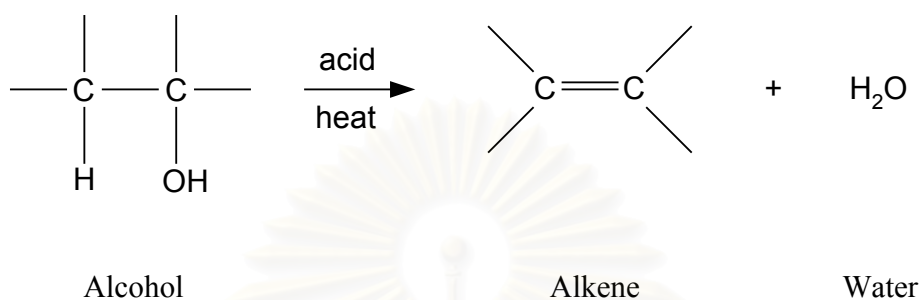
The various classes of alcohols differ widely in ease of dehydration, the order of reactivity being

Ease of dehydration of alcohol $3^o > 2^o > 1^o$
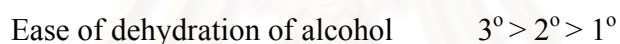
3.3 Cobalt oxide catalyst

Cobalt oxide is an interesting material in the fields of heterogeneous catalysis. Among the transition metal oxide Co_3O_4 shows the highest catalytic activity for the combustion of organic compounds, CO, diesel soot, NO, and ammonia. In addition, it is also active for hydrogenation and hydrodesulphurization reaction [Busca *et al*. (1990)].

Co_3O_4 is a black material having the structure of a normal spinel; it is thermodynamically stable up to $900^o C$ with respect to the lower oxide CoO. This implies that Co_3O_4 is the oxide stable under the conditions of catalytic oxidation. Both Co_3O_4 and CoO are readily reduced to the metal in the hydrogen flow near $300^o C$. The surface of Co_3O_4 shows Co^{3+} ions in excess. This surface is very reactive, even with respect to a stable molecule such as ammonia and methanol, which are readily decomposed at room temperature [Busca *et al*. (1990)].

For the gas-phase oxidation of hydrogen, ammonia, methane, ethylene, propylene, carbon monoxide, or toluene, the order of activity varied somewhat with the reactant, but the general pattern of activity found was [Satterfield (1991)].

$$Ti < V < Cr < \underline{Mn} > Fe < \underline{Co} > Ni < Cu > Zn$$

In almost all cases the most active catalyst was cobalt oxide and manganese oxide; the least active were the oxides of titanium or zinc.

3.4 Effect of support on catalytic performance

Many researches found that the catalytic performance of catalyst depending on the type of support. Suitable support not only improves catalytic activity, but also increases the thermal stability and therefore the lifetime of the catalyst. For the oxidative dehydrogenation of propane, MgO was used as support for V_2O_5 catalyst that showed high catalytic performance in the oxidation of propane. It is suggested that the loading of V_2O_5 catalyst on metal oxide having solid-base properties or the formation of complex metal oxide between V_2O_5 and basic metal oxides, reduce the strong oxidation ability of V_2O_5 to attain higher selectivity to oxidative dehydrogenation [Chaar *et al*. (1988)].

Titanium (IV) oxide is widely used as catalyst supports for the selective catalytic reduction (SCR) of NOx with ammonia and the selective oxidation of hydrocarbon, and as photocatalysts for various reactions. For catalytic applications, it is usually prepared from titanium oxysulfate ($TiO(SO_4)$), sulfate ($TiO(SO_4)_2$), or chloride ($TiCl_4$) by the precipitation (or hydrolysis method). Large-surface area is one of the important factors for the use of titanium (IV) oxide as catalyst supports. Generally, large-surface areas are required for catalyst supports to disperse a catalyst material effectively and to increase the number of active site in the catalyst.

3.5 Surface reducibility and basicity

A general agreement is that the reducibility of the catalyst plays an important role in the reaction course on the activation of propane [Gao *et al*. (1994)]. In V-Mg-O catalysts, where one V atom is replaced by one Mg atom, the involved lattice V-O-M oxygen atom is less mobile and thus the catalyst surface is less reducible: these catalysts led to dominant propylene selectivity [Corma *et al*. (1993)]. The basic catalyst surface also increases the alkene selectivity during the oxidative dehydrogenation of alkanes [Owen *et al*. (1992)]. For that reason, it may be possible to postulate the role of reducibility V-Mg-O systems to cover supported Co-Mg-O catalyst to explain the behavior of the selective oxidation reaction of alcohols.

CHAPTER IV
EXPERIMENTAL

The experimental systems and procedures used in this work are divided into three parts:

1. The preparation of catalysts
2. The characterization of catalysts
3. The catalytic activity measurements

The details of the experiments are described as the following.

The scope of this study.

The reaction conditions are chosen as follows:

Catalysts	:	Co-Mg-O/TiO$_2$, Co-Mg-O/Al$_2$O$_3$ (8%wtCo, 1%wtMg)
Reactant liquid	:	1-C$_3$H$_7$OH and 2-C$_3$H$_7$OH
Flow rate of reactant	:	100 ml/min
Reaction temperature	:	200-500°C
Gas hourly space velocity	:	20,000 hr^{-1}

4.1 Preparation of catalysts

4.1.1 Chemicals

The details of chemicals used in this experiment are shown in table 4.1.

Table 4.1 the chemicals used in this experiment.

Chemical	Grade	Manufacture
Cobaltous acetate tetrahydrate ($Co(CH_3COO)_2 \cdot 4H_2O$)	Analytical	Fluka, Switzerland
Magnesium nitrate ($Mg(NO_3)_2$)	Analytical	Fluka, Switzerland
Titanium dioxide (TiO_2) JRC-TIO4	Japan reference catalyst	Department of Material Sience, Shimane University
Alumina (Al_2O_3) JRC-ALO2	Japan reference catalyst	Catalysts and Chemicals Ind. Co., Ltd.

4.1.2 Preparation of catalyst

To study the effect of sequence of cobalt and magnesium loading, then three types of Co-Mg-O/TiO_2 catalyst (8%wtCo, 1%wtMg) were prepared. In the first type of preparation, an appropriate amount of TiO_2 powder was added to an aqueous solution of cobaltous acetate tetrahydrate ($Co(CH_3COO)_2.4H_2O$) at 70°C.   The suspension was evaporated at 80°C, then dried in the oven at 110°C in air over night. The resulting solid was calcined in air at 550°C for 6 hours. Magnesium was introduced into the calcined solid by impregnation from a magnesium nitrate ($Mg(NO_3)_2$) solution, evaporated at 80°C and dried at 110°C in air overnight. After drying the catalyst was calcined in air at 550°C for 6 hours. This catalyst was denoted as 8Co1MgTi catalyst.

In the second type of sample, magnesium was firstly introduced in the way given above on to pure titania surface and then cobalt was deposited on Mg-doped

TiO_2 support by the incipient wetness impregnation method. The catalyst was dried at 110°C in air overnight and calcined in air for 6 hours at 550°C. This catalyst was denoted as 1Mg8CoTi catalyst.

The third one was prepared by co-impregnation of cobalt and magnesium. An appropriate TiO_2 was added to an aqueous solution containing both $Co(CH_3COO)_2.4H_2O$ and $Mg(NO_3)_2$. The conditions of drying and calcination liked previous samples. This catalyst was denoted as co-8Co1MgTi catalyst.

Three types of Co-Mg-O/Al_2O_3 catalysts were prepared using similar method to the three types of Co-Mg-O/TiO_2 catalysts. The symbols of the three types of Co-Mg-O/Al_2O_3 catalysts liked the three types of Co-Mg-O/TiO_2 catalysts too i.e. 8Co1MgAl, 1Mg8CoAl, co-8Co1MgAl.

4.2 The characterization of catalyst

4.2.1 Determination of composition content of catalyst

The actual composition contents of all catalysts were determined by atomic absorption spectroscopy (AAS) at the center service of science. The calculation of the sample preparation is shown in Appendix A.

4.2.2 Surface area measurement

The BET surface area was determined by nitrogen absorption in an automatic apparatus ASAP 2000 constructed by Micromeritics, U.S.A. The data obtained were recorded by a microcomputer.

4.2.3 X-ray diffraction (XRD)

The phase structure of samples were determined by X-ray diffraction, Siemens D 5000 X-ray diffractometer using CuKα radiation with Ni filter in the 2θ range of 4-

80°. The sample is placed into XRD plate before placing on the measured position of XRD diffractometer.

4.2.4 Fourier transform Infrared (FT-IR)

The functional group on the catalyst surface was determined by FT-IR using Nicolet model Impact 400. Each sample was mixed with KBr with ratio of sample: KBr equal to 1:100 and then pressed into a thin wafer. Infrared spectra were recorded between 400 and 2000 cm^{-1} on a microcomputer.

4.3 The catalytic activity measurements

4.3.1 Equipment

The 1-propanol and 2-propanol system consists of a reactor, a saturator, an automatic temperature controller, an electrical furnace and a gas controlling system. 1-propanol and 2-propanol reactant is liquid phase so they are passed through the saturator in order to evaporate them into gas phase before passing to the microreactor. Flow diagram of the oxidation reaction system is shown in figure 4.1.

The reactor is made from a stainless steel tube. Sampling points are provided above and below the catalyst bed. Catalyst is placed between two quartz wool layers.

An automatic temperature controller consists of a magnetic contactor model Telex 87114. Temperature was measured at the bottom of the catalyst bed in the reactor. The temperature control set point is adjustable within the range of 0-800°C at maximum voltage of 220 volt.

The electrical furnace supplies heat to the reactor for 1-propanol and 2-propanol oxidation. The reactor can be operated from room temperature up to 800°C at maximum voltage of 220 volt.
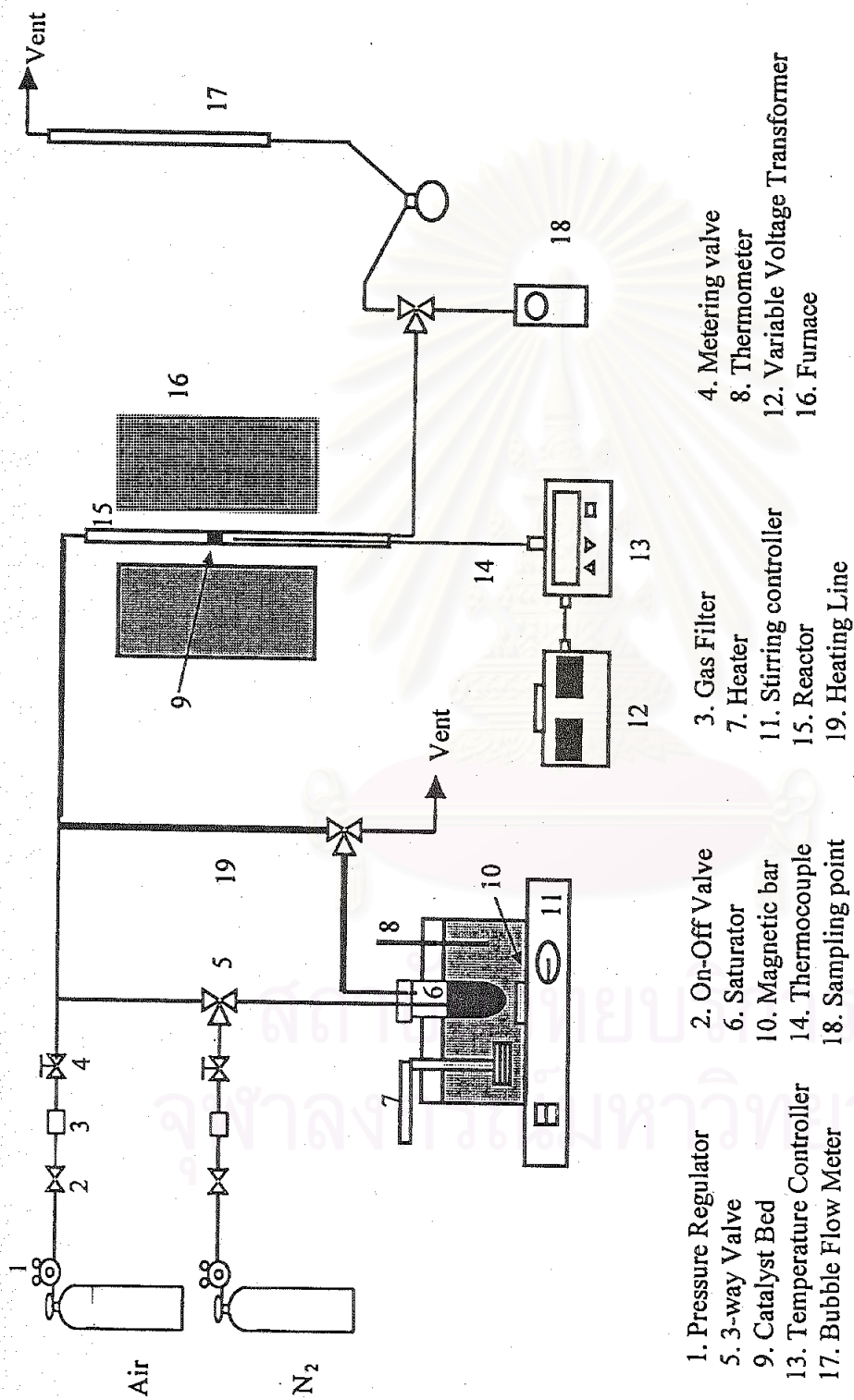
Figure 4.1 Flow diagram of 1-propanol and 2- propanol oxidation system

1. Pressure Regulator
2. On-Off Valve
3. Gas Filter
4. Metering valve
5. 3-way Valve
6. Saturator
7. Heater
8. Thermometer
9. Catalyst Bed
10. Magnetic bar
11. Stirring controller
12. Variable Voltage Transformer
13. Temperature Controler
14. Thermocouple
15. Reactor
16. Furnace
17. Bubble Flow Meter
18. Sampling point
19. Heating Line

The gas supplying system consists of cylinders of ultra high purity nitrogen and air, each equipped with pressure regulators (0-120 psig), on-off valves and fine-meter valves used for adjusting the flow rate of these gases.

The composition of oxygenated compound in the feed and product stream was analyzed by flame ionization detector gas Chromatograph Shimadzu GC14A.

The composition of hydrocarbons in the product stream was measured by flame ionization detector gas Chromatograph Shimadzu GC14B.

A Shimadzu GC8A gas chromatograph equipped with a thermal conductivity detector was used to analyze permanent gases and water. Two columns, a 5A molecular sieve to separate oxygen and Co and a Porapak-Q column to separate CO_2 and water were operated in parallel. The operating conditions of GC are listed in the Table 4.2.

Table 4.2 Operating condition for gas chromatograph

Gas chromatograph	Shimadzu GC8A	Shimadzu GC14A	Shimadzu GC14B
Detector	TCD	FID	FID
Column	MS-5A, Porapak-Q	Capillary	VZ10
Carrier gas	He (99.999%)	N_2 (99.999%)	N_2 (99.999%)
Carrier gas flow	25 ml/min	25 ml/min	25 ml/min
Column temperature			
- Initial	100	40	70
- Final	100	140	70
Detector temperature	130	150	150
Injector temperature	130	100	100
Analyzed gas	CO, CO_2, H_2O	Oxygenates	Hydrocarbon C_1-C_4

4.3.2 Oxidation procedure

The oxidation procedures are described in the detail below.

1. 0.1 gram of catalyst was packed in the middle of the stainless steel microreactor located in the electrical furnace.

2. The total flow rate was 100 ml/min. Flow rate of 1-propanol and 2-propanol, nitrogen and air were adjusted to the required values.
- The gas mixtures for 1-propanol oxidation were 8 vol.% 1-propanol, 5 vol.% oxygen and balance with nitrogen.
- The gas mixtures for 2-propanol oxidation were 8 vol.% 2-propanol, 5 vol.% oxygen and balance with nitrogen.

3. The reaction temperature was between 200-500°C. The effluent gases were analyzed by using the FID and TCD gas chromatograph. The chromatograph data were changed into mole of methane, ethylene, propane, propylene, methanol, ethanol, 1-propanol, 2-propanol, formaldehyde, acetaldehyde, propionaldehyde, and CO_2 by calibration curves in Appendix C.

4. The result of catalytic test was calculated in the term of

$$\%A \text{ conversion (C)} = \frac{\text{mole of A converted}}{\text{mole of A in feed}}$$

$$\%\text{selectivity (S) to B} = \frac{\text{mole of B formed}}{\text{mole of A converted}} \times \frac{\text{no. of C atom of B}}{\text{no. of C atom of A}} \times 100$$

$$\%\text{yield (Y) to B} = \frac{\%A \text{ conversion} \times \%\text{selectivity to B}}{100\%}$$

where A is reactant

B is product

CHAPTER V
RESULTS AND DISCUSSION

The results and discussion in this chapter are divided into two major parts including the catalyst characterization and the catalytic oxidation reaction of 1-propanol and 2-propanol, respectively.

5.1 Catalyst characterization

5.1.1 Determination of composition content and BET surface area of catalyst

The results of metal composition and BET surface area of all catalysts, which are analyzed by Atomic Absorption Spectroscopy (AAS) and BET surface area are summarized in Table 5.1.

Table 5.1 The composition of catalyst and BET surface area

Catalyst	%Cobalt content	%Magnesium content	BET surface area (m^2/g)
TiO_2	-	-	48
8Co1MgTi	7.4	0.85	40
1Mg8CoTi	8.3	0.73	37
co-8Co1MgTi	8.2	0.77	35
Al_2O_3	-	-	251
8Co1MgAl	7.7	0.93	242
1Mg8CoAl	7.7	0.82	247
co-8Co1MgAl	8.4	0.90	235

The above data in Table 5.1 show that the cobalt and magnesium content in all catalysts are close to the calculated value. The catalysts 8Co1MgTi, 1Mg8CoTi, co-8Co1MgTi, 8Co1MgAl, 1Mg8CoAl, co-8Co1MgAl have slightly lower surface area than TiO_2 and Al_2O_3 supports, respectively. It can be seen that the surface areas of the catalysts, prepared in different order metal loading, are quite the same. Therefore, the sequence of cobalt and magnesium loading seems to have no effect on the surface area.

5.1.2 X-ray Diffraction (XRD)

The crystal structure of the catalysts was identified by X-ray diffraction technique. Figures 5.1-5.8 reveal the results of XRD spectra of catalysts (TiO_2, 8Co1MgTi, 1Mg8CoTi, co-8Co1MgTi, Al_2O_3, 8Co1MgAl, 1Mg8CoAl, and co-8Co1MgAl catalysts).

From previous research, XRD pattern of Co_3O_4 catalyst shows 6 peaks at $20°$, $32°$, $37°$, $45°$, $60°$, and $65.5°$ [Jan Petryk and co-workers (2000)]. Figure 5.1, XRD spectrum of TiO_2, shows peaks at 2θ values that can be attributed to anatase phase ($25°$, $37.6°$, $48°$, $54°$, $56°$) and the rutile phase ($27.3°$, $36°$, $41°$, $57°$).

For Co-Mg-O/TiO_2 system, the spectra of all catalysts have the 2θ values which belong to TiO_2 (figures 5.2 to 5.4) but the level of intensity is lower than TiO_2. The crystalline Co_3O_4 peaks appear at $32°$ in Co-Mg-O/TiO_2 system but the strongest peak of Co_3O_4 at $37°$ cannot be detected possibly because this peak has the same position as TiO_2, therefore it may be hidden by the XRD spectrum of TiO_2 support. From this result, it cannot conclude what structure of Co_3O_4 formed on TiO_2 surface. Cobalt oxide may form a Co_3O_4 crystal structure on the TiO_2 support or may react with MgO to form a new Co-Mg-O compound. The structure of Co-Mg-O/TiO_2 catalyst is similar to TiO_2 but more amorphous.

In the case of Co-Mg-O/Al$_2$O$_3$ catalyst, the XRD patterns of these catalysts (figures 5.6 to 5.8) are the same as Al$_2$O$_3$ support. The XRD pattern of Al$_2$O$_3$ catalyst (figure 5.5) shows 7 peaks at 31°, 37°, 45°, 46°, 56°, 59° and 65.5° that are the same positions as Co$_3$O$_4$ catalyst. This means that the crystalline Co$_3$O$_4$ catalyst peaks in Co-Mg-O/Al$_2$O$_3$ catalyst are not measurable because in these regions the XRD patterns of Co$_3$O$_4$ are hidden by the XRD patterns of Al$_2$O$_3$ support. The XRD pattern of Co-Mg-O/Al$_2$O$_3$ catalyst is the same as Al$_2$O$_3$ support but the level of intensity is lower than Al$_2$O$_3$ support. Therefore, the structure of Co-Mg-O/Al$_2$O$_3$ catalyst is similar to Al$_2$O$_3$ support, but more amorphous.
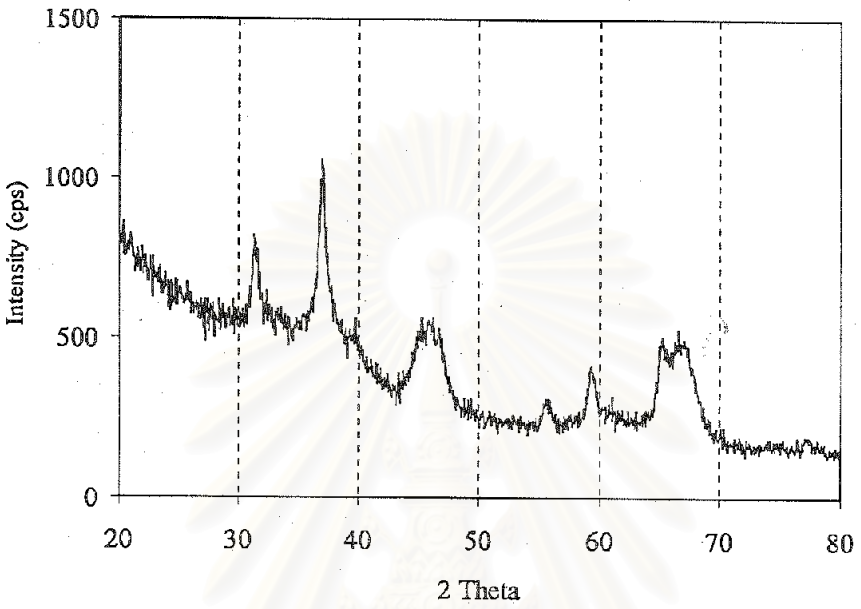
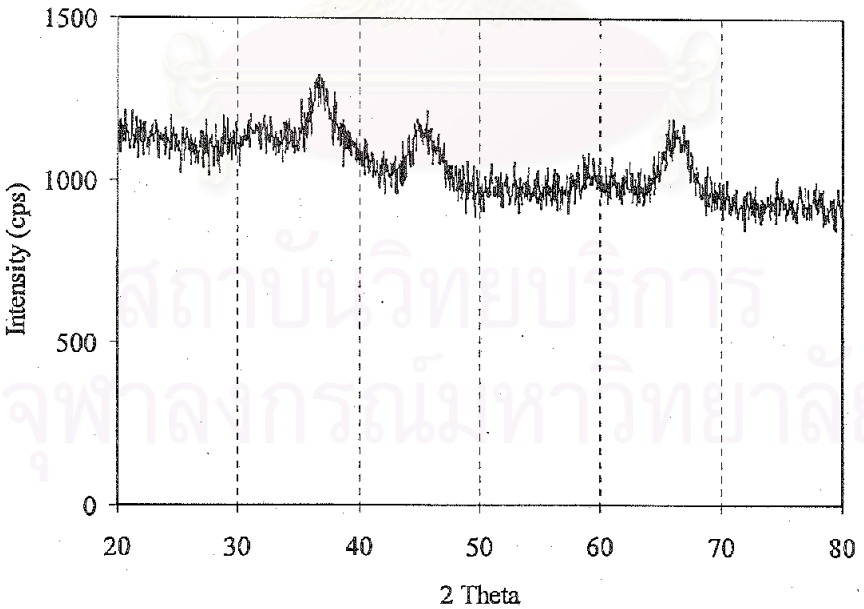Figure 5.5 The XRD pattern of Al_2O_3 catalyst

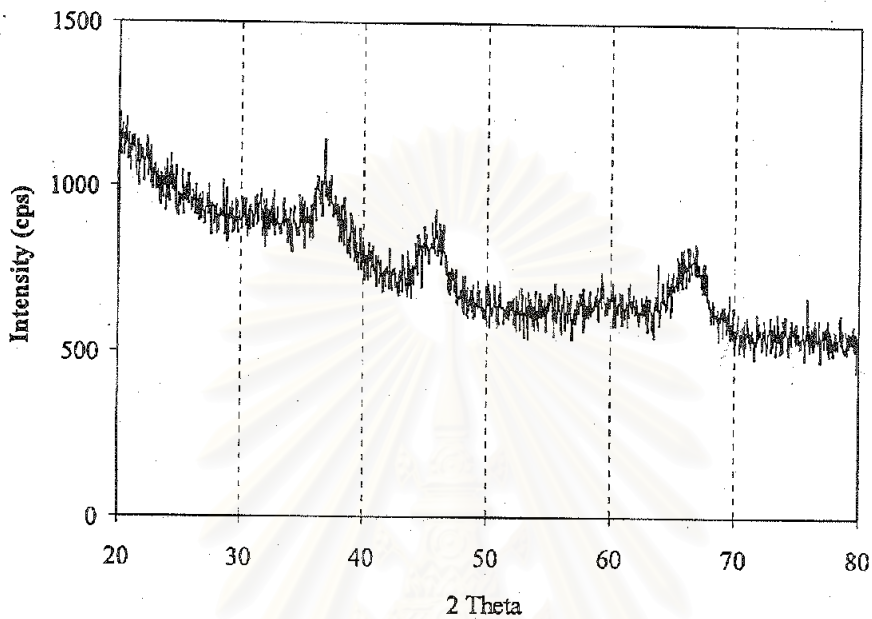Figure 5.6 The XRD pattern of 8Co1MgAl catalyst

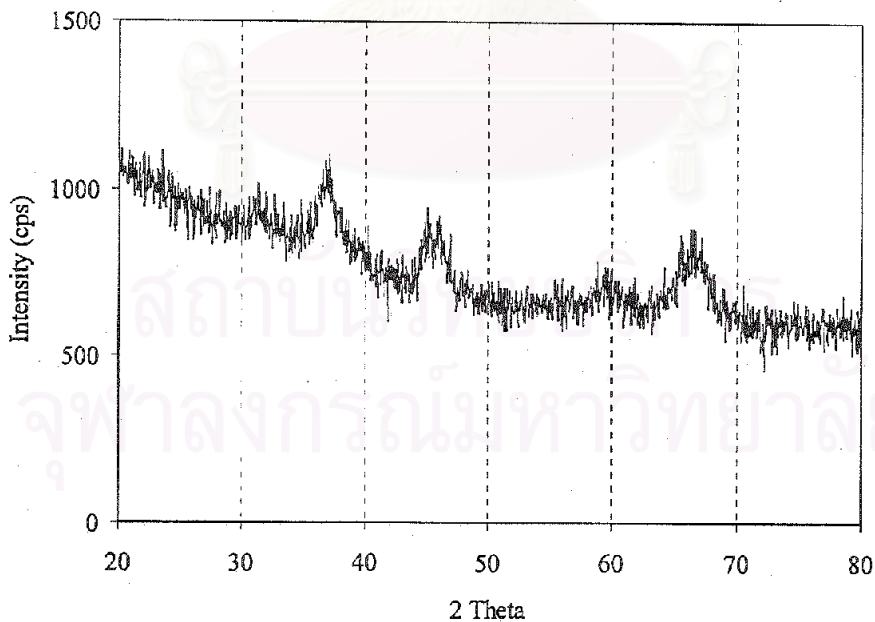**Figure 5.7** The XRD pattern of 1Mg8CoAl catalyst

Figure 5.8 The XRD pattern of co-8Co1MgAl catalyst

5.1.3 Fourier Transform Infrared Spectrometer (FT-IR)

The IR spectrum in the proper wavelength of 400-2000 cm^{-1} for determining the solid surface is used to identify the functional group on the surface of catalyst.

Figure 5.9 shows the IR spectrum of TiO_2 support. Strong absorption IR bands at 520 and 620 cm^{-1} are observed. The absorption peaks of 8Co1MgTi, 1Mg8CoTi, co-8Co1MgTi catalysts (figures 5.10, 5.11, and 5.12, respectively) are detected at 580, $667cm^{-1}$ and also exhibits the same pattern as TiO_2. From literature reviews, the IR absorption bands of cobalt oxide occur at 385, 580, and 667 cm^{-1} [Busca et al. (1990)]. This means that cobalt oxide appears in the forms of crystalline Co_3O_4 on the TiO_2 surface for all Co-Mg-O/ TiO_2 system.

The IR spectra of Al_2O_3 and Co-Mg-O/Al_2O_3 catalysts are shown in figures 5.13-5.16. The IR absorption bands of cobalt oxide are also found in Co-Mg-O/Al_2O_3 samples. It is indicated that cobalt species on these three catalysts form a Co_3O_4 crystal on Al_2O_3 support.
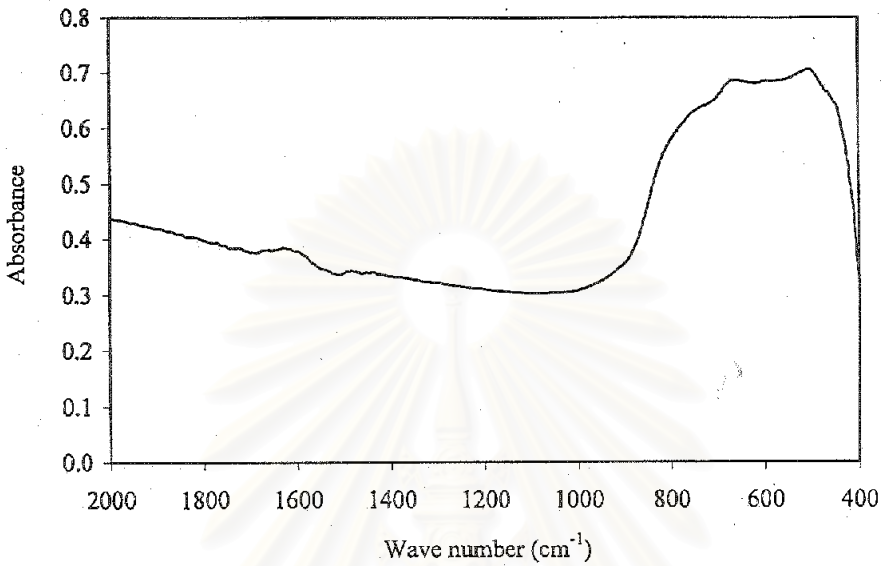
Figure 5.9 IR spectrum of TiO_2 catalyst

Figure 5.10 IR spectrum of 8Co1MgTi catalyst

Figure 5.11 IR spectrum of 1Mg8CoTi catalyst

Figure 5.12 IR spectrum of co-8CoMgTi catalyst

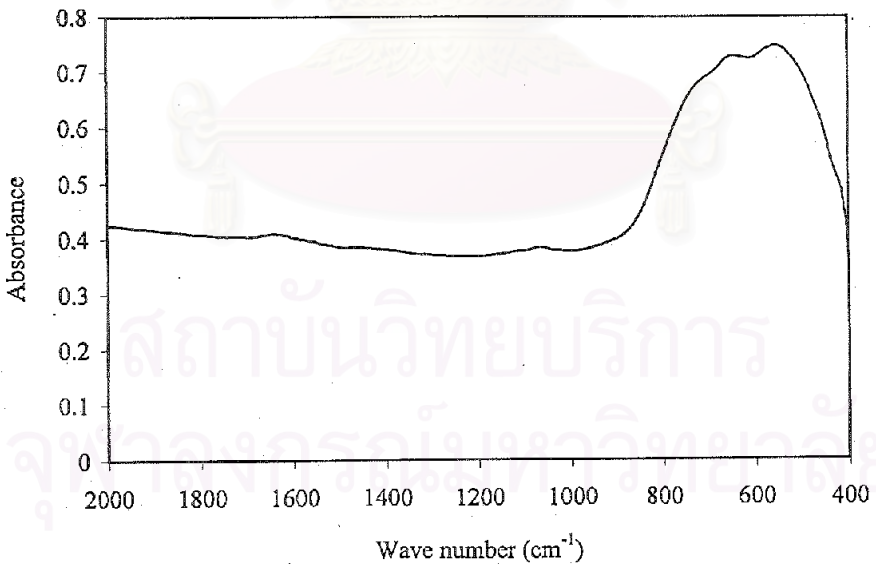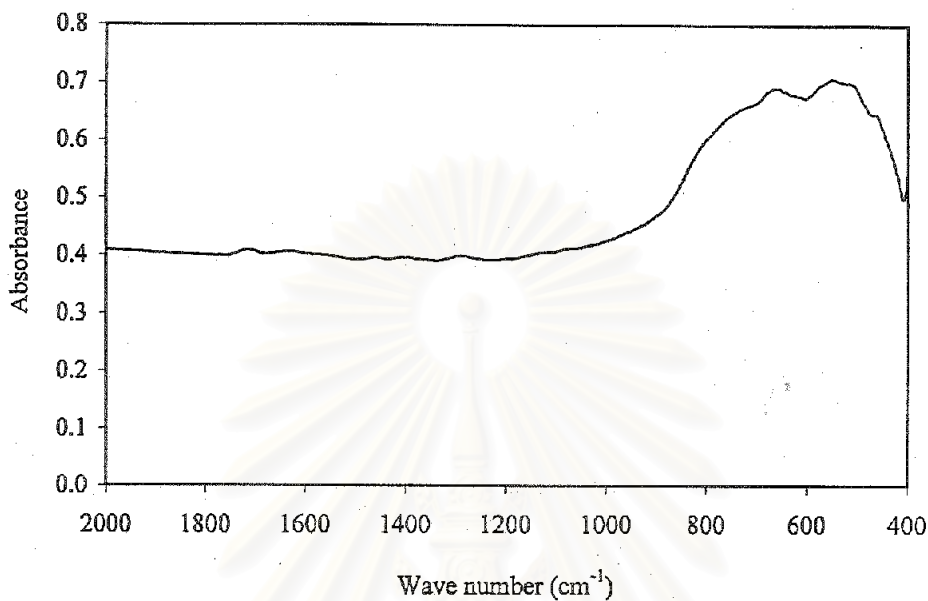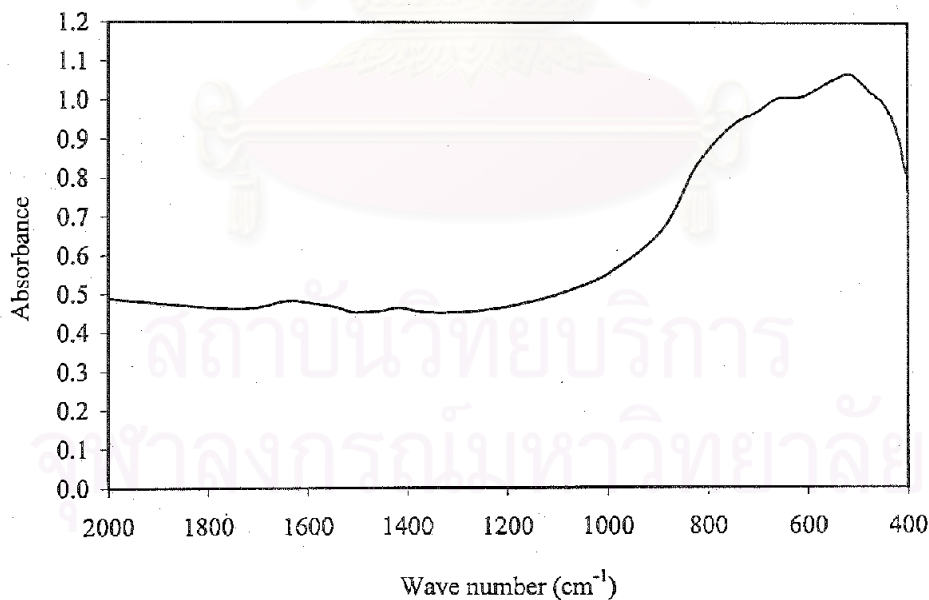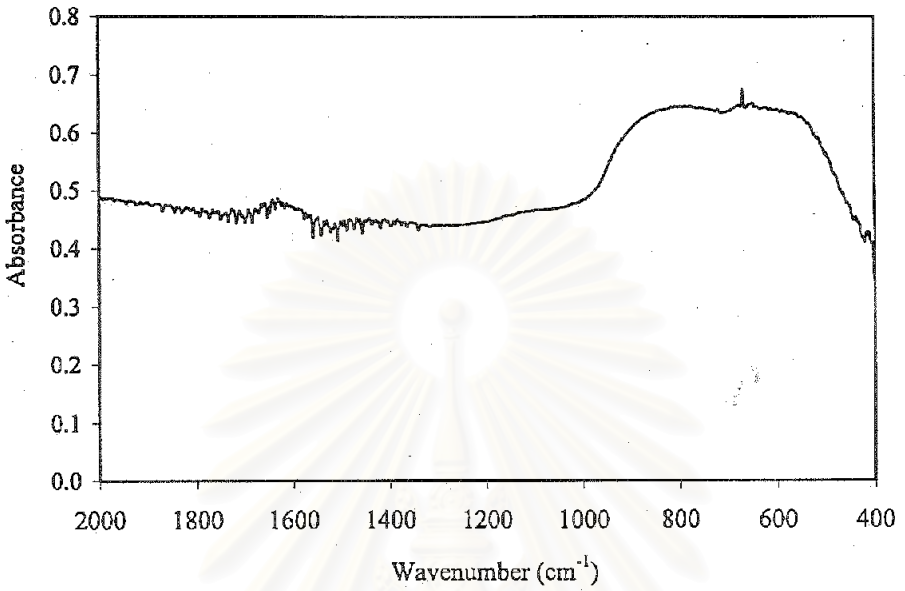**Figure 5.13** IR spectrum of Al$_2$O$_3$ catalyst
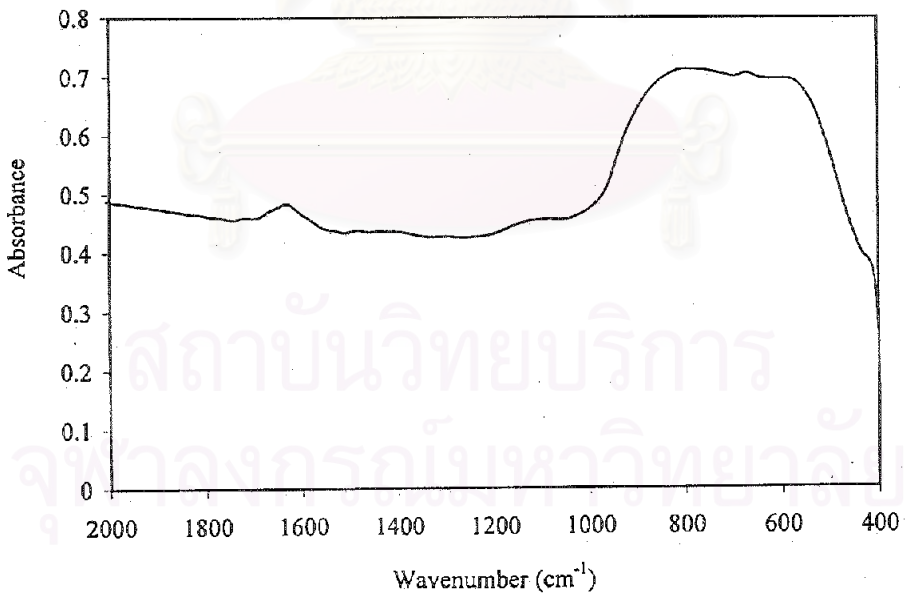
Figure 5.14 IR spectrum of 8Co1MgAl catalyst
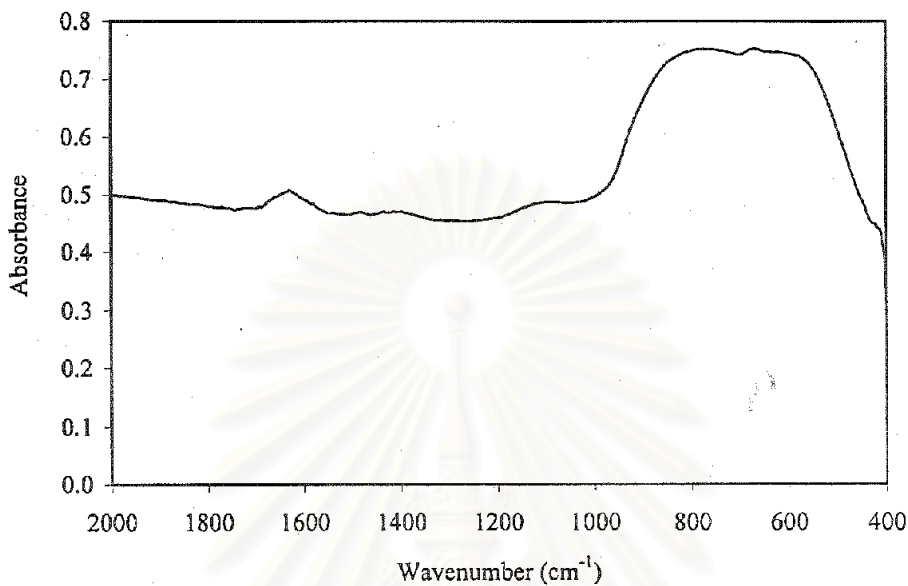
Figure 5.15 IR spectrum of 1Mg8CoAl catalyst
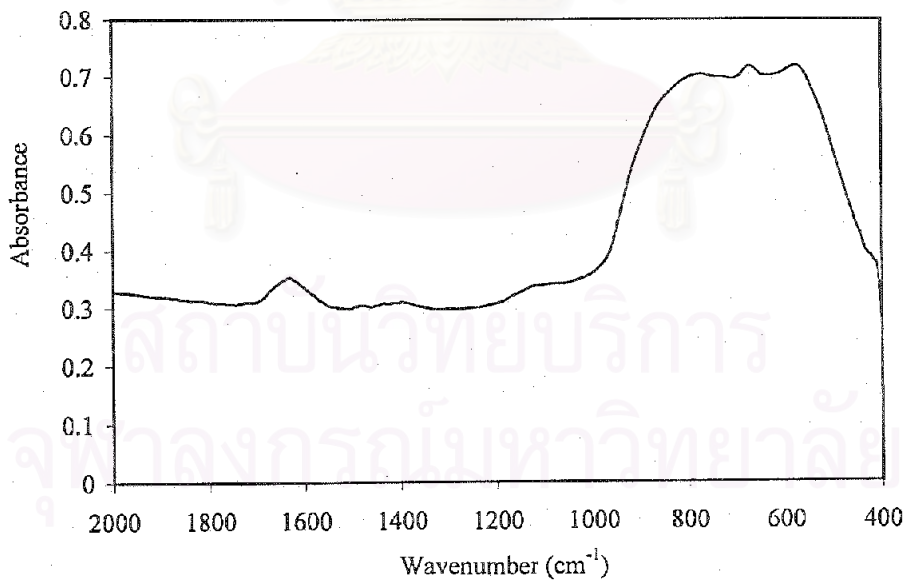
Figure 5.16 IR spectrum of co-8Co1MgAl catalyst

5.2 Catalytic reaction

In this work, the effect of the sequence of cobalt and magnesium loading and the effect of supports are received much attention. Since Co-Mg-O/TiO_2 and Co-Mg-O/Al_2O_3 systems are a novel system that have no information about its catalytic property. Therefore, the oxidation properties of 8Co1MgTi, 1Mg8CoTi, co-8Co1MgTi, 8Co1MgAl, 1Mg8CoAl, co-8Co1MgAl catalysts are studied by using the oxidation reaction on 1-propanol and 2-propanol as test reaction.

5.2.1 1-Propanol oxidation

- **8Co1MgTi catalyst**

The catalytic property of 8Co1MgTi catalyst on 1-propanol oxidation is illustrated in figure 5.17. In the reaction temperature range 200-250°C, 1-propanol conversion gradually rises from 3% to 7% and rapidly increases to 77% at 350°C. Beyond 350°C, the conversion of 1-propanol slightly increases up to 87% at 500°C.

At low 1-propanol conversion (200-300°C) the major reaction product is propionaldehyde. Also, there are some formations of other reaction products i.e., formaldehyde, acetaldehyde, ethylene, propylene, and CO_2. While at high 1-propanol conversion (350-500°C) the main product are propionaldehyde, propylene and CO_2 and with traces of formaldehyde, acetaldehyde, methane, and ethylene. Consequently, the selectivity of propionaldehyde moderately falls from 94% to 64% and the selectivities of CO_2 and propylene slightly rise from 0% to 13% and 0% to 14%, respectively, with increasing reaction temperature from 200-500°C. Acetaldehyde selectivity is rather constant about 4-6% at all reaction temperature. From these results the maximum yield of propionaldehyde is ca. 57% at 350°C.
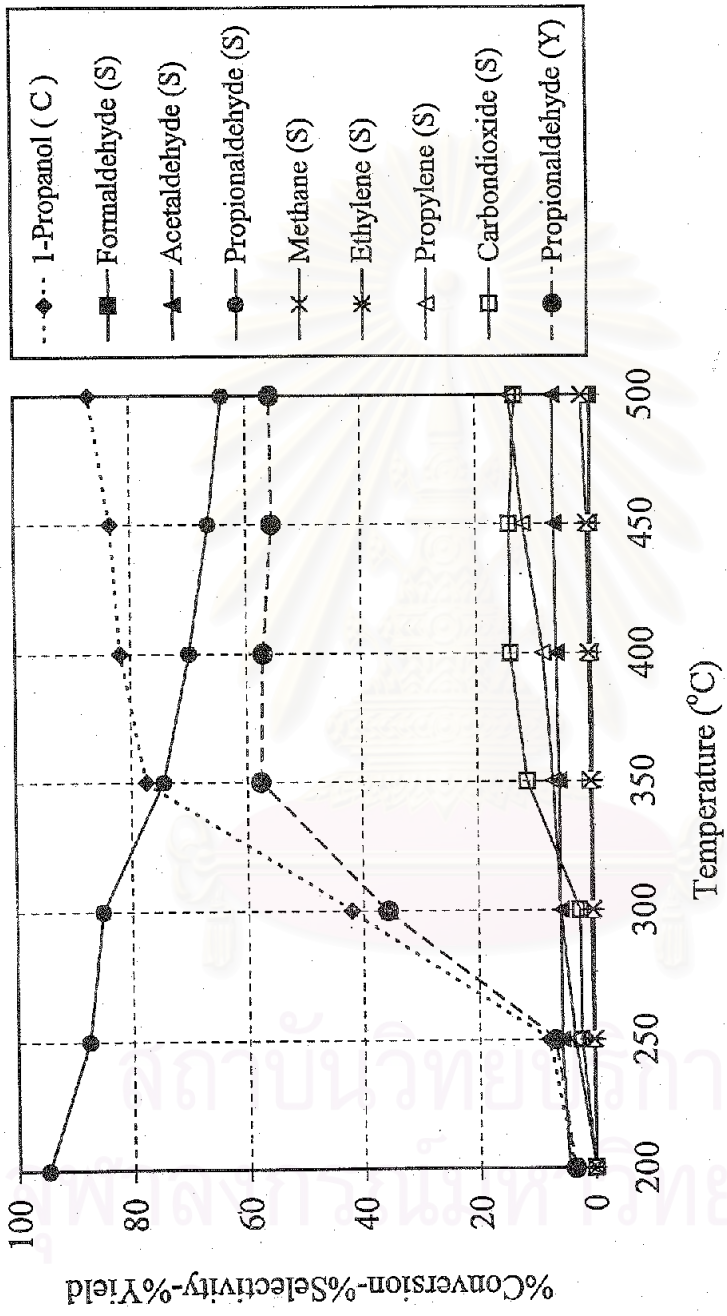
C – Conversion, S – Selectivity, Y – Yield

Figure 5.17 Catalytic property of 8Co1MgTi catalyst in the 1-propanol oxidation

- **1Mg8CoTi catalyst**

Figure 5.18 shows the catalytic activity of 1Mg8CoTi catalyst for 2-propanol oxidation reaction. At low reaction temperature the activity of 1Mg8CoTi catalyst slightly increases from 4% to 8% 1-propanol conversion on the increase of reaction temperature from 200 to 250°C. The conversion of 1-propanol significantly rises from 8% to 70% in the temperature range 250-350°C and then gradually increases up to 82% at 500°C.

At the initial reaction temperature (200-300°C) the main product is propionaldehyde and there are some formations of acetaldehyde, propylene, CO_2 and with traces amount of formaldehyde and ethylene. When increasing reaction temperature (350-500°C), the main product are propionaldehyde, propylene and CO_2 and with traces of formaldehyde, acetaldehyde, methane, and ethylene. Consequently, the selectivity of propionaldehyde moderately falls from 99% to 64% and the selectivities of CO_2 and propylene slightly rise from 0% to 15% and 0% to13%, respectively, with increasing reaction temperature from 200-500°C. Acetaldehyde selectivity still slightly increases from 0% to 2% at low 1-propanol conversion and becomes constant at around 3-4% at high 1-propanol conversion. From these results the maximum yield of propionaldehyde is ca. 55% at 350°C.

- **co-8Co1MgTi catalyst**

The result of the catalytic oxidation of 1-propanol on co-8Co1MgTi is shown in figure 5.19. Increasing the reaction temperature from 200°C to 250°C results in the increase in 1-propanol conversion from 3% to 9%. When the reaction temperature is higher than 250°C the 1-propanol conversion rapidly rises to 76% at 350°C and then slightly increase up to 84% at 500°C.

At low 1-propanol conversion the main oxidation product is propionaldehyde with small amounts of propylene and CO_2. At high 1-propanol conversion (above 250°C) the main product are propionaldehyde, propylene and CO_2. Traces of methane

Figure 5.18 Catalytic property of 1Mg8CoTi catalyst in the 1-propanol oxidation

C - Conversion, S - Selectivity, Y - Yield
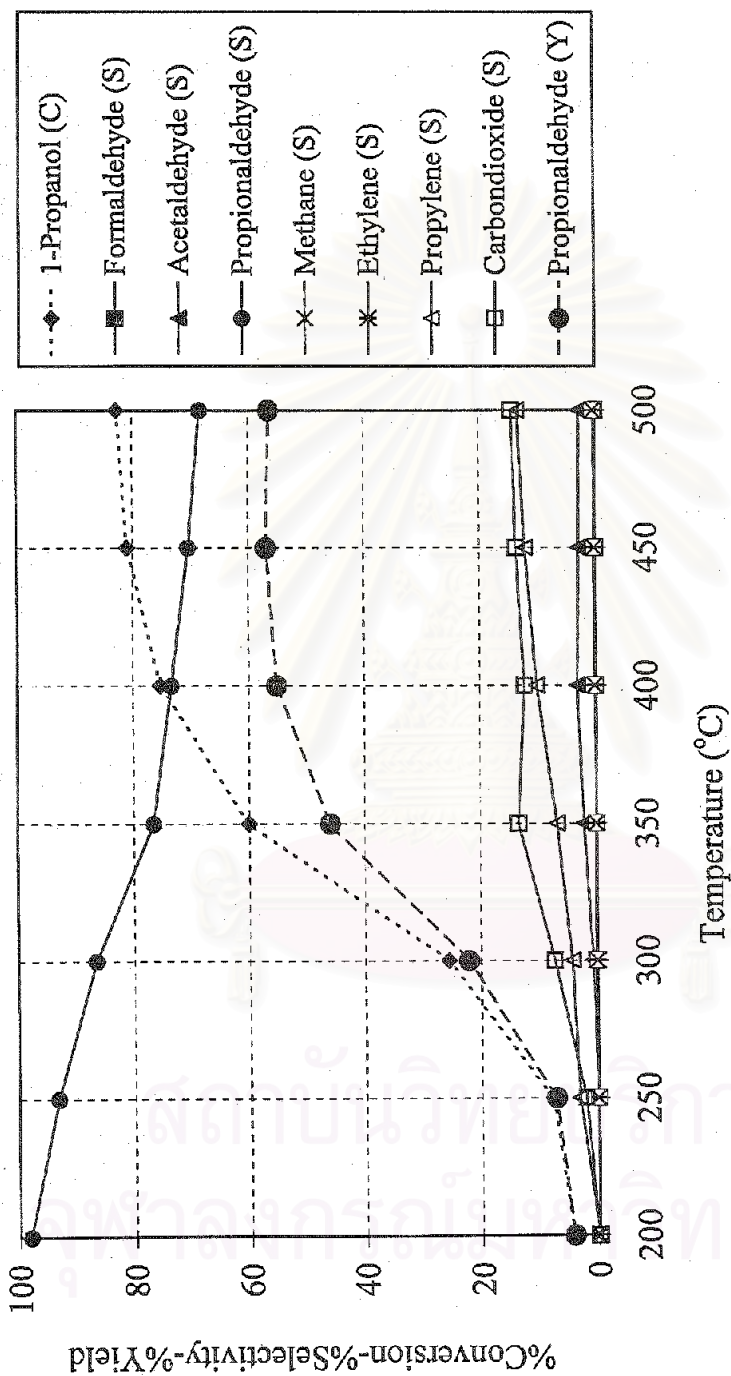
C - Conversion, S - Selectivity, Y - Yield

Figure 5.19 Catalytic property of co-8Co1MgTi catalyst in the 1-propanol oxidation

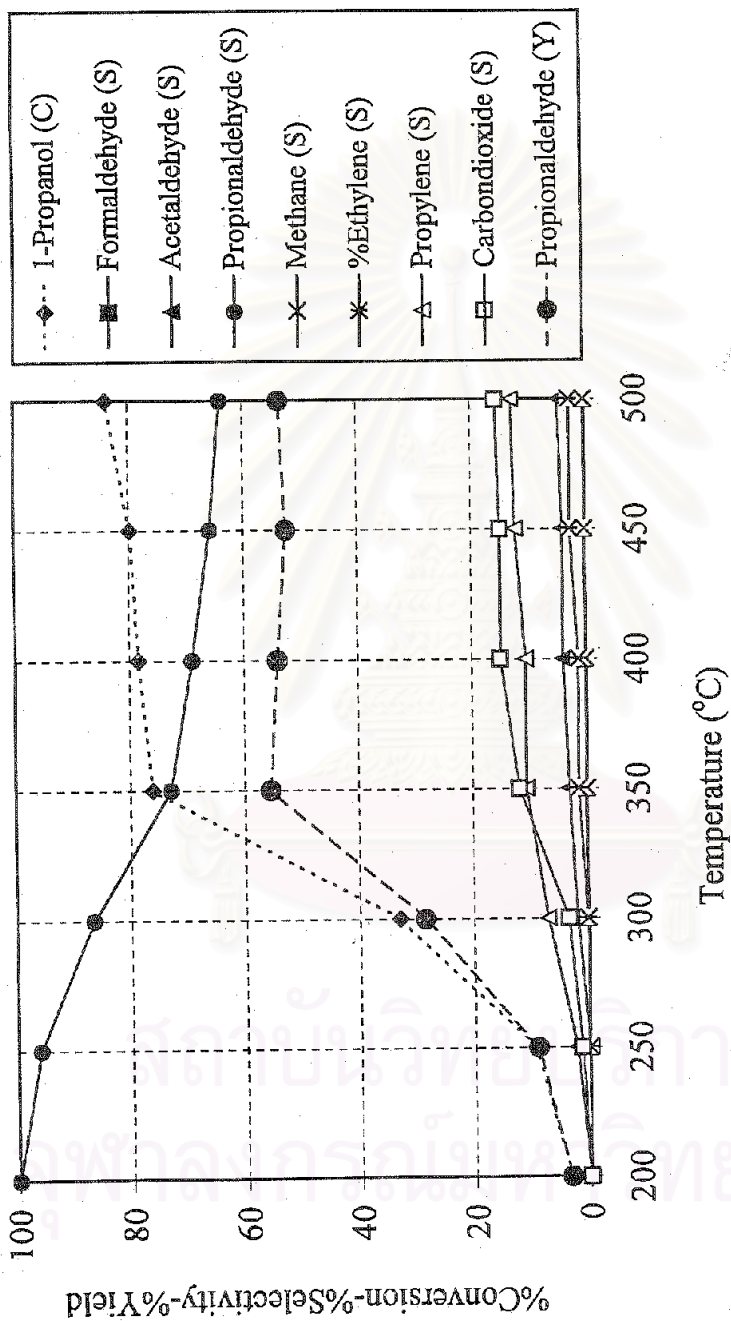ethylene, formaldehyde, and acetaldyhyde are detected at high temperature range. Consequently, the selectivity of propionaldehye moderately falls from 98% to 68% and the selectivities of CO_2 and propylene slightly rise from 0% to 14% and 0% to 1%, respectively, with increasing reaction temperature from 200-500°C. The maximum yield of propionaldehye is ca. 56% at 450°C.

After Co-Mg-O/TiO$_2$ system is tested as catalysts in 1-propanol oxidation, it can be concluded that the main useful product obtained from this reaction is propionaldehyde. In addition, the effect of sequence of cobalt and magnesium loading seem to have no effect on the structure and then the catalytic performance of Co-Mg-O/TiO$_2$ catalyst in 1-propanol oxidation because the catalytic property of 8Co1MgTi, 1Mg8CoTi, co-8Co1MgTi catalysts are almost the same.

- **8Co1MgAl catalyst**

The behavior of 8Co1MgAl catalyst for 1-propanol oxidation is illustrated in figure 5.20. In the initial reaction temperature, the conversion of 1-propanol gradually increases from 9% to 16% on the increase reaction temperature from 200 to 250°C. When the reaction temperature is higher than 250°C the 1-propanol conversion of this catalyst rapidly rises to 80% at 400°C and slightly increases up to 89% at 500°C.

At low 1-propanol conversion the main oxidation product is propionaldehyde with small amount of propylene and CO_2. At high 1-propanol conversion (above 250°C) propionaldehyde selectivity rapidly decreases while CO_2 and propylene selectivities quickly increase. The selectivity to propylene is higher than in case of Co-Mg-O/TiO$_2$ catalyst at all reaction temperature. The maximum selectivities to CO_2 and propylene are about 21% and 24% at 500°C, respectively. The maximum yield of propionaldehyde is ca. 41% at 350°C.

C – Conversion, S – Selectivity, Y – Yield

Figure 5.20 Catalytic property of 8Co1MgAl catalyst in the 1-propanol oxidation

- 1Mg8CoAl catalyst

The catalytic property of 1Mg8CoAl catalyst is illustrated in figure 5.21. The activity of this catalyst gradually increases at the beginning of reaction and then rapidly increases to about 85% at 500°C. The main product observed at the initial reaction temperature is propionaldehyde with small amounts of CO_2, propylene, and acetaldehyde. Further increasing reaction temperature propionaldehyde, CO_2, and propylene are the main products. At the temperature range 200-500°C the selectivity to propylene decreases rapidly from 91% to 42% while CO_2 and propylene selectivities increase from 0% to 20% and 8% to 23%, respectively.

- co-8Co1MgAl catalyst

The result of catalytic test on co-8Co1MgAl catalyst is shown in figure 5.22. The conversion of propionaldehyde steadily increases from 10% to 83% on the increase of reaction temperature from 200°C to 450°C and the slightly increases up to 85% at 500°C. An increase of reaction temperature from 200°C to 500°C causes selectivity to propionaldehyde steadily falls from 95% to 47% while CO and propylene selectivity rises from 2% to 20% and 2% to 21%, respectively. Small amount of acetaldehyde (~5%) and ethylene (~4%) are observed.

From the above results, it can be seen that the activities of these Co-Mg-O/Al_2O_3 catalysts in the 1-propanol oxidation have the same trends. Therefore, it may be concluded that the sequence of introduction of cobalt and magnesium has no effect on the catalytic property of Co-Mg-O/Al_2O_3 catalyst for 1-propanol oxidation reaction. In addition, the selectivity to propylene of these three catalysts is higher than in case of Co-Mg-O/TiO_2 catalyst at all the temperature range. Propionaldehyde selectivity is still to be the main product but rather lower than Co-Mg-O/TiO_2 catalyst.

C - Conversion, S - Selectivity, Y - Yield

Figure 5.21 Catalytic property of 1Mg8CoAl catalyst in the 1-propanol oxidation
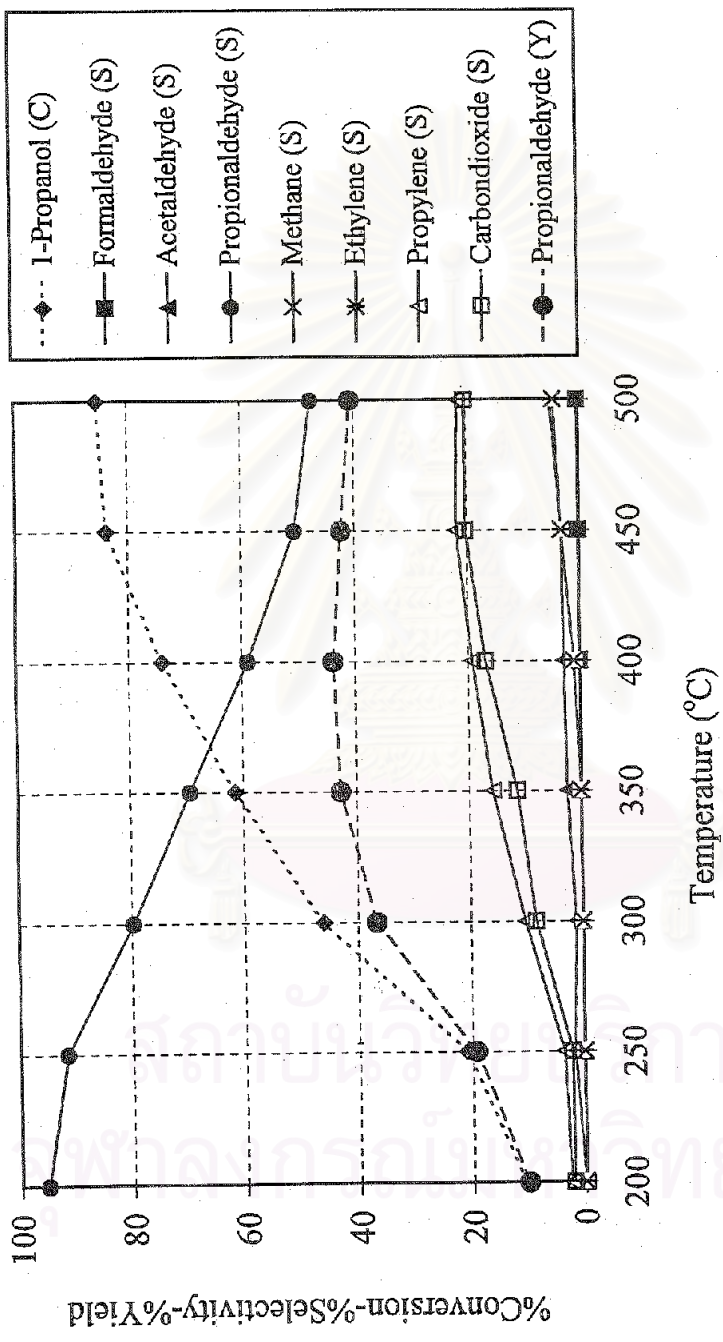
C - Conversion, S - Selectivity, Y - Yield

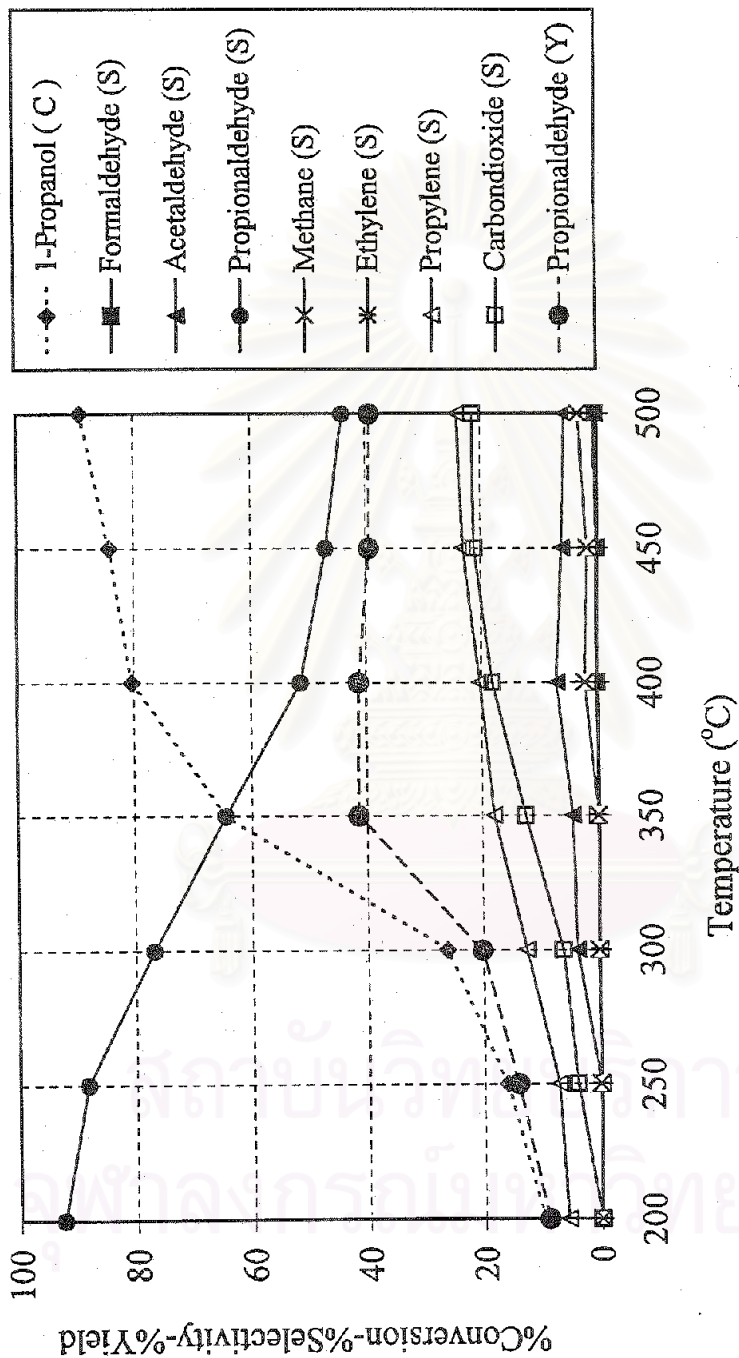**Figure 5.22** Catalytic property of co-8Co1MgAl catalyst in the 1-propanol oxidation

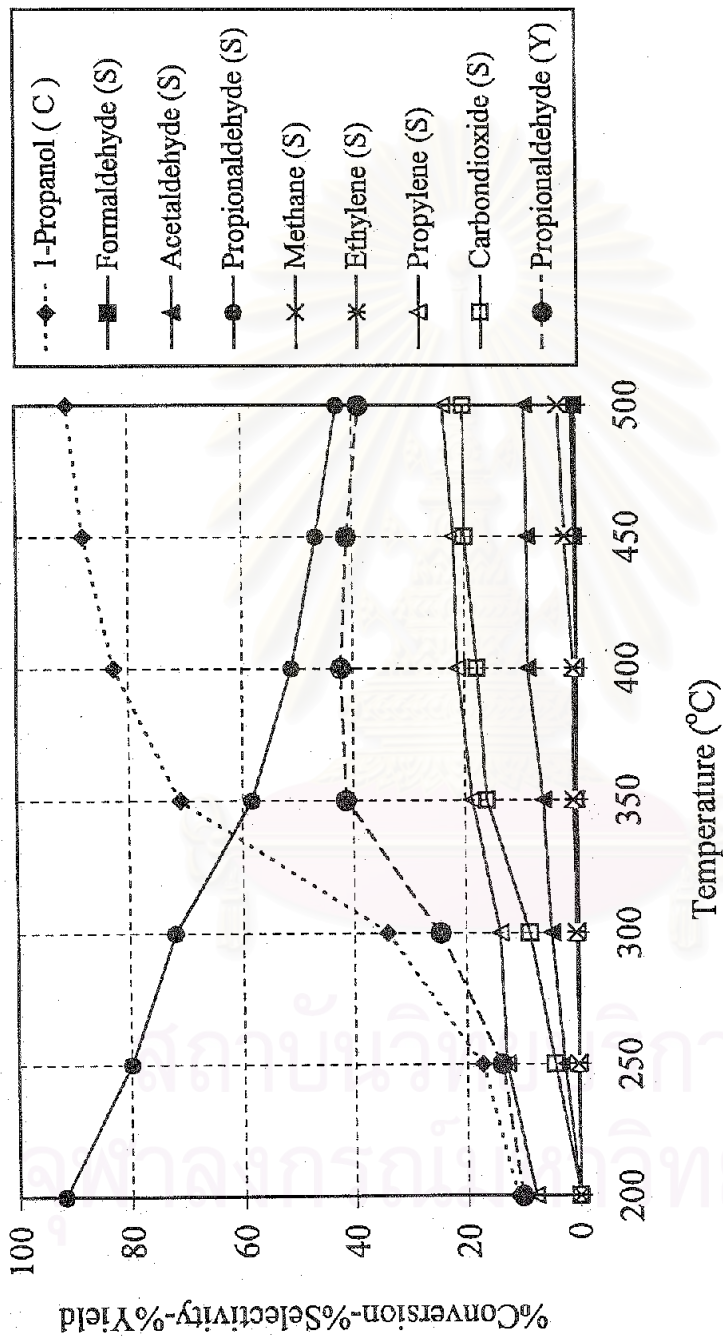### 5.2.2 2-Propanol oxidation

- **8Co1MgTi catalyst**

The behavior of the 8Co1MgTi catalyst in 2-propanol oxidation is described in figure 5.23. Increasing the reaction temperature from $200^{o}C$ to $350^{o}C$ results in the increase in 2-propanol conversion from 7% to 89%. Further increasing temperature 100% conversion is obtained at reaction temperature $400^{o}C$.

In the beginning (reaction temperature $200\text{-}250^{o}C$), the main reaction product is propylene with traces amount of formaldehyde and CO_2. At the reaction temperature higher than $250^{o}C$ propylene and propionaldehyde are the main products. Consequently, the selectivity of propylene substantially falls from 96% to 33% with increasing reaction temperature from $250\text{-}500^{o}C$. In the reaction temperature range $250\text{-}300^{o}C$ the propionaldehyde selectivity rapidly increases from 0% to 37%. Beyond $300^{o}C$, the selectivity of propionaldehyde steadily rises from 37% to 56% at $500^{o}C$. CO_2 selectivity is rather constant about 7-8% at high 2-propanol conversion.

- **1Mg8CoTi catalyst**

Figure 5.24 demonstrates the catalytic property of 1Mg8CoTi in the 2-propanol oxidation. At low reaction temperature the conversion of 2-propanol steadily increases from 5% to 25% with increasing temperature from $200^{o}C$ to $300^{o}C$. In the temperature range $300\text{-}350^{o}C$ the 2-propanol conversion rapidly increases from 25% to 86%. Beyond $350^{o}C$, the conversion of 2-propanol gradually rises up to 100% at $500^{o}C$.

At the initial reaction temperature ($200\text{-}250^{o}C$) the main product is propylene with traces of CO_2 and formaldehyde whereas at high reaction temperature ($300\text{-}500^{o}C$) the main products are propylene and propionaldehyde. The selectivity to propylene rapidly decreases from 97% to 28% while the selectivity to propionaldehhyde increases from 0% to 60% in the temperature range $250\text{-}500^{o}C$.
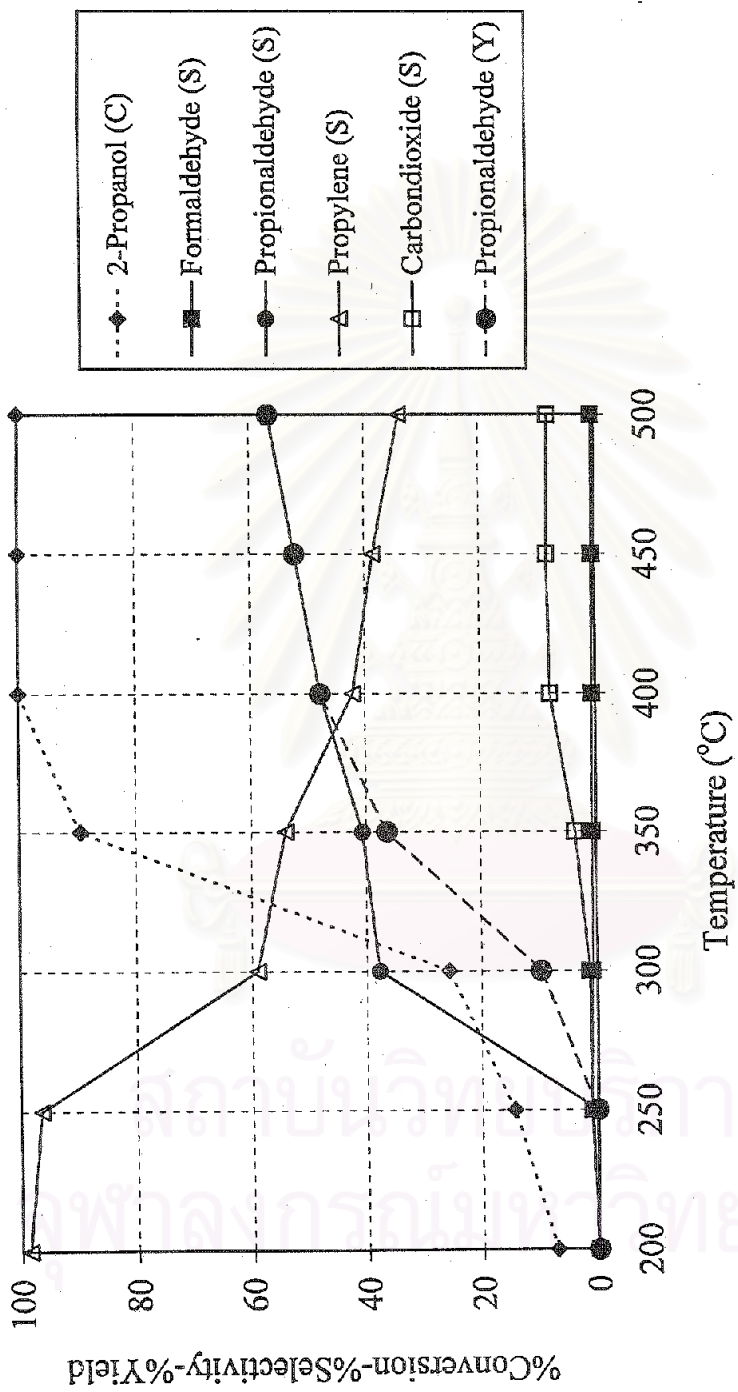
C - Conversion, S - Selectivity, Y - Yield

Figure 5.23 Catalytic property of 8Co1MgTi catalyst in the 2-propanol oxidation
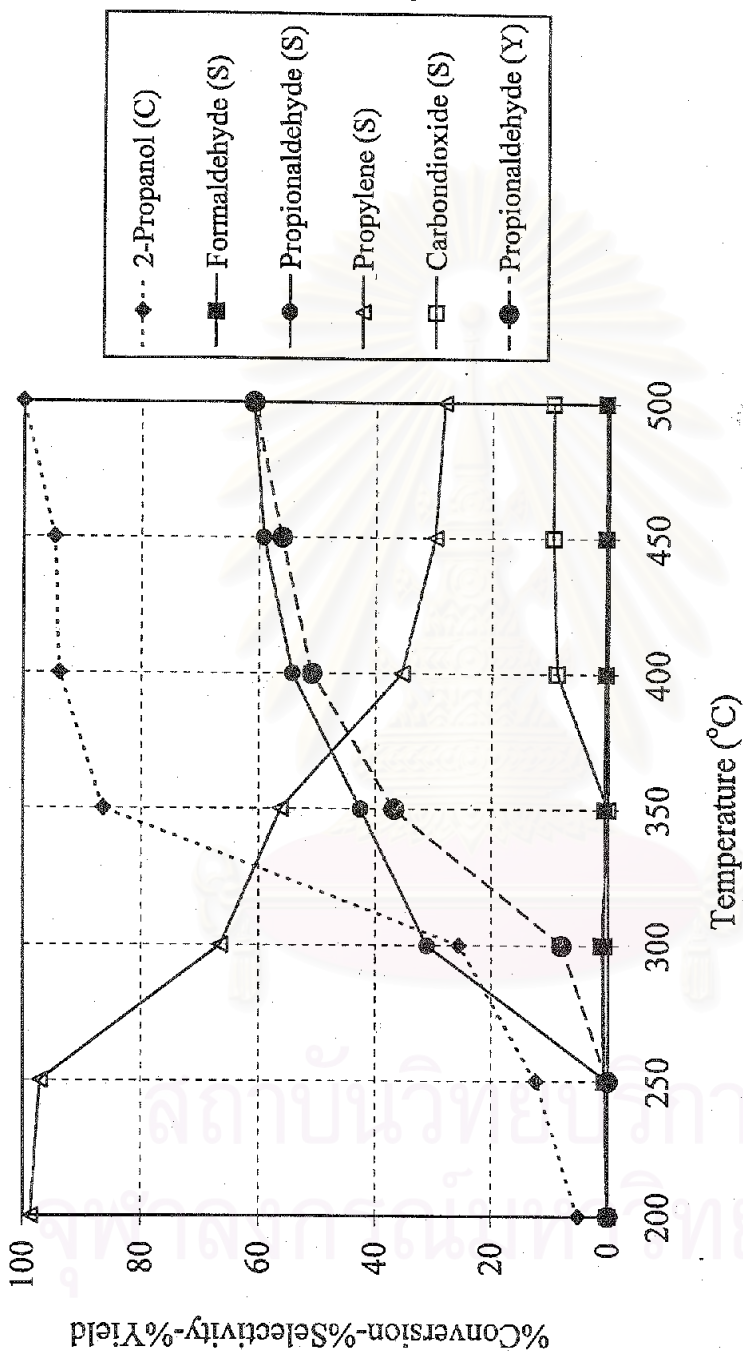
C – Conversion, S – Selectivity, Y – Yield

Figure 5.24 Catalytic property of 1Mg8CoTi catalyst in the 2-propanol oxidation

- **co-8Co1MgTi catalyst**

The result of the catalytic oxidation of 2-propanol on co-8Co1MgAl catalyst is shown in figure 5.25. Increasing the reaction temperature from $200^{o}C$ to 350 co-8Co1MgTi catalyst results in the increase in 2-propanol conversion from 7% to 89%. Further increasing temperature above $400^{o}C$ effects the conversion of co-8Co1MgTi catalyst reach a steady value of 100%. Propionaldehyde selectivity rapidly enhances from 0% to 60% while propylene selectivity significantly decrease from 97% to 26% at reaction temperature range 250-500°C. From these results the maximum yield of propylene is ca. 48% at $350^{o}C$.

According to the above results, it is observed that Co-Mg-O/TiO$_2$ catalyst has the high potential to produce propylene from 2-propanol at low reaction temperature. The sequence of cobalt and magnesium loading seems to have no effect to catalytic behavior of Co-Mg-O/TiO$_2$ catalyst in 2-propanol oxidation reaction.

- **8Co1MgAl catalyst**

The catalytic property of 8Co1MgAl catalyst on 2-propanol oxidation is illustrated in figure 5.26. The conversion of 2-propanol steadily increases from 1% to 95% at the temperature range 200-350°C and slightly increases to 100% at $400^{o}C$.

At the initial reaction temperature (200-250°C) the main product is propylene and traces of CO$_2$ and formaldehyde whereas at high reaction temperature (300-500°C) the main products are propylene and propionaldehyde. The selectivity to propylene rapidly decreases from 97% to 66% while the selectivity to propionaldehyde increases from 0% to 30% in the temperature range 250-300°C. Above $300^{o}C$, the selectivity to propionaldehyde slightly increases up to 39% at $500^{o}C$. Propylene selectivity gradually goes down from 66% to 47% in the temperature range 300-500°C. On the other hand, the selectivity to CO$_2$ slightly rises from 0% to 12% at all reaction temperature range. From these results the maximum yield of propylene is ca. 59% at $350^{o}C$.

C - Conversion, S - Selectivity, Y - Yield

Figure 5.25 Catalytic property of co-8Co1MgTi catalyst in the 2-propanol oxidation
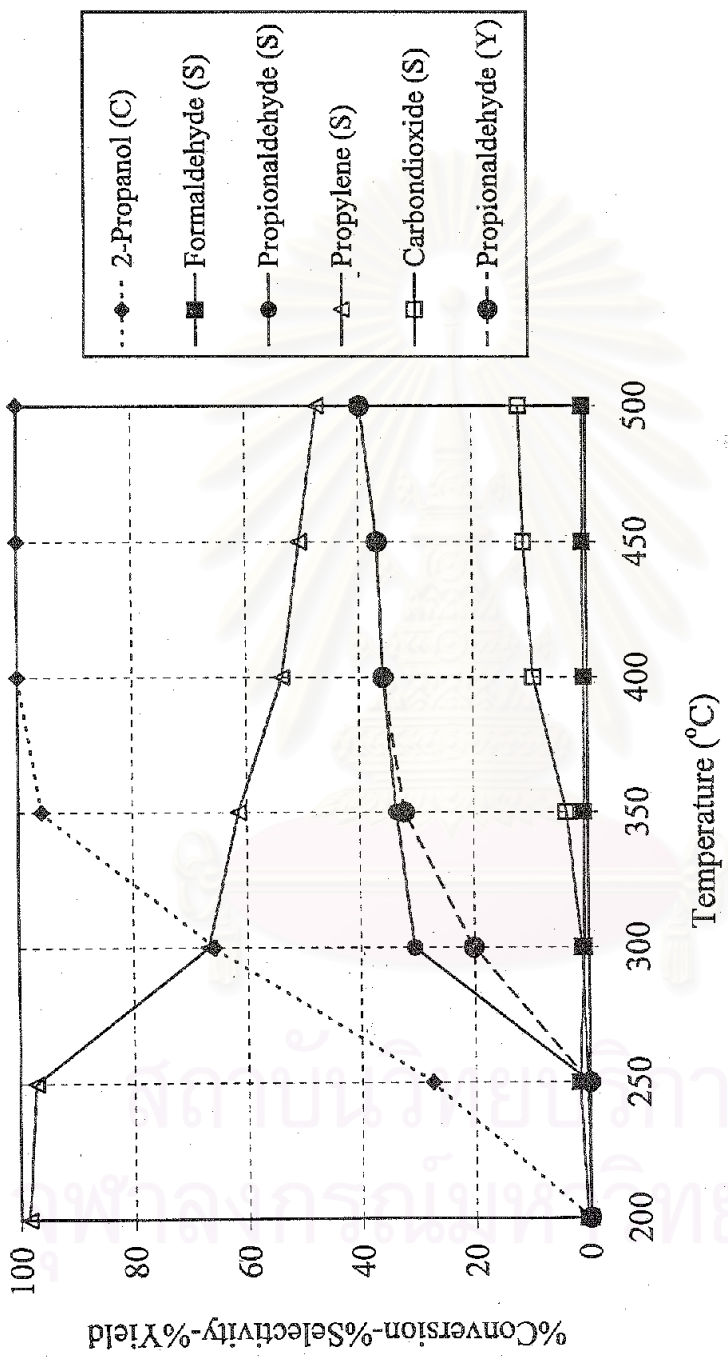
C - Conversion, S - Selectivity, Y - Yield

Figure 5.26 Catalytic property of 8Co1MgAl catalyst in the 2-propanol oxidation
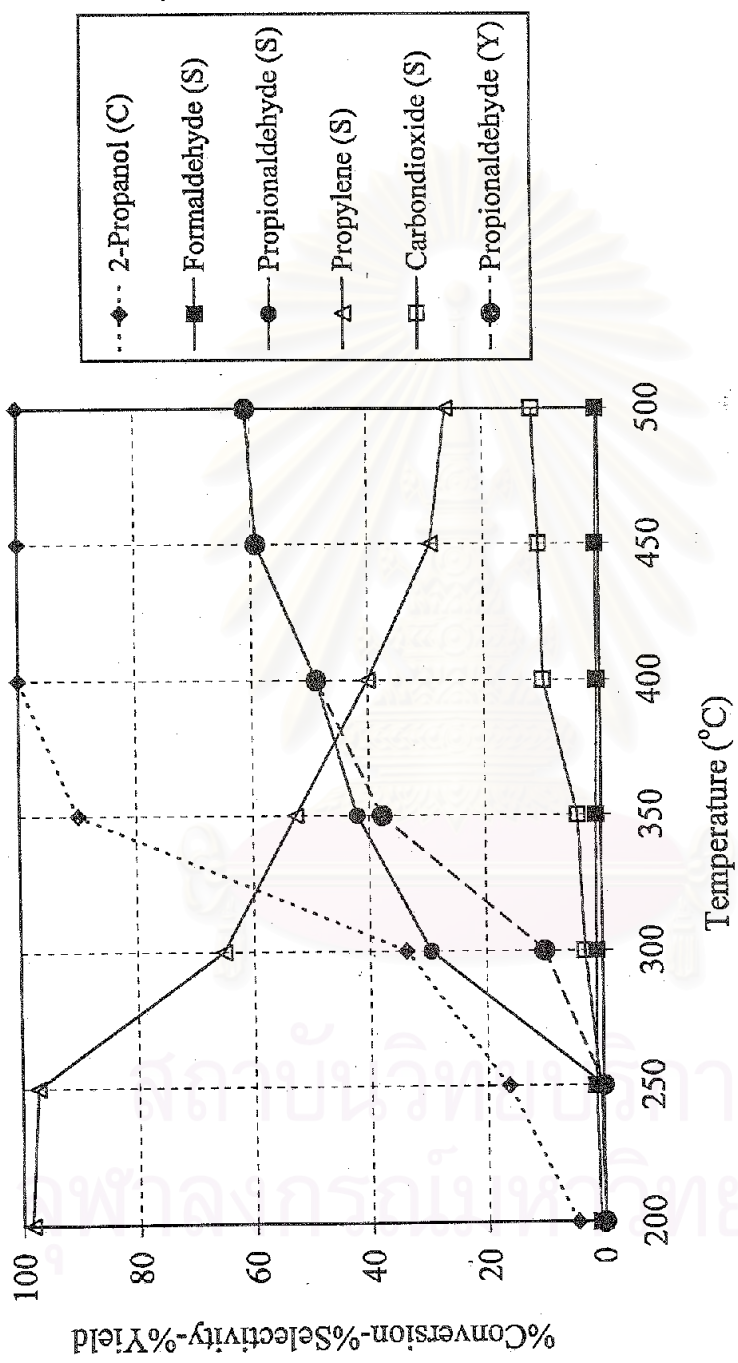
- **1Mg8CoAl catalyst**

Figure 5.27 shows the activity of 1Mg8CoAl catalyst for 2-propanol oxidation reaction. At low reaction temperature the conversion of 2-propanol slightly increases from 6% to 19% with increasing temperature from $200^{\circ}C$ to $250^{\circ}C$. In the temperature range 250-350°C the 2-propanol conversion rapidly increases form 19% to 96%. Beyond 350°C, the conversion of 2-propanol gradually rises up to 100% at 500°C. Propionaldehyde selectivity rapidly enhances from 0% to 25% and steadily increases to 38% at reaction temperature range 250-300°C and 300-500°C, respectively. On the other hand, propylene selectivity significantly decreases from 92% to 50% at reaction temperature range 250-500°C. The maximum selectivity to CO_2 is about 9% and the maximum yield of propylene is ca. 62% at 350°C.

- **co-8Co1MgAl catalyst**

The behavior of co-8Co1MgAl catalyst for 2-propanol oxidation is described in figure 5.28. The 2-propanol conversion rapidly rises from 8% to 95%, and then slightly enhances up to 100% at the temperature range 200-350°C and 350-400°C. At the initial reaction temperature (200-250°C) the main product is propylene with traces of CO_2 and formaldehyde whereas at high reaction temperature (300-500°C) the main product are propylene and propionaldehyde. The selectivity to propylene rapidly decreases from 98% to 67% while the selectivity to propionaldehyde increases from 0% to 26% in the temperature range 250-300°C. Above 300°C, the selectivity to propionaldehyde slightly increases up to 38% at 500°C. Propylene selectivity gradually goes down from 67% to 50% in the temperature range 300-500°C. The maximum selectivity to CO_2 is about 10% and the maximum yield of propylene is ca. 58% at 350°C.

From the results of 2-propanol oxidation over $Co-Mg-O/Al_2O_3$ catalyst that are shown above, it turns out that the activities of these three catalysts have almost the same patterns as $Co-Mg-O/TiO_2$ catalyst but $Co-Mg-O/Al_2O_3$ catalyst gives propylene selectivity higher than $Co-Mg-O/TiO_2$ catalyst.

C - Conversion, S - Selectivity, Y - Yield

Figure 5.27 Catalytic property of 1Mg8CoAl catalyst in the 2-propanol oxidation
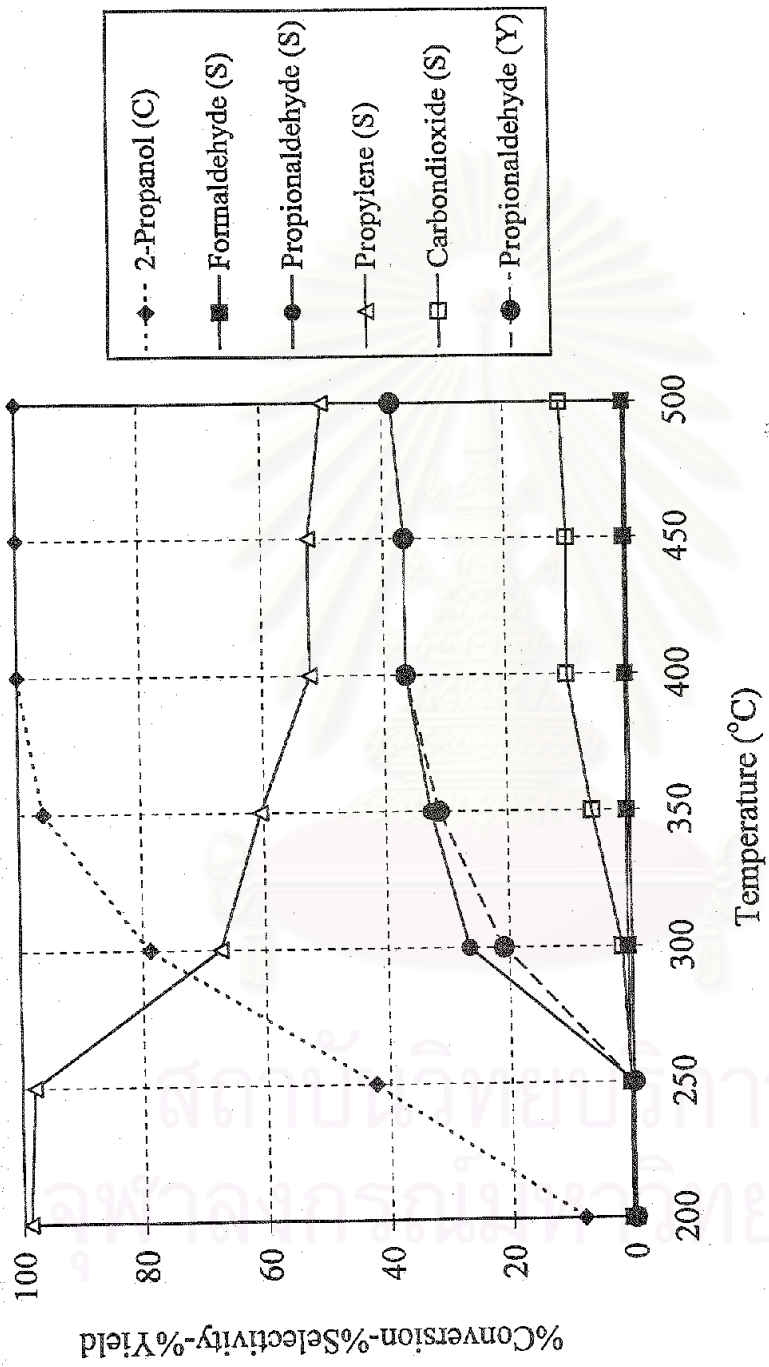
C – Conversion, S – Selectivity, Y – Yield

Figure 5.28 Catalytic property of co-8Co1MgAl catalyst in the 2-propanol oxidation
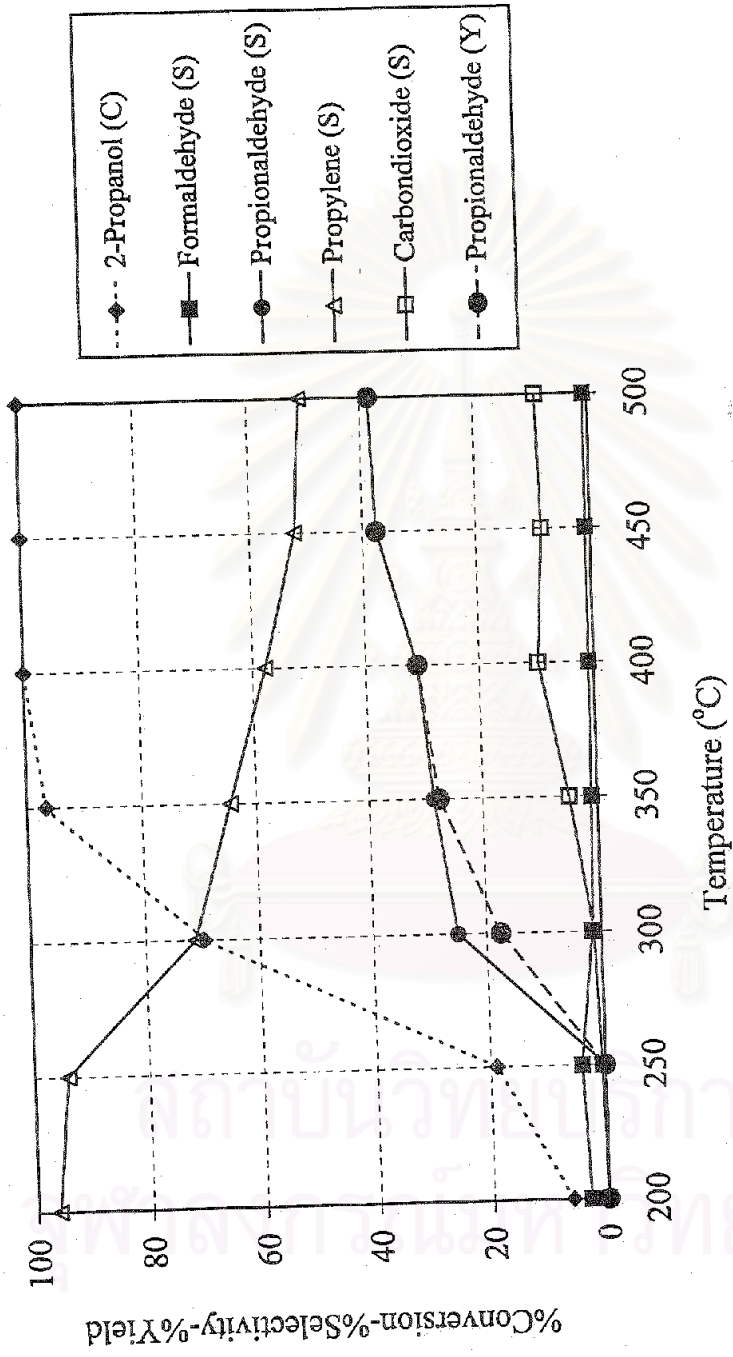
5.2.3 Effect of sequence of metal loading

To investigate the effect of sequence of cobalt and magnesium loading on the oxidation property of Co-Mg-O/TiO$_2$ and Co-Mg-O/Al$_2$O$_3$ catalyst, then 8Co1MgTi, 1Mg8CoTi, co-8Co1MgTi and 8Co1MgAl, 1Mg8CoAl, co-8Co1MgAl catalysts are prepared.

From the above results, it can be seen that the catalytic property of 8Co1MgTi, 1Mg8CoTi, and co-8Co1MgTi catalysts in 1-propanol and 2-propanol oxidation exhibit similar trend. The XRD pattern and IR spectrum of these three catalysts also showed the same pattern and the crystalline Co$_3$O$_4$ peaks could be detected. It indicated that these three catalysts might have same structure. Therefore, it may be concluded that the sequence of introduction of metal has no effect on the catalytic property of Co-Mg-O/TiO$_2$ system.

From previous studies, the sequence of introduction of magnesium has an effect on the catalytic property of V-Mg-O/TiO$_2$ system. It may be explained that vanadium with first deposited on TiO$_2$ forms a dispersed vanadia species on TiO$_2$ surface calcination at 550°C. Though the melting point of pure V$_2$O$_5$ is 700°C, when vanadia is dispersed on TiO$_2$ surface, it can be melted at a lower temperature than bulk V$_2$O$_5$. Therefore, after the impregnation of magnesium, the catalyst is then calcined at 550°C and vanadia species can be melted at this calcination temperature and react with MgO to from a new V-Mg-O compound, not from vanadium oxide. The similar phenomenon occurs in the case of co-impregnation of vanadium and magnesium. In contrast, magnesium forms a stable MgO on the TiO$_2$ surface after the calcination at 550°C when it is first impregnated on TiO$_2$. The melting point of MgO is about 2800°C thus, after vanadium is impregnated on MgO/TiO$_2$ and them calcined at 550°C, MgO is not melted at this calcination temperature. Vanadium can not react with magnesium to form V-Mg-O compound but it appears in the forms of crystalline V$_2$O$_5$ on the TiO$_2$ surface.

In the case of 8Co1MgTi catalyst with cobalt first deposited on TiO_2, after impregnation of magnesium and then calcined at 550°C, Co_3O_4 cannot be melted at this temperature and does not react with MgO to form a new Co-Mg-O compound, because the melting point of Co_3O_4 is 895°C which higher than V_2O_5. Therefore, the structure of cobalt species on Co-Mg-O/TiO_2 catalyst is Co_3O_4 that can be seen from the XRD and IR spectrum of this catalyst. The similar phenomenon occurs in the case of co-impregnation of cobalt and magnesium (co-8Co1MgTi catalyst). For 1Mg8CoTi catalyst, it can be explained in the same way as V-Mg-O/TiO_2 which magnesium is first deposited on TiO_2 support.

For Co-Mg-O/Al_2O_3 system, the catalytic properties in 1-propanol and 2-propanol oxidation of these three catalysts (8Co1MgAl, 1Mg8CoAl, co-8Co1MgAl) have the same trend. In addition, the XRD and IR spectrum give the same patterns and can be detected the Co_3O_4 peaks too. From this results it may be concluded that Co-Mg-O/Al_2O_3 catalyst, which the difference order of metal loading have the same structure of cobalt species on Al_2O_3 surface and the sequence of cobalt and magnesium loading have no effect. The reasons of this phenomenon can be explained as the Co-Mg-O/TiO_2 system.

5.2.4 Pathway of 1-propanol and 2-propanol oxidation

From the results of 1-propanol oxidation over Co-Mg-O/TiO$_2$ and Co-Mg-O/Al$_2$O$_3$ catalysts, propionaldehyde is the main product at low reaction temperature while propylene and CO$_2$ become significant at high reaction temperature. It can be proposed that propylene is produced directly from 1-propanol by dehydration reaction. On the other hand, CO$_2$ has propionaldehyde as an intermediate produced by oxidation reaction of 1-propanol.

For 2-propanol oxidation reaction over Co-Mg-O/TiO$_2$ and Co-Mg-O/Al$_2$O$_3$ catalysts, all catalyst provided high propylene selectivity at low reaction temperature. Further increasing temperature propionaldehyde forms when propylene selectivity decreases at the same temperature. It indicates that propionaldehyde is secondary product for 2-propanol oxidation that is produced via the oxidation reaction of propylene. To investigate this assumption, propylene is used as reactant on the oxidation reaction of Co-Mg-O/TiO$_2$ and Co-Mg-O/Al$_2$O$_3$ catalysts. Because the sequence of introduction of cobalt and magnesium has no effect on catalytic property of Co-Mg-O/TiO$_2$ and Co-Mg-O/Al$_2$O$_3$, only co-8Co1MgTi and co-8Co1MgAl catalysts are chosen as representative to investigate.

The behavior of co-8Co1MgTi and co-8Co1MgAl as catalyst for propylene oxidation is illustrated in figures 5.29 and 5.30, respectively. In the initial reaction temperature (200-250°C) the absence of selectivities curves at the reaction temperature between 200-250°C is because of zero conversion. When the temperature is higher than 250°C, the activity of co-8Co1MgTi and co-8Co1MgAl catalysts increase gradually up to 22% and 20%, respectively and the main product is propionaldehyde and CO$_2$. co-8Co1MgTi catalyst shows propionaldehyde selectivity rises continuously with temperature from 50% to 72%, while the selectivity to CO$_2$ drops from 49% to 27%. The propionaldehyde selectivity of co-8Co1MgAl catalyst presents the same trend but lower than that of co-8Co1MgTi catalyst (48% to 60%), while CO$_2$ selectivity drops from 52% to 40% at the reaction temperature between 300-500°C.
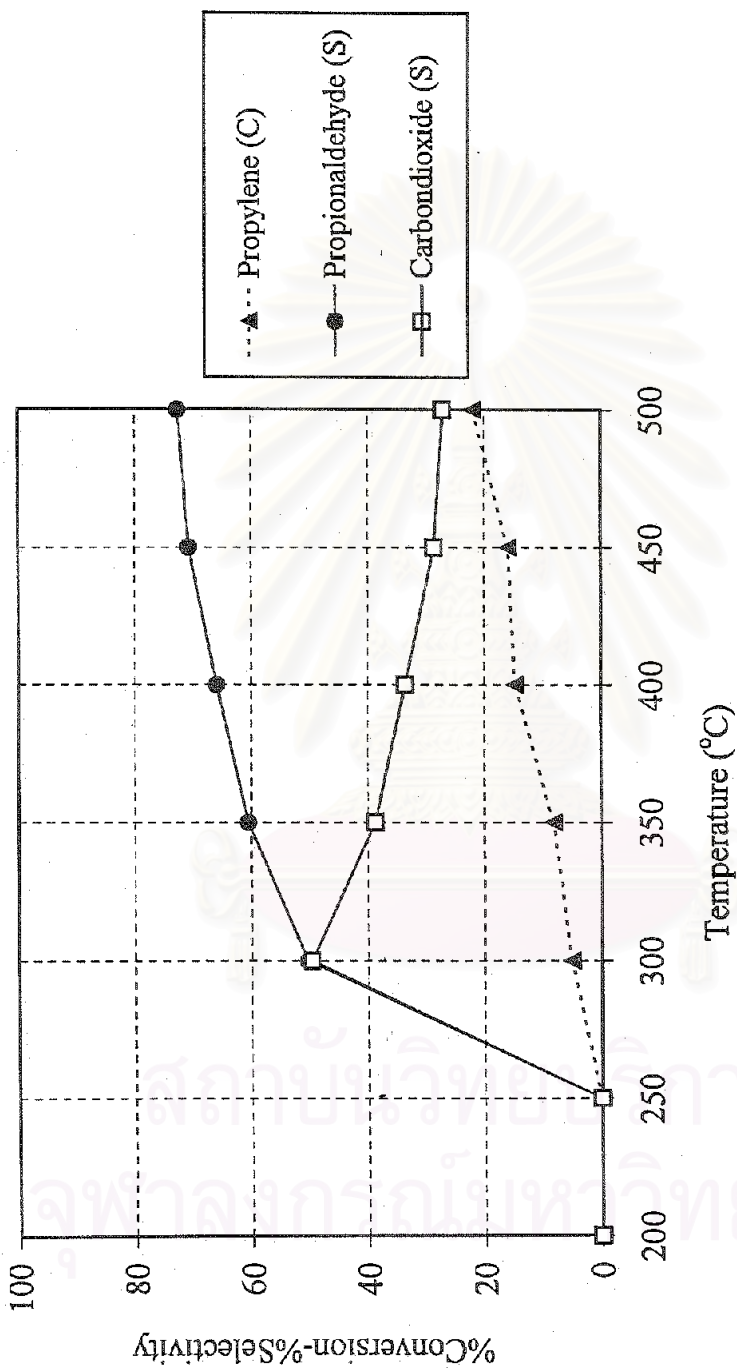
C - Conversion, S - Selectivity

Figure 5.29 Catalytic property of co-8Co1MgTi catalyst in the propylene oxidation
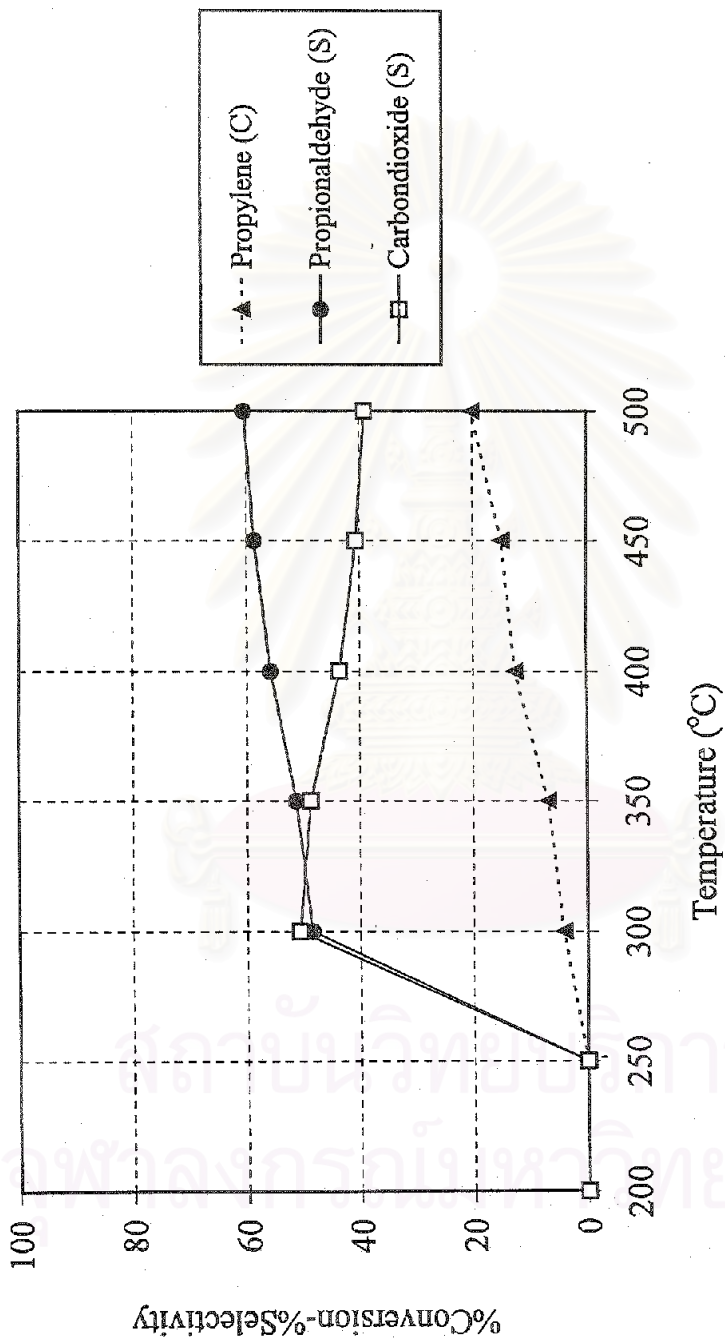
C – Conversion, S – Selectivity

Figure 5.30 Catalytic property of co-8Co1MgAl catalyst in the propylene oxidation

From the result of catalytic test on co-8Co1MgTi and co-8Co1MgAl catalysts in the propylene oxidation that are shown above, this means that propionaldehyde from 2-propanol oxidation reaction over Co-Mg-O/TiO_2 and Co-Mg-O/Al_2O_3 catalysts is the secondary product of 2-propanol that is produced directly from propylene.

In addition, it can be seen that the propionaldehyde selectivity increases while CO_2 selectivity decreases with increasing the reaction temperature. This phenomenon can be explained that at high reaction temperature, the rate of propylene oxidation with O_2 to form propionaldehyde is faster than at low temperature. The concentration of O_2 used in the catalytic combustion of propylene to formed CO_2 decreases, therefore CO_2 selectivity decreases with increasing the reaction temperature.

The routes of product formation in 1-propanol and 2-propanol oxidation is shown in scheme 1.

$$2\text{-propanol} \rightarrow \text{propylene} \rightarrow \text{propionaldehyde} \rightarrow CO_2$$
$$\uparrow$$
$$1\text{-propanol}$$
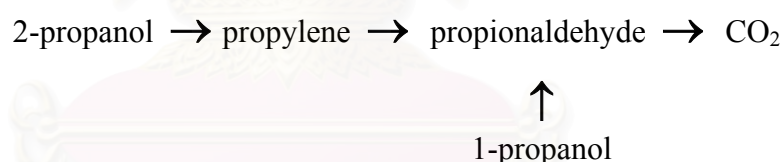
Scheme 1 Routes of product formation in 1-propanol and 2-propanol oxidation.

As seen in 1-propanol and 2-propanol oxidation reaction, 100% conversion of 2-propanol is obtained at high reaction temperature while conversion of 1-propanol rises to reach the maximum value about 90%. From this result, it may be concluded that propylene formed in 2-propanol oxidation reaction is produced from dehydration reaction that does not use O_2 in reaction. On the other hand, dehydrogenation reaction of 1-propanol to formed propionaldehyde used O_2 and in this reaction O_2 is limiting agent.

5.2.5 Effect of support to supported cobalt catalyst

For this work, 1-propanol and 2-propanol oxidation over Co-Mg-O/TiO$_2$ and Co-Mg-O/Al$_2$O$_3$ catalysts are studied to investigate the effect of support on catalytic property of supported cobalt catalyst. It has been known that alcohol can be oxidized, and the products of oxidation depend on the class of the alcohol. Primary alcohol and secondary alcohol can lose one of α-hydrogen (dehydrogenation reaction) to from an aldehyde and a ketone, respectively, or lose molecule of water (dehydration reaction) to form alkene. In general, secondary alcohol can lose molecule of water easier than primary alcohol. From the results of 1-propanol oxidation, the main product of two catalyst systems is propionaldehyde, but Co-Mg-O/TiO$_2$ catalyst give the selectivity to propionaldehyde higher than in case of Co-Mg-O/Al$_2$O$_3$ catalyst while the selectivity to propylene is lower.

It has long been recognized that acid/base properties of catalysts play an important role in many catalytic reactions, including polymerization, isomerization, cracking, dehydration, dehydrogenation, and alkylation. From the previous studies, it has been reported that acidity can promote the dehydration reaction of alcohol to olefin and basicity can promote the dehydrogenation reaction of alcohol to oxygenated compound [Murthy *et al*. (1994)]. Because TiO$_2$ exhibit stronger basic character than Al$_2$O$_3$, so Co-Mg-O/TiO$_2$ catalyst provides propionaldehyde selectivity higher than Co-Mg-O/Al$_2$O$_3$ catalyst.

Moreover, compared with previous study, Co-Mg-O/Al$_2$O$_3$ catalyst gives the maximum propionaldehyde yield (~40%) higher than Co/Al$_2$O$_3$ catalyst (~30%) [Kittikerdkulchai (1999)] at the same reaction condition. This result can be explained by the acid-base properties of catalyst too. When MgO is loaded on Al$_2$O$_3$, its essentially basic surface character increases the basic property of catalyst, thus Co-Mg-O/Al$_2$O$_3$ catalyst gives the propionaldehyde yield higher than Co/Al$_2$O$_3$ catalyst.

For 2-propanol oxidation, the main product at the lower temperature is propylene but at the higher temperature the main products are propylene and propionaldehyde. At all reaction temperature, Co-Mg-O/Al_2O_3 catalyst gives the propylene yield higher than Co-Mg-O/TiO_2 catalyst because Co-Mg-O/Al_2O_3 catalyst has acid property higher than Co-Mg-O/TiO_2 catalyst. In addition, the result of propylene oxidation indicated that Co-Mg-O/TiO_2 catalyst give the conversion of propylene to propionaldehyde and the propionaldehyde selectivity higher than Co-Mg-O/Al_2O_3 catalyst.

Recently, the oxidation property of the Co-Mg-O (8wt%Co) catalyst was investigated by using the oxidation reaction of methanol, ethanol, 1-propanol, 2-propanol, and 1-butanol as test reactions [Kittikerdkulchai (1999)]. To compare the catalytic performance of Co-Mg-O catalyst with Co-Mg-O/TiO_2 catalyst (co-8Co1MgTi), the result of the catalytic oxidation of 1-propanol on 8Co/MgO catalyst is shown in figure 5.31.

It can be seen that at low reaction temperature the conversion of 1-propanol steadily increases from 2% to 6% with increasing reaction temperature from 200°C to 250°C. In the reaction temperature range 250-400°C the 1-propanol conversion rapidly increases from 6% to 74%. Beyond 400°C, the conversion of 1-propanol gradually rises up to 76% at 500°C. At low 1-propanol conversion (200-250°C) the major reaction product is propionaldehyde. Also, there are some formations of other reaction products i.e., methane, ethylene, propylene, formaldehyde, and CO_2. While at high 1-propanol conversion (400-500°C) the main products are propionaldehyde and CO_2. Consequently, the selectivity of propionaldehyde moderately falls from 91% to 68% and the selectivity of CO_2 slightly rises from 5% to 20% with increasing reaction temperature from 200-500°C. Propylene selectivity is rather constant about 1-2% at all reaction temperature. From these results the maximum yield of propionaldehyde is ca. 53% at 400°C.
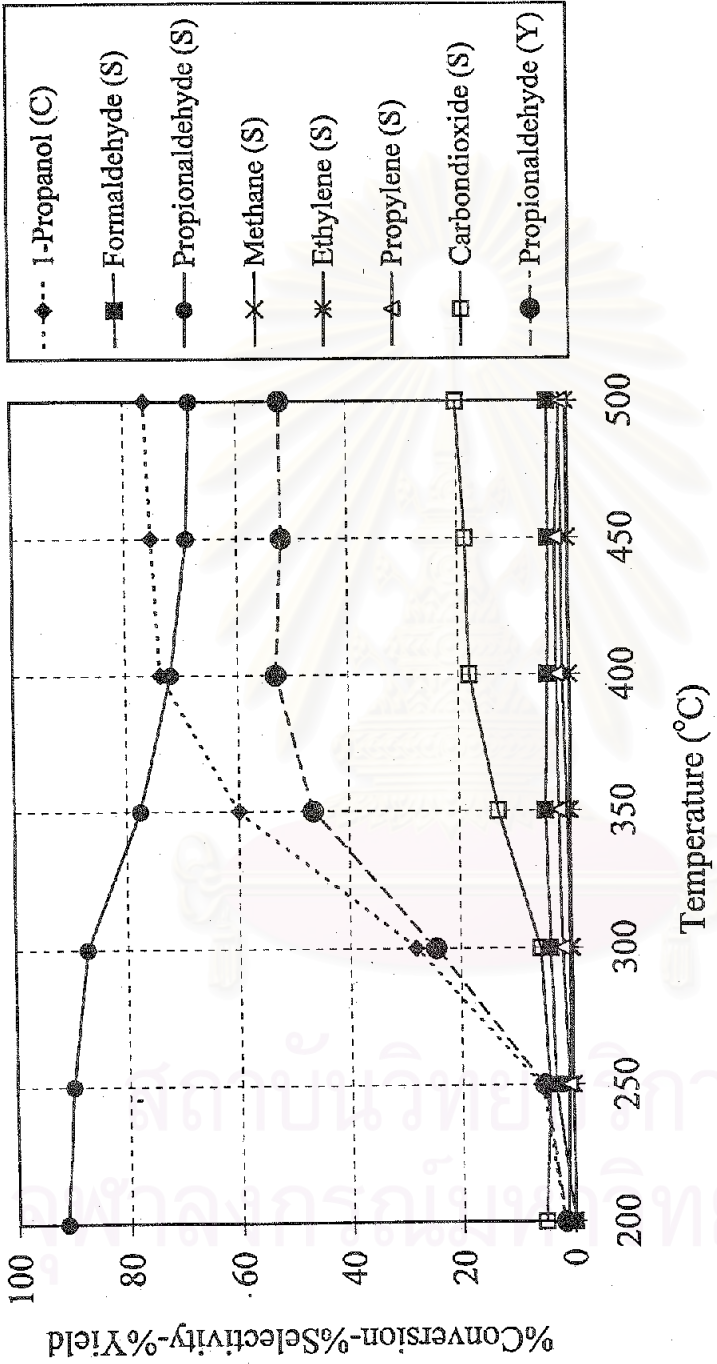
C - Conversion, S - Selectivity, Y - Yield

Figure 5.31 Catalytic property of 8Co/MgO catalyst in 1-propanol oxidation [Kiitikerdkulchai (1999)]

Table 5.2 shows the catalytic activity and the main product yield of Co-Mg-O/TiO_2 catalyst compared with 8Co/MgO catalyst.

Table 5.2 The comparison of catalytic property of Co-Mg-O/TiO_2 (Data from figure 5.19) and 8Co/MgO catalysts

Catalyst	8Co/MgO	Co-Mg-O/TiO_2
Maximum 1-propanol converted/catalyst 1 g	5.8%	6.6%
Maximum 1-propanol converted/Co-Mg-O 1 g	0.5%	7.4%
Maximum propionaldehyde yield/catalyst 1 g	53.0%	57.0%
Maximum propionaldehyde yield/Co-Mg-O 1 g	5.3%	63.3%

Therefore, it can be concluded that catalytic property of 8Co/MgO catalyst has the same pattern as Co-Mg-O/TiO_2 catalyst but shows slightly lower 1-propanol conversion. The main product of these two catalysts is propionaldehyde and the same by products (methane, ethylene, propylene formaldehyde, and CO_2) formed. However the selectivities to propionaldehyde and propylene of 8Co/MgO catalyst are slightly lower than in case of Co-Mg-O/TiO_2 catalyst while CO_2 selectivity is higher. From these results it may be concluded that Co-Mg-O/TiO_2 catalyst is a better selective oxidation catalyst than 8Co/MgO catalyst.

CHAPTER VI
CONCLUSIONS AND RECOMMENDATIONS

6.1 Conclusions

The conclusions of the present research are the following:

1. The catalytic activity of 8Co-Mg-O/Al_2O_3 and 8Co-Mg-O/TiO_2 catalysts is high for the oxidation of 1-propanol and 2-propanol.

2. The sequences of metal loading have no effect on the structure and catalytic property of 8Co-Mg-O/Al_2O_3 and 8Co-Mg-O/TiO_2 catalysts.

3. From 1-propanol oxidation, the major product is propionaldehyde and 8Co-Mg-O/TiO_2 catalyst give the highest propionaldehyde yield.

4. The main products obtained from the 2-propanol oxidation are propylene and propionaldehyde and 8Co-Mg-O/Al_2O_3 catalyst give the highest propylene yield.

5. From propylene oxidation, since propionaldehyde is the main product proposed that propylene forms in 2-propanol oxidation further oxidized to propionaldehyde.

6. The acid/base properties of support effect the catalytic performance of catalysts. TiO_2, the basic support, promote dehydrogenation reaction of 1-propanol and 2-propanol to form propionaldehyde while Al_2O_3, the acid support, promote dehydration reaction to from propylene.

6.2 Recommendations for future studies

     1. 8Co-Mg-O/Al$_2$O$_3$ and 8Co-Mg-O/TiO$_2$ catalysts are suitable to use in selective oxidation reaction of 1-propanol and 2-propanol. Therefore it will be interesting to further study the oxidation property of 8Co-Mg-O/Al$_2$O$_3$ and 8Co-Mg-O/TiO$_2$ catalysts in the other alcohol oxidation such as ethanol, butanol and unsaturated alcohol.

     2. For this research, the amounts of cobalt and magnesium content are fixed to study other effects. A variation of the cobalt and magnesium content will be interesting to study the optimum content that gives the best catalyst.

REFERENCES

Aramendia, M. A., Benitez, J. A., Borau, V., Jimenez, C., Marinas, J. M., Ruiz, J. R. and Urbano, F., "Study of MgO and Pt/MgO systems by XRD, TPR, and H MAS NMR", *Langmuir*, 1999, **15**, 1192-1197.

Baldi, M., Finocchio, E., Milella, F. and Busa, G., "Catalytic combustion of C3 hydrocarbons and oxygenated over Mn_3O_4", *Appl. Catal. B*, 1998, **16**, 43-51.

Besson, M., Gallezot, P., "Selective oxidation of alcohols and aldehydes on metal catalysts", *Catalysis today*, 2000, **57**, 127-141.

Bettasar, M. M., Costentin, G., Savary, L. and Lavalley, J. C., "On the Partial oxiation of propane and propylene on mixed metal oxide catalysts", *Appl. Catal. A*, 1996, **145**, 1-48.

Busca, G., Guidetti, R. and Lorenzelli, V., "Fourier-transform Infrared study of the surface properties of cobalt oxides", *J. Chem. Soc., Faraday Trans.*, 1990, **86**, 989-994.

Cassidy, F. E. and Hodnett, B. K., "Selective oxidation catalysts: an evaluation of the discriminating capacity of active sites on oxides catalysts with molecular oxygen as oxidant", *Catal. Tech.*, 1998, **2**, 173-180.

Chan, T.K. and Smith, K.J., "Oxidative coupling of methane over cobalt-magnesium and manganese-magnesium mixed oxide catalysts", *Appl. Catal.*, 1990, **60**, 13-31.

Chang, Y. F. and Heinemann, H., "Partial oxidation of methane to syngas over Co/MgO catalysts. Is it low temperature?", *Catal. Lett.*, 1993, **21**, 215-224.

Chernavskii, P.A., Pankina, G. V. and Lunin, V. V., "The influence of oxide-oxide interaction of the catalytic properties of Co/Al_2O_3 in CO hydrogenation", *Catal. Lett.*, 2000, **66**, 121-124.

Chin, R. L. and Hercules, D. M., "Surface spectroscopic characterization of cobalt-alumina catalysts", *J. Phys. Chem.*, 1982, **86**, 360-367.

Finocchio, E., Willey, R. J., Busca, G. and Lorenzelli, V., "FTIR studies on the selective oxidation and combustion of light hydrocarbons at metal oxide surfaces", *J. Chem. Soc., Faraday Trans.*, 1997, **93**, 175-180.

Fishel, T. and Davis, J., "Use of catalytic reactions to probe Mg-Al mixed oxide surfaces", *Catal. Lett.*, 1994, **25**, 87-95.

Garbowski, E., Guenin, M., Marion, M-C. and Primet, M., "Catalytic properties and surface states of cobalt containing oxidation catalysts", *Appl. Catal.*, 1990, **64**, 209-224.

Grzybowska-Swierkosz, B., "Thirty years in selective oxidation on oxides: what have we learned?", *Topics in Catalysis*, 2000, **11/12**, 23-42.

Haga, F., Nakajima, T., Yamashita, K. and Mishima, S., "Effect of crystallite size on the catalysis of alumina-supported cobalt catalyst for steam reforming of ethanol", *React. Kinet. Catal. Lett.*, 1998, **63**, 253-259.

Kitayama, Y., Satoh, M. and Kodama, T., "Preparation of large surface area nickel magnesium silicate and its catalytic activity for conversion of ethanol into buta-1,3-diene", *Catal. Lett.*, 1996, **36**, 95-97.

Kittikerdkulchat, S., *Master of Engineering thesis Chulalongkorn University*, 1999.

Leklertsunthorn, R., *Master of Engineering thesis Chulalongkorn University*, 1998.

Mars, P. and van Krevelen, D. W., "Oxidations carried out by means of vanadium oxide catalysts", *Chem. Eng. Sc.*, 1954, **3**, 41-59.

Murthy, I.A.P.S., "Catalytic decomposition of 2-propanol on $Co_{1+x} Al_{2-x} O_4$ spinel system", *Catal. Lett.*, 1994, **27**, 103-112.

Novochinsky, I. I., Chernavsky, P. A., Ryabchenko, P. V., and Lunin, V. V. "Cobalt catalysts in selective catalytic reduction of NO by methane", *Catal. Lett.*, 1998, **51**, 191-194.

Okamoto, Y., Adachi, T., Nagata, K., Odawara, M. and Imanaka, T., "Effects of starting cobalt salt upon the cobalt-alumina interactions and hydrodesulfurization activity of CoO/Al_2O_3", *Appl. Catal.*, 1991, **73**, 249-265.

Petryk, J. and Kolakowska, E., "Cobalt oxide catalysts for ammonia oxidation activated with cerium and lanthanum", *Appl. Catal. B.*, 2000, **24**, 121-128.

Querini, C. A., Ulla, M. A., Requejo, F., Soria, J., Sedran, U. A. and Miro, E. E., "Catalytic combustion of diesel soot particles. Activity and characterization of Co/MgO and Co,K/MgO catalysts", *Appl. Catal. B*, 1998, **15**, 5-19.

Querini, C. A., Cornaglia, L. M., Ulla, M. A. and Miro, E. E., "Catalytic combustion of diesel soot on Co,K/MgO catalysts. Effect of the potassium loading on activity and stability", *Appl. Catal. B*, 1999a, **20**, 165-177.

Querini, C. A., Miro, E. E., Ravelli, F., Ulla, M. A. and Cornaglia, L. M., "Catalytic combustion of diesel soot on Co,K supported catalysts", *Catalysis Today*, 1999b, **53**, 631-638.

Reid, R. C., Prausnitz, J. M. and Poling, B. E., The properties of Gases & Liquids, McGraw-Hill Company, 1988, Fourth Edition.

Riva, R., Miessner, H., Vitali, R. and Del piero, G., "Metal-support interaction in Co/SiO_2 and Co/TiO_2", *Appl. Catal. A*, 2000, **196**, 111-123.

Ruckenstein, E. and Wang, H. Y., "Effect of calcination conditions on the species formed and the reduction behavior of the cobalt-magnesia catalysts", *Catal. Lett*., 2000, **70**, 15-21.

Santos, A., Menendez, M., Monzon, A., Santamaria, J., Miro, E. E. and Lombardo, E. A., "Oxidation of methane to synthesis gas in fluidized bed reactor using MgO-based catalysts", *J. Catal*., 1996, **158**, 83-91.

Satterfield, C. N., Heterogeneous., "Catalytic Oxidation", *Heterogeneous Catalysis in Industrial Practice*, McGraw-Hill, 1980, Second Edition, 180-192.

Sewell, G. S., van Steen, E. and O'Connor, C. T., "Use of TPR/TPO for characterization of supported cobalt catalysts", *Catal. Lett*., 1996, **37**, 255-260.

Sinha, A. S. K. and Shankar, V., "Low-Temperature Catalysts for Total Oxidation of n-Hexane', *Ind. Eng. Chem. Res*., 1993, **32**, 1061-1065.

Szalowski, K. S., Krawczyk, K., and Petryk, J., "The properties of cobalt oxide catalyst for ammonia oxidation", *Appl. Catal. A*, 1998, **175**, 147-157.

Xanthopoulou, G., "Oxide catalysts for pyrolysis of diesel fuel made by self-propagating high-temperature synthesis. Part I: cobalt-modified Mg-Al spinel catalysts", *Appl. Catal. A*, 1999, **182**, 285-295.

Wang, W. J. and Chen Y. W., "Influence of metal loading on the reducibility and hydrogenation activity of cobalt/alumina catalysts", *Appl. Catal. A*, 1991, **71**, 223-233.

Youngwanishsate, W., *Master of Engineering thesis Chulalongkorn University*, 1998.

APPENDICES

APPENDIX A
CALCULATION OF CATALYST PREPARATION

Preparation of 8Co-Mg-O/TiO$_2$ and 8Co-Mg-O/Al$_2$O$_3$ catalysts by the Wet Impregnation Method is shown as follow:

Reagent: - Cobalt acetate tetrahydrate [Co(CH$_3$COO)$_2 \cdot$4H$_2$O]

         Molecular weight = 249 g.

     - Magnesium nitrate [Mg(NO$_3$)$_2$]

         Molecular weight = 256.41 g.

Support   - Titanium dioxide [TiO$_2$]

     - Alumina [Al$_2$O$_3$]

Calculation for the preparation of the 8Co-Mg-O/TiO$_2$ catalyst.

The 8Co-**Mg-O**/TiO$_2$ **aqueous** solution used in catalyst preparation consists of Co 8wt% and TiO$_2$ 92wt%. The amount of cobalt in 8Co-**Mg-O**/TiO$_2$ catalyst is calculated as follows:

Basis: TiO$_2$ 1 g.

If the weight of catalyst was 100 gram, 8Co-**Mg-O**/TiO$_2$ would compose of cobalt 8 g. and TiO$_2$ 92 g. Therefore, in this system,

the amount of Co   = 8/92 × 1

                                         = 0.0869 g.

Cobalt (Co) 0.0869 g. was prepared from Co(CH$_3$COO)$_2 \cdot$4H$_2$O 99% and molecular weight of Co = 59, then

the Co(CH$_3$COO)$_2 \cdot$4H$_2$O content   = (249×0.0869×100)/(59×99)

                                         = 0.3712 g.

Then, Mg 1% was loaded on 8Co/TiO$_2$ catalyst 100 gram.

The amount of Mg $= (0.0869+1)/100$

$= 0.010869$ g.

Magnesium (Mg) 0.010869 g. was impregnated from Mg(NO$_3$)$_2$ solution 99% and molecular weight of Mg = 24.305 g.

Thus, the amount of Mg(NO$_3$)$_2$ used $= (0.010869×256.41)/24.305$

$= 0.1157$ g.

Calculation for the preparation of the 8Co-Mg-O/ Al$_2$O$_3$ catalyst.

The calculation for the preparation of 8Co-Mg-O/Al$_2$O$_3$ catalyst is the same as the preparation of 8Co-**Mg-O**/TiO$_2$ catalyst.

APPENDIX B
CALCULATION OF DIFFUSIONAL LIMITATION EFFECT

In the present work there are doubt whether the external and internal diffusion limitations interfere with the propane reaction. Hence, the kinetic parameters were calculated based on the experimental data so as to prove the controlled system. The calculation is divided into two parts; one of which is the external diffusion limitation, and the other is the internal diffusion limitation.

1. External diffusion limitation

The 1-propanal oxidation reaction is considered to be an irreversible first order reaction occurred on the interior pore surface of catalyst particles in a fixed bed reactor. Assume isothermal operation for the reaction.

In the experiment, 8% 1-propanol, 5% O_2 balance with nitrogen was used as the unique reactant in the system. Molecular weight of 1-propanol and air (O_2 5%) are 60 and 28.2, respectively. Thus, the average molecular weight of the gas mixture was calculated as follows:

$$M_{AB} \quad = \quad 0.08 \times 60 + 0.92 \times 28.2$$
$$= \quad 30.744 \text{ g/mol}$$

Calculation of reactant gas density

Consider the 1-propanol oxidation is operated at low pressure and high temperature. We assume that the gases are respect to ideal gas law. The density of such gas mixture reactant at various temperatures is calculated in the following.

$$\rho = \frac{PM}{RT} = \frac{1.0 \times 10^5 \times 30.744 \times 10^{-3}}{8.314T}$$

We obtained : $\rho = 0.782$ kg/m^3 at T = 200°C

$\rho = 0.706$ kg/m^3 at T = 250°C

$\rho = 0.645$ kg/m^3 at T = 300°C

$\rho = 0.594$ kg/m^3 at T = 350°C

Calculation of the gas mixture viscosity

The simplified methods for determining the viscosity of low pressure binary are described anywhere (Reid, 1988). The method of Wilke is chosen to estimate the gas mixture viscosity.

For a binary system of 1 and 2,

$$\mu_m = \frac{y_1 \mu_1}{y_1 + y_2 \Phi_{12}} + \frac{y_2 \mu_2}{y_2 + y_1 \Phi_{21}}$$

where μ_m = viscosity of the mixture

μ_1, μ_2 = pure component viscosity

y_1 , y_2 = mole fractions

$$\phi_{12} = \frac{\left[1 + \left(\frac{\mu_1}{\mu_2}\right)^{1/2} \left(\frac{M_1}{M_2}\right)^{1/4}\right]^2}{\left[8\left(1 + \frac{M_1}{M_2}\right)\right]^{1/2}}$$

$$\phi_{21} = \phi_{12} \left(\frac{\mu_2}{\mu_1}\right) \left(\frac{M_1}{M_2}\right)$$

M_1, M_2 = molecular weight

Let 1 refer to 1-propanol and 2 to air (O$_2$ 5%)

$M_1 = 60$ and $M_2 = 28.2$

From Perry the viscosity of pure 1-propanol at 200°C, 250°C, 300°C, 350°C, 400°C, 450°C and 500°C are 0.0124, 0.0135, 0.015 and 0.0162 cP, respectively. The viscosity of pure air at 200°C, 250°C, 300°C and 350°C are 0.0248, 0.0265, 0.0285 and 0.030 cP, respectively.

<u>At 200°C :</u>

$$\phi_{12} = \frac{\left[1+\left(\dfrac{0.0124}{0.0248}\right)^{1/2}\left(\dfrac{28.2}{60}\right)^{1/4}\right]^2}{\left[8\left(1+\dfrac{60}{28.2}\right)\right]^{1/2}} = 0.502$$

$$\phi_{21} = 0.502\left(\frac{0.0248}{0.0124}\right)\left(\frac{60}{28.2}\right) = 2.14$$

$$\mu_m = \frac{0.08\times0.0124}{0.08+0.92\times0.502} + \frac{0.92\times0.0248}{0.92+0.08\times2.14} = 0.0227cP = 2.27\times10^{-5}\,kg/m-\sec$$

<u>At 250^{0}C :</u>

$$\phi_{12} = \frac{\left[1+\left(\dfrac{0.0135}{0.0265}\right)^{1/2}\left(\dfrac{28.2}{60}\right)^{1/4}\right]^2}{\left[8\left(1+\dfrac{60}{28.2}\right)\right]^{1/2}} = 0.506$$

$$\phi_{21} = 0.506\left(\frac{0.0265}{0.0135}\right)\left(\frac{60}{28.2}\right) = 2.113$$

$$\mu_m = \frac{0.08\times0.0135}{0.08+0.92\times0.506} + \frac{0.92\times0.0265}{0.92+0.08\times2.113} = 0.0244cP = 2.44\times10^{-5}\,kg/m-\sec$$

<u>At 300°C :</u>

$$\phi_{12} = \frac{\left[1+\left(\dfrac{0.015}{0.0285}\right)^{1/2}\left(\dfrac{28.2}{60}\right)^{1/4}\right]^2}{\left[8\left(1+\dfrac{60}{28.2}\right)\right]^{1/2}} = 0.512$$

$$\phi_{21} = 0.512\left(\frac{0.0285}{0.015}\right)\left(\frac{60}{28.2}\right) = 2.07$$

$$\mu_m = \frac{0.08 \times 0.015}{0.08 + 0.92 \times 0.512} + \frac{0.92 \times 0.0285}{0.92 + 0.08 \times 2.07} = 0.0263 cP = 2.63 \times 10^{-5} \, kg/m-\sec$$

At $350^{\circ}C$:

$$\phi_{12} = \frac{\left[1 + \left(\frac{0.0162}{0.030} \right)^{1/2} \left(\frac{28.2}{60} \right)^{1/4} \right]^2}{\left[8\left(1 + \frac{60}{28.2} \right) \right]^{1/2}} = 0.517$$

$$\phi_{21} = 0.517 \left(\frac{0.030}{0.0162} \right) \left(\frac{60}{28.2} \right) = 2.037$$

$$\mu_m = \frac{0.08 \times 0.0162}{0.08 + 0.92 \times 0.517} + \frac{0.92 \times 0.030}{0.92 + 0.08 \times 2.037} = 0.0278 cP = 2.78 \times 10^{-5} \, kg/m-\sec$$

Calculation of diffusion coefficients

Diffusion coefficients for binary gas system at low pressure calculated by empirical correlation are proposed by Reid (1988). Wilke and Lee method is chosen to estimate the value of D_{AB} due to the general and reliable method. The empirical correlation is

$$D_{AB} = \frac{\left(3.03 - \frac{0.98}{M_{AB}^{1/2}} \right) (10^{-3}) T^{3/2}}{P M_{AB}^{1/2} \sigma_{AB}^2 \Omega_D}$$

where D_{AB} = binary diffusion coefficient,cm^2/s

T = temperature,K

M_A ,M_B = molecular weights of A and B ,g/mol

$$M_{AB} = 2 \left[\left(\frac{1}{M_A} \right) + \left(\frac{1}{M_B} \right) \right]^{-1}$$

P = pressure,bar

σ = characteristic length,^{0}A

Ω_D = diffusion collision integral, dimensionless

    The characteristic Lennard-Jones energy and Length, ε and σ, of nitrogen and propane are as follows: (Reid,1988)

For $C_3 H_7OH$: $\sigma(C_3 H_7OH) = 4.549\ ^0A$, $\varepsilon/k = 576.7$
For air   : $\sigma(air) = 3.711\ ^0A$, $\varepsilon/k = 78.6$

The sample rules are usually employed.

$$\sigma_{AB} = \frac{\sigma_A + \sigma_B}{2} = \frac{4.549 + 3.711}{2} = 4.13$$

$$\varepsilon_{AB}/k = \left(\frac{\varepsilon_A \varepsilon_B}{k^2}\right)^{1/2} = (576.7 \times 78.6)^{1/2} = 212.9$$

    Ω_D is tabulated as a function of kT/ε for the Lennard-Jones potential. The accurate relation is

$$\Omega_D = \frac{A}{(T^*)^B} + \frac{C}{\exp(DT^*)} + \frac{E}{\exp(FT^*)} + \frac{G}{\exp(HT^*)}$$

where $T^* = \dfrac{kT}{\varepsilon_{AB}}$, A = 1.06036 , B = 0.15610 , C = 0.19300 , D = 0.47635 , E = 1.03587 , F = 1.52996 , G = 1.76474 , H = 3.89411

Then $T^* = \dfrac{473}{212.9} = 2.222$ at 200^oC

       $T^* = \dfrac{523}{212.9} = 2.456$ at 250^oC

       $T^* = \dfrac{573}{212.9} = 2.691$ at 300^oC

       $T^* = \dfrac{623}{212.9} = 2.926$ at 350^oC

$$\Omega_D = \frac{1.06036}{(T^*)^{0.15610}} + \frac{0.19300}{\exp(0.47635T^*)} + \frac{1.03587}{\exp(1.52996T^*)} + \frac{1.76474}{\exp(3.89411T^*)}$$

Ω_D = 1.038 ; 200°C

Ω_D = 1.006 ; 250°C

Ω_D = 0.979 ; 300°C

Ω_D = 0.956 ; 350°C

With Equation of D_{AB},

At 200°C : $D(C_3H_7OH\text{-air})$ = $\dfrac{\left(3.03 - \dfrac{0.98}{30.24^{0.5}}\right)(10^{-3})473^{3/2}}{1 \times 30.24^{0.5} \times 4.13^2 \times 1.038}$

= 3.01×10^{-5} m^2/s

At 250°C : $D(C_3H_7OH\text{-air})$ = $\dfrac{\left(3.03 - \dfrac{0.98}{30.24^{0.5}}\right)(10^{-3})523^{3/2}}{1 \times 30.24^{0.5} \times 4.13^2 \times 1.006}$

= 3.62×10^{-5} m^2/s

At 300°C : $D(C_3H_7OH\text{-air})$ = $\dfrac{\left(3.03 - \dfrac{0.98}{30.24^{0.5}}\right)(10^{-3})573^{3/2}}{1 \times 30.24^{0.5} \times 4.13^2 \times 0.979}$

= 4.26×10^{-5} m^2/s

At 350°C : $D(C_3H_7OH\text{-air})$ = $\dfrac{\left(3.03 - \dfrac{0.98}{30.24^{0.5}}\right)(10^{-3})623^{3/2}}{1 \times 30.24^{0.5} \times 4.13^2 \times 0.956}$

= 5.04×10^{-5} m^2/s

Reactant gas mixture was supplied at 100 ml/min. in tubular microreactor used in the 1-propanol oxidation system at 30^oC

1-propanol flow rate through reactor = 100 ml/min. at 30^oC

The density of 1-propanol , $\rho = \dfrac{1.0 \times 10^5 \times 30.744 \times 10^{-3}}{8.314(273 + 30)} = 1.236 \text{ kg/s}$

Mass flow rate = $1.236 \left(\dfrac{100 \times 10^{-6}}{60} \right) = 2.06 \times 10^{-6} \text{ kg/s}$

Diameter of quartz tube reactor = 8 mm

Cross-sectional area of tube reactor = $\dfrac{\pi(8 \times 10^{-3})^2}{4} = 5.03 \times 10^{-5} \text{ m}^2$

Mass Velocity , $G = \dfrac{2.06 \times 10^{-6}}{5.03 \times 10^{-5}} = 0.04 \text{ kg/m}^2\text{-s}$

Catalysis size = 40-60 mesh = 0.178-0.126 mm

Average catalysis = (0.126+0.178)/2 = 0.152 mm

Find Reynolds number, Re_p, which is well known as follows:

$$Re_p = \frac{d_p G}{\mu}$$

We obtained

<u>At 200^oC</u> : $Re_p = \dfrac{(0.152 \times 10^{-3} \times 0.04)}{2.27 \times 10^{-5}} = 0.268$

<u>At 250^oC</u> : $Re_p = \dfrac{(0.152 \times 10^{-3} \times 0.04)}{2.44 \times 10^{-5}} = 0.249$

<u>At 300^oC</u> : $Re_p = \dfrac{(0.152 \times 10^{-3} \times 0.04)}{2.63 \times 10^{-5}} = 0.231$

<u>At 350^oC</u> : $Re_p = \dfrac{(0.152 \times 10^{-3} \times 0.04)}{2.78 \times 10^{-5}} = 0.219$

Average transport coefficient between the bulk stream and particles surface could be correlated in terms of dimensionless groups, which characterize the flow conditions. For mass transfer the Sherwood number, $k_m\rho/G$, is an empirical function of the Reynolds number, d_pG/μ, and the Schmit number, $\mu/\rho D$. The j-factors are defined as the following functions of the Schmidt number and Sherwood numbers:

$$j_D = \frac{k_m\rho}{G}\left(\frac{a_m}{a_t}\right)(\mu/\rho D)^{2/3}$$

The ratio (a_m/a_t) allows for the possibility that the effective mass-transfer area a_m, may be less than the total external area, a_t, of the particles. For Reynolds number greater than 10, the following relationship between j_D and the Reynolds number well represents available data.

$$j_D = \frac{0.458}{\varepsilon_B}\left(\frac{d_pG}{\mu}\right)^{-0.407}$$

where G = mass velocity(superficial) based upon cross-sectional area of empty reactor

$\quad$ (G = uρ)

$\quad$ d_p = diameter of catalyst particle for spheres

$\quad$ μ = viscosity of fluid

$\quad$ ρ = density of fluid

$\quad$ ε_B = void fraction of the interparticle space (void fraction of the bed)

$\quad$ D = molecular diffusivity of component being transferred

Assume $\varepsilon_B = 0.5$

<u>At 200°C</u> ; $j_D = \dfrac{0.458}{0.5}(0.268)^{-0.407} = 1.565$

<u>At 250°C</u> ; $j_D = \dfrac{0.458}{0.5}(0.249)^{-0.407} = 1.613$

<u>At 300°C</u> ; $j_D = \dfrac{0.458}{0.5}(0.231)^{-0.407} = 1.663$

<u>At 350°C</u> ; $j_D = \dfrac{0.458}{0.5}(0.219)^{-0.407} = 1.699$

A variation of the fixed bed reactor is an assembly of screens or gauze of catalytic solid over which the reacting fluid flows. Data on mass transfer from single screens has been reported by Gay and Maughan. Their correlation is of the form

$$j_D = \dfrac{\varepsilon k_m \rho}{G}(\mu / \rho D)^{2/3}$$

Where ε is the porosity of the single screen.

Hence, $k_m = \left(\dfrac{j_D G}{\mu}\right)(\mu / \rho D)^{2/3}$

$k_m = \left(\dfrac{0.458 G}{\varepsilon_B \rho}\right)\mathrm{Re}^{-0.407} Sc^{-2/3}$

Find Schmidt number, Sc : $Sc = \dfrac{\mu}{\rho D}$

<u>At 200°C</u> : $Sc = \dfrac{2.27 * 10^{-5}}{0.782 * 3.01 * 10^{-5}} = 0.964$

<u>At 250°C</u> : $Sc = \dfrac{2.44 * 10^{-5}}{0.706 * 3.62 * 10^{-5}} = 0.955$

At 300$^{\text{o}}$C : Sc = $\dfrac{2.63*10^{-5}}{0.645*4.26*10^{-5}} = 0.957$

At 350$^{\text{o}}$C : Sc = $\dfrac{2.78*10^{-5}}{0.594*5.04*10^{-5}} = 0.928$

Find k_m :   At 200$^{\text{o}}$C, $k_m = \left(\dfrac{1.565\times 0.04}{0.782}\right)(0.964)^{-2/3} = 0.082$ m/s

At 250$^{\text{o}}$C, $k_m = \left(\dfrac{1.613\times 0.04}{0.706}\right)(0.955)^{-2/3} = 0.094$ m/s

At 300$^{\text{o}}$C, $k_m = \left(\dfrac{1.663\times 0.04}{0.645}\right)(0.957)^{-2/3} = 0.106$ m/s

At 350$^{\text{o}}$C, $k_m = \left(\dfrac{1.699\times 0.04}{0.594}\right)(0.928)^{-2/3} = 0.12$ m/s

Properties of catalyst

Density = 0.375 g/ml catalyst

Diameter of 40-60 mesh catalyst particle = 0.152 mm

Weight per catalyst particle = $\dfrac{\pi(0.152\times 0^{-1})^3 \times 0.375}{6} = 6.895*10^{-7}$ g/particle

External surface area per particle = $\pi(0.152\times 10^{-3})^2 = 7.26\times 10^{-7}$ m^2/particle

a_m = $\dfrac{7.26\times 10^{-7}}{6.895\times 10^{-7}} = 1.052\times 10^{-2}$ m^2/gram catalyst

Volumetric flow rate of gaseous feed stream = 100 ml/min

Molar flow rate of gaseous feed stream = $\dfrac{(1\times 10^5)\left(\dfrac{100\times 10^{-6}}{60}\right)}{8.314(273+30)} = 6.62\times 10^{-5}$ mol/s

1-propanol molar feed rate = 0.08×6.62×10^{-5} = 5.29×10^{-6} mol/s

1-propanol conversion (experimental data): 1.78   % at 200°C

5.73   % at 250°C

28.07 % at 300°C

59.93 % at 350°C

The estimated rate of 1-propanol oxidation reaction is based on the ideal plug flow reactor which there is no mixing in the direction of flow and complete mixing perpendicular to the direction of flow (i.e., in the radial direction). The rate of reaction will vary with reaction length. Plug flow reactors are normally operated at steady state so that properties at any position are constant with respect to time. The mass balance around plug flow reactor becomes
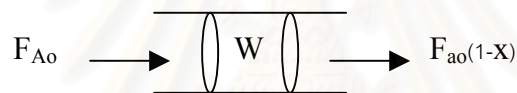
{rate of i into volume element} - {rate of i out of volume element}

+ {rate of production of i within the volume element}

= {rate of accumulation of i within the volume elecment }

$F_{Ao} = F_{Ao}(1-x) + (r_W W)$

$(r_W W) = F_{Ao} - F_{Ao}(1-x) = F_{Ao} = F_{Ao}x$

$$r_W = \frac{F_{Ao}x}{W} = \frac{5.29 \times 10^{-6} \times 0.0178}{0.1} = 4.717 \times 10^{-7} \quad \text{mol/s-gram catalyst at } 200^{\circ}\text{C}$$

$$r_W = \frac{F_{Ao}x}{W} = \frac{5.29 \times 10^{-6} \times 0.0573}{0.1} = 1.518 \times 10^{-6} \quad \text{mol/s-gram catalyst at } 250^{\circ}\text{C}$$

$$r_W = \frac{F_{Ao}x}{W} = \frac{5.29 \times 10^{-6} \times 0.28}{0.1} = 7.42 \times 10^{-6} \quad \text{mol/s-gram catalyst at } 300^{\circ}\text{C}$$

$$r_W = \frac{F_{Ao}x}{W} = \frac{5.29 \times 10^{-6} \times 0.599}{0.1} = 1.587 \times 10^{-5} \quad \text{mol/s-gram catalyst at } 350^{\circ}\text{C}$$

At steady state the external transport rate may be written in terms of the diffusion rate from the bulk gas to the surface. The expression is:

$$R_{obs} = k_m a_m (C_b - C_s)$$

$$= \frac{1\text{-propanol converted (mole)}}{(\text{time})(\text{gram of catalyst})}$$

where C_b and C_s are the concentrations in the bulk gas and at the surface, respectively.

<u>At 200°C</u>, $(C_b - C_s) = \dfrac{r_{obs}}{k_m a_m} = \dfrac{4.717 \times 10^{-7}}{0.082 \times 1.052 \times 10^{-1}} = 5.47 \times 10^{-4}$ mol/m³

<u>At 250°C</u>, $(C_b - C_s) = \dfrac{r_{obs}}{k_m a_m} = \dfrac{1.518 \times 10^{-6}}{0.094 \times 1.052 \times 10^{-1}} = 1.53 \times 10^{-4}$ mol/m³

<u>At 300°C</u>, $(C_b - C_s) = \dfrac{r_{obs}}{k_m a_m} = \dfrac{7.42 \times 10^{-6}}{0.106 \times 1.052 \times 10^{-1}} = 6.65 \times 10^{-3}$ mol/m³

<u>At 350°C</u>, $(C_b - C_s) = \dfrac{r_{obs}}{k_m a_m} = \dfrac{1.587 \times 10^{-5}}{0.12 \times 1.052 \times 10^{-1}} = 1.26 \times 10^{-3}$ mol/m³

From C_b (1-propanol) = 1.59 mol/m³

Consider the difference of the bulk and surface concentration is small. It means that the external mass transport has no effect on the 1-propanol oxidation reaction rate.

2. Internal diffusion limitation

Next, consider the internal diffusion limitation of the 1-propanol reaction. An effectiveness factor, η, was defined in order to express the rate of reaction for the whole catalyst pellet, r_p, in terms of the temperature and concentrations existing at the outer surface as follows:

$$\eta = \frac{\text{actual rate of whole pellet}}{\text{rate evaluated at outer surface conditions}} = \frac{r_p}{r_s}$$

The equation for the local rate (per unit mass of catalyst) may be expected functionally as $r = f(C,T)$.

Where C represents, symbolically, the concentrations of all the involved components

Then, $\qquad r_p = \eta r_s = \eta f(C_s, T_s)$

Suppose that the 1-propanol oxidation is an irreversible reaction A$\rightarrow$B and first order reaction, so that for isothermal conditions $r = f(C_A) = k_1 C_A$. Then $r_p = \eta k_1 (C_A)_s$.

For a spherical pellet, a mass balance over the spherical-shell volume of thickness Δr. At steady state the rate of diffusion into the element less the rate of diffusion out will equal the rate of disappearance of reactant with in the element. This rate will be $\rho_p k_1 C_A$ per unit volume, where ρ_p is the density of the pellet. Hence, the balance may be written, omitting subscript A on C,
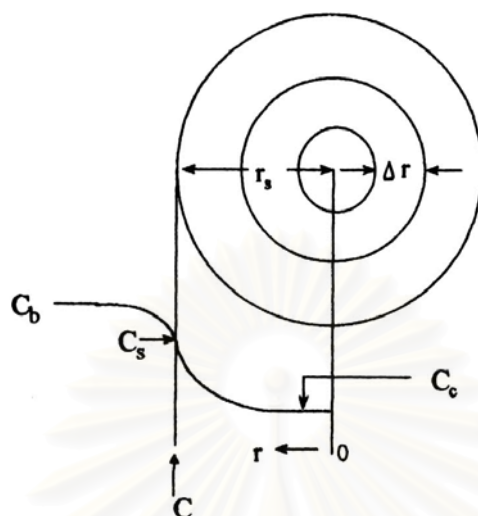
Figure B1. Reactant (A) concentration vs. position for first-order reaction on a spherical catalyst pellet.

$$\left(-4\pi r^2 D_e \frac{dC}{dr}\right)_r - \left(-4\pi r^2 D_e \frac{dC}{dr}\right)_{r+\Delta r} = -4\pi r^2 \, \Delta r_p k_1 C$$

Take the limit as $\Delta r \to 0$ and assume that the effective diffusivity is independent of the concentration of reactant, this difference equation becomes

$$\frac{d^2C}{dr^2} + 2\frac{dC}{dr} - \frac{k_1 \rho_p C}{D_e} = 0$$

At the center of the pellet symmetry requires

$$\frac{dC}{dr} = 0 \text{ at } r = 0$$

and at outer surface

$$C = C_s \text{ at } r = r_s$$

Solve linear differential equation by conventional methods to yield

$$\frac{C}{C_s} = \frac{r_s \sinh\left(3\phi_s \dfrac{r}{r_s}\right)}{r \sinh 3\phi_s}$$

where ϕ_s is Thiele modulus for a spherical pellet defined by $\phi_s = \dfrac{r_s}{3}\sqrt{\dfrac{k_1 \rho_p}{D_e}}$

Both D_e and k_1 are necessary to use $r_p = \eta k_1 (C_A)_s$. D_e could be obtained from the reduced pore volume equation in case of no tortuosity factor.

$$D_e = (\varepsilon_s^2 D_{AB})$$

<u>At 200°C</u>, $D_e = (0.5)^2 (3.01 \times 10^{-5}) = 7.53 \times 10^{-6}$

<u>At 250°C</u>, $D_e = (0.5)^2 (3.62 \times 10^{-5}) = 9.04 \times 10^{-6}$

<u>At 300°C</u>, $D_e = (0.5)^2 (4.26 \times 10^{-5}) = 1.06 \times 10^{-5}$

Substitute radius of catalyst pellet, $r_s = 0.107 \times 10^{-3}$ m with ϕ_s equation

$$\phi_s = \frac{0.076 \times 10^{-3} \text{ m}}{3} \sqrt{\frac{k(m^3/s\text{-kg cat.}) \times 1000(kg/m^3)}{7.53 \times 10^{-6}(m^2/s)}} \text{, at 200°C}$$

$\phi_s = 0.292\sqrt{k}$ (dimensionless) at 200°C

$\phi_s = 0.266\sqrt{k}$ (dimensionless) at 250°C

$\phi_s = 0.246\sqrt{k}$ (dimensionless) at 300°C

Find k (at 200°C) from the mass balance equation around plug-flow reactor.

$$r_w = \frac{F_{Ao} \, dx}{dW}$$

where $r_w = kC_A$

Thus,
$$kC_A = \frac{F_{Ao}}{dW} dx$$

$$kC_{Ao}(1-x) = \frac{F_{Ao}}{dW} dx$$

$$W = \frac{F_{Ao}}{kC_{Ao}} \int_0^{0.1} \frac{1}{1-x} dx$$

$$W = \frac{F_{Ao}}{kC_{Ao}} \left[-\ln(1-x) \right]_0^{0.1} = \frac{F_{Ao}}{kC_{Ao}} (-\ln(0.9))$$

$$k = \frac{F_{Ao}}{WC_{Ao}} (-\ln(0.9822))$$

$$k = \frac{5.29 \times 10^{-6} \ (\text{mol/s})}{0.1 \times 10^{-3} \ (\text{kg}) \times 1.03 (\text{mol/m}^3)} (-\ln(0.9822)$$

$$= 0.92 \times 10^{-4} \ \text{m}^3/\text{s-kg catalyst}$$

Calculate ϕ_s : $\phi_s = 0.292 \sqrt{0.92 \times 10^{-4}} = 0.0028$ at 200°C

$$\phi_s = 0.266 \sqrt{3.03 \times 10^{-3}} = 0.015 \ \text{at } 250°C$$

$$\phi_s = 0.246 \sqrt{1.68 \times 10^{-2}} = 0.032 \ \text{at } 300°C$$

For such small values of ϕ_s it was concluded that the internal mass transport has no effect on the rate of 1-propanol oxidation reaction.

APPENDIX C
CALIBRATION CURVE

Flame ionization detector gas chromatographs, model 14A and 14B, were used to analyze the concentrations of oxygenated compounds and light hydrocarbons, respectively. 1-propanol, 2-propanol, formaldehyde, acetaldehyde, and propionaldehyde were analyzed by GC model 14A while methane, ethylene, and propylene were analyzed by GC model 14B.

Gas chromatograph with the thermal conductivity detector, model 8A, was used to analyze the concentration of CO_2 and CO by using Porapak-Q and Molecular Sieve 5-A column, respectively.

The calibration curves of methane, ethylene, propylene, 1-propanol, 2-propanol, CO_2, formaldehyde, acetaldehyde, and propionaldehyde are illustrated in the following figures.

Figure C1 The calibration curve of methane

$y = 6.97E\text{-}13x$

Figure C2 The calibration curve of ethylene

$y = 4.12E\text{-}13x$

Figure C3 The calibration curve of propylene
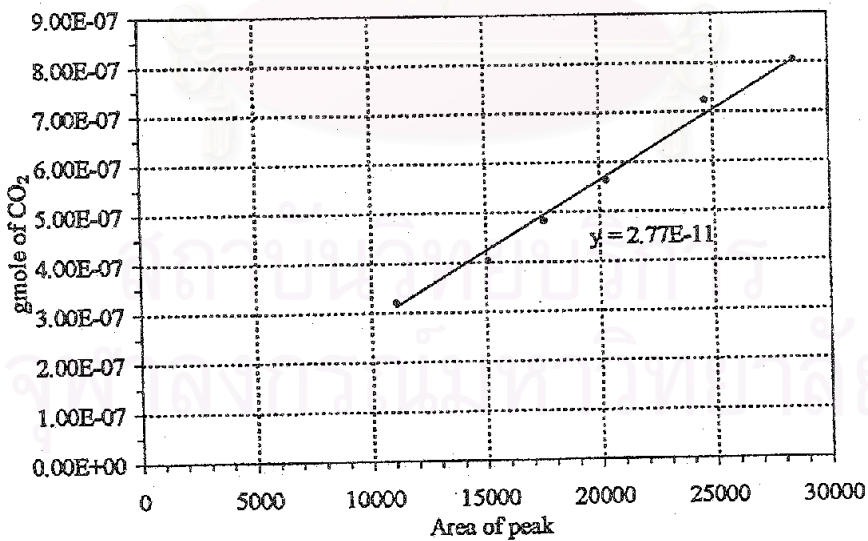
Figure C4 The calibration curve of CO_2
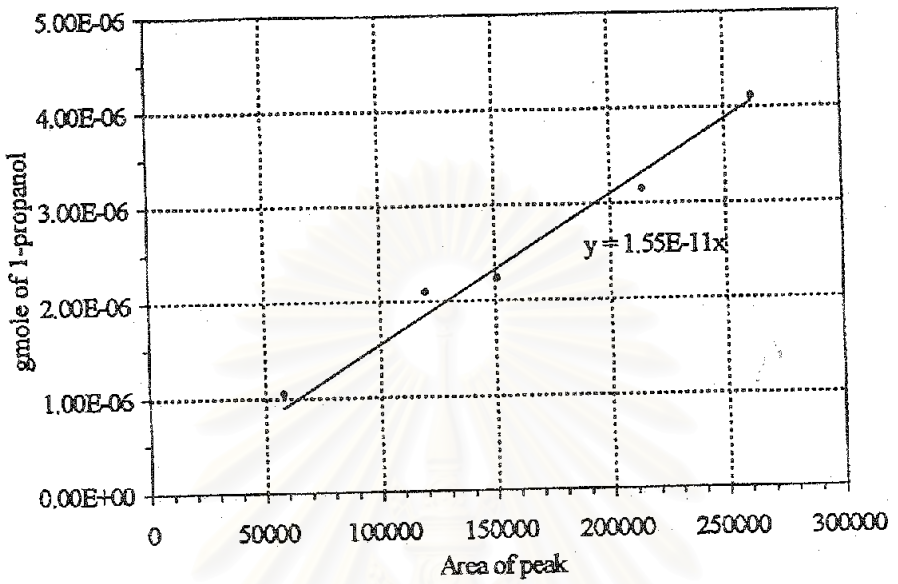
Figure C5 The calibration curve of 1-propanol

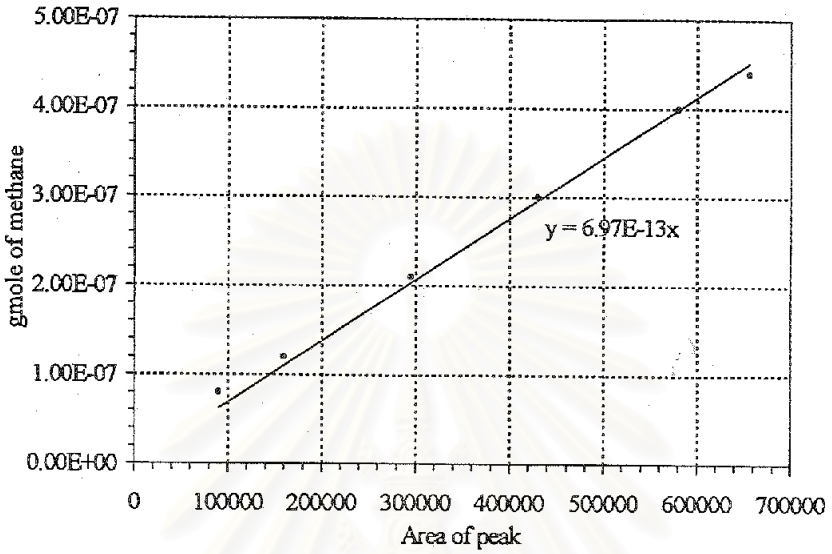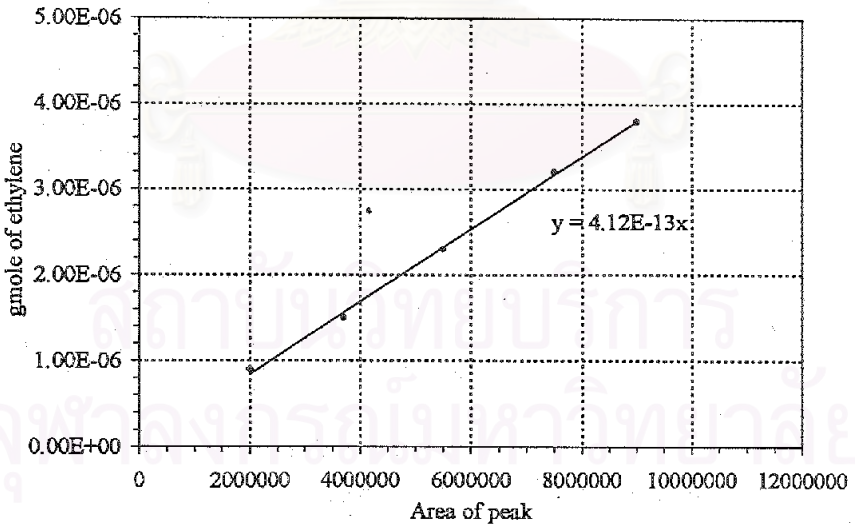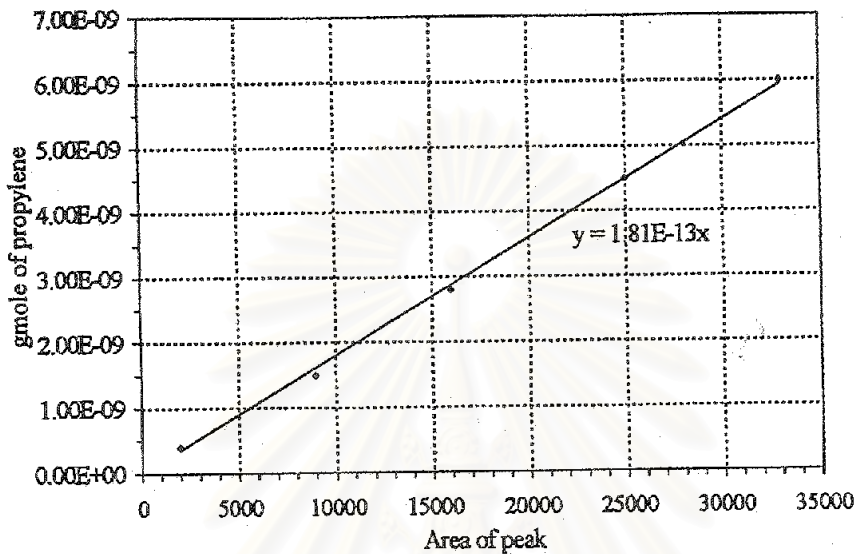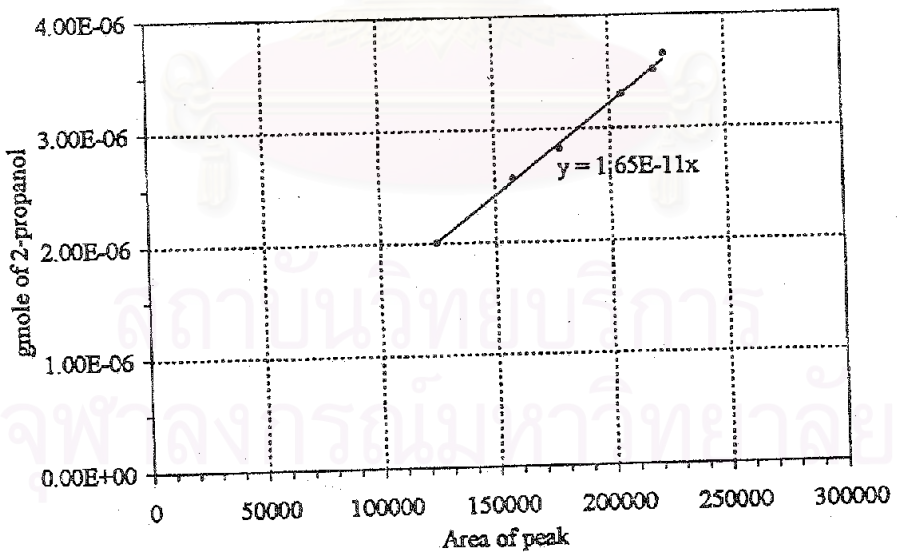Figure C6 The calibration curve of 2-propanol
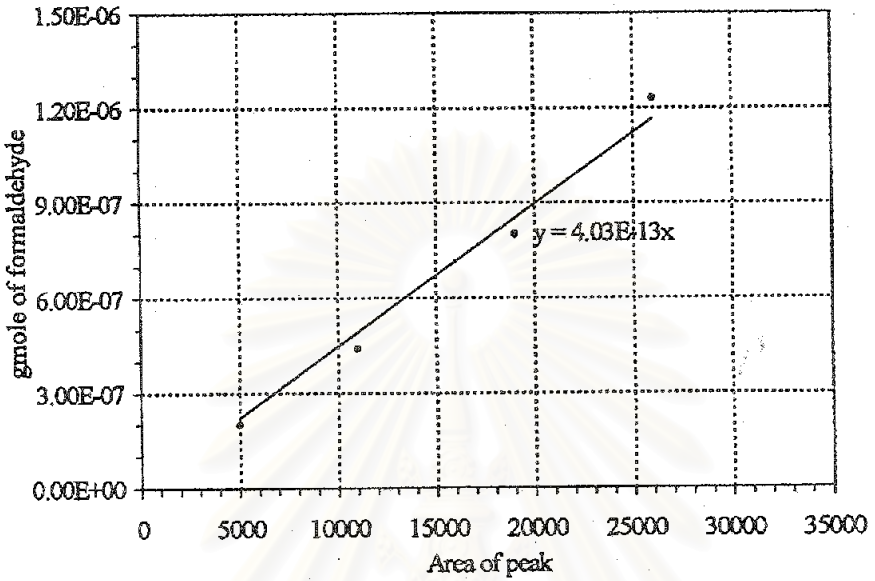
Figure C7 The calibration curve of formaldehyde
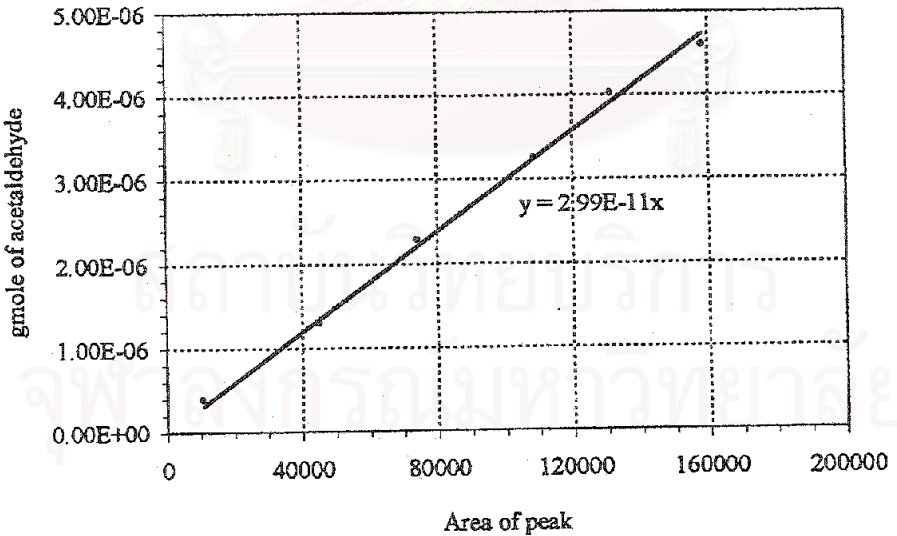
Figure C8 The calibration curve of acetaldehyde
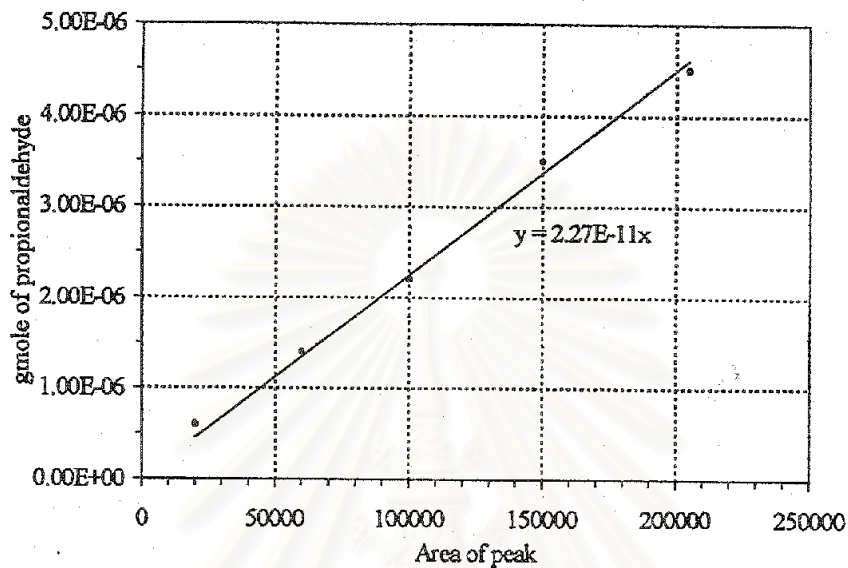
Figure C9 The calibration curve of propionaldehyde

APPENDIX D
DATA OF EXPERIMENTS

D1 The data of 1-propanol oxidation reaction test

Table D1 Data of figure 5.17

Component	Temperature (°C)						
	200	250	300	350	400	450	500
%1-Propanol (C)	3.69	7.86	41.99	77.41	81.74	83.44	87.09
%Formaldehyde (S)	0	0.27	0.46	0.38	0.23	0.21	0.10
%Acetaldehyde (S)	4.59	5.72	5.70	5.80	6.10	6.40	6.60
%Propionaldehyde (S)	94.79	87.62	85.05	74.46	69.89	66.53	64.03
%Methane (S)	0	0	0	0.01	0.02	0.07	0.18
%Ethylene (S)	0	0.10	0.08	0.23	0.44	0.63	1.45
%Propylene (S)	0	3.38	5.76	6.85	8.38	11.80	14.17
%Carbondioxide (S)	0	0.24	0.37	11.40	14.07	14.14	13.14
%Propionaldehyde (Y)	3.49	6.89	35.71	57.64	57.12	55.51	55.76

Table D2 Data of figure 5.18

Component	Temperature (°C)						
	200	250	300	350	400	450	500
%1-Propanol (C)	4.34	7.82	35.62	70.04	75.22	80.90	82.68
%Formaldehyde (S)	0	0.01	0.06	0.06	0.05	0.06	0.05
%Acetaldehyde (S)	0	0	1.82	3.08	4.00	4.02	4.61
%Propionaldehyde (S)	99.87	95.88	86.53	72.89	69.03	65.86	64.00
%Methane (S)	0	0	0	0	0.02	0.07	0.11
%Ethylene (S)	0	0.04	0.07	1.51	1.35	2.64	2.70
%Propylene (S)	0	2.24	7.06	10.61	10.57	12.27	12.82
%Carbondioxide (S)	0	1.35	3.51	11.81	14.91	14.97	15.58
%Propionaldehyde (Y)	3.32	9.00	28.49	55.44	54.14	52.56	53.70

Table D3 Data of figure 5.19

Component	Temperature (°C)						
	200	250	300	350	400	450	500
%1-Propanol (C)	3.33	9.38	32.93	76.07	78.43	79.81	83.92
%Formaldehyde (S)	0	0.05	0.22	0.09	0.06	0.06	0.06
%Acetaldehyde (S)	0	0	0.81	2.21	3.26	3.01	2.86
%Propionaldehyde (S)	98.14	93.2	86.49	76.59	73.37	70.38	68.32
%Methane (S)	0	0	0	0	0.01	0.03	0.06
%Ethylene (S)	0	0.04	0.05	0.07	0.17	0.22	0.34
%Propylene (S)	0	3.23	4.42	6.9	10.28	12.23	13.52
%Carbondioxide (S)	0	2.16	7.42	13.50	12.36	13.77	14.46
%Propionaldehyde (Y)	4.26	7.29	30.8	53.64	55.19	56.94	56.48

Table D4 Data of figure 5.20

Component	Temperature (°C)						
	200	250	300	350	400	450	500
%1-Propanol (C)	9.63	15.97	26.27	64.31	80.38	84.08	89.08
%Formaldehyde (S)	0	0.02	0.10	0.14	0.20	0.21	0.30
%Acetaldehyde (S)	0	0	3.87	4.51	7.04	6.04	5.49
%Propionaldehyde (S)	92.46	88.28	76.81	64.40	51.44	46.99	44.09
%Methane (S)	0	0.02	0.03	0	0.18	0.26	0.74
%Ethylene (S)	0	0.04	0.2	0.10	2.26	1.80	3.18
%Propylene (S)	5.76	7.15	12.50	18.00	20.29	23.19	24.10
%Carbondioxide (S)	0	3.89	6.52	12.54	18.14	21.17	21.43
%Propionaldehyde (Y)	8.90	14.10	20.18	41.42	41.34	39.5	39.27

Table D5 Data of figure 5.21

Component	Temperature (°C)						
	200	250	300	350	400	450	500
%1-Propanol (C)	11.07	17.27	34.09	70.94	82.58	87.91	90.75
%Formaldehyde (S)	0.02	0.06	0.20	0.15	0.08	0.25	0.23
%Acetaldehyde (S)	0	2.54	4.76	6.02	8.63	8.76	9.06
%Propionaldehyde (S)	91.78	79.91	72.02	58.28	51.09	46.68	42.83
%Methane (S)	0	0.02	0.05	0	0.05	0.41	0.71
%Ethylene (S)	0.02	0.14	0.41	0.70	0.53	2.06	3.15
%Propylene (S)	7.87	12.98	13.96	18.74	21.17	21.87	23.73
%Carbondioxide (S)	0	4.28	8.66	16.16	17.74	19.93	20.05
%Propionaldehyde (Y)	10.16	13.80	24.55	41.34	42.19	41.03	38.86

Table D6 Data of figure 5.22

Component	Temperature (°C)						
	200	250	300	350	400	450	500
%1-Propanol (C)	10.62	20.98	45.99	61.48	74.18	83.78	85.41
%Formaldehyde (S)	0	0.01	0.01	0.11	0.08	0.12	0.18
%Acetaldehyde (S)	0	1.74	1.15	2.53	2.84	3.06	5.04
%Propionaldehyde (S)	95.26	91.61	79.74	69.52	59.04	50.52	47.56
%Methane (S)	0	0	0	0	0.01	0.04	0.14
%Ethylene (S)	0	0.02	0.03	0.10	1.11	3.17	4.43
%Propylene (S)	2.56	3.61	10.24	15.86	19.24	22.00	21.59
%Carbondioxide (S)	2.01	2.17	8.24	11.40	16.93	20.26	20.37
%Propionaldehyde (Y)	10.33	19.63	36.67	42.74	43.79	42.32	40.62

D2 The data of 2-propanol oxidation reaction test

Table D7 Data of figure 5.23

Component	Temperature (°C)						
	200	250	300	350	400	450	500
%2-Propanol (C)	7.14	14.37	25.62	89.41	100	100	100
%Formaldehyde (S)	0.08	0.91	0.69	0.70	0.58	0.50	0.45
%Propionaldehyde (S)	0	0	37.72	40.60	47.81	52.18	56.72
%Propylene (S)	98.67	96.40	59.10	54.01	42.15	38.57	33.92
%Carbondioxide (S)	0	1.11	1.20	3.65	7.78	8.26	8.01
%Propylene (Y)	7.05	13.85	15.14	48.29	42.15	38.57	33.92

Table D8 Data of figure 5.24

Component	Temperature (°C)						
	200	250	300	350	400	450	500
%2-Propanol (C)	5.10	12.34	25.62	86.38	93.85	94.67	100
%Formaldehyde (S)	0.08	0.57	0.70	0.55	0.49	0.43	0.41
%Propionaldehyde (S)	0	0	31.13	42.56	54.26	59.25	60.95
%Propylene (S)	98.68	97.08	66.54	56.20	35.56	29.86	28.31
%Carbondioxide (S)	0	0.64	1.10	4.89	8.75	9.55	9.49
%Propylene (Y)	5.03	11.98	17.04	48.54	33.37	28.26	28.31

Table D9 Data of figure 5.25

Component	Temperature (°C)						
	200	250	300	350	400	450	500
%2-Propanol (C)	4.60	16.30	33.82	89.80	100	100	100
%Formaldehyde (S)	0.65	1.30	1.00	0.86	0.51	0.67	0.39
%Propionaldehyde (S)	0	0	29.51	42.05	48.88	59.13	60.81
%Propylene (S)	98.68	97.31	65.23	52.67	40.09	29.10	26.32
%Carbondioxide (S)	98.51	6.52	2.98	4.08	9.78	10.44	11.51
%Propylene (Y)	4.53	15.86	22.06	47.29	40.09	29.10	26.32

Table D10 Data of figure 5.26

Component	Temperature (^oC)						
	200	250	300	350	400	450	500
%2-Propanol (C)	0.23	27.43	65.85	95.84	100	100	100
%Formaldehyde (S)	0.46	1.73	0.80	0.68	0.59	0.69	0.64
%Propionaldehyde (S)	0	0	30.52	33.52	35.80	36.71	39.71
%Propylene (S)	98.56	97.23	66.82	61.46	53.64	50.53	47.32
%Carbondioxide (S)	0	0.36	1.19	3.74	9.39	11.00	11.74
%Propylene (Y)	0.23	26.67	44.00	58.90	53.64	50.53	47.32

Table D11 Data of figure 5.27

Component	Temperature (^oC)						
	200	250	300	350	400	450	500
%2-Propanol (C)	6.11	18.93	69.82	96.64	100	100	100
%Formaldehyde (S)	2.99	4.09	1.54	0.99	0.86	0.82	0.71
%Propionaldehyde (S)	0	0	25.07	28.62	30.95	37.58	38.54
%Propylene (S)	96.26	92.24	71.42	64.57	57.80	52.08	50.82
%Carbondioxide (S)	0	0.59	1.27	4.94	9.69	8.52	9.20
%Propylene (Y)	5.89	17.84	49.86	62.40	57.80	52.08	50.82

Table D12 Data of figure 5.28

Component	Temperature (^oC)						
	200	250	300	350	400	450	500
%2-Propanol (C)	8.32	42.26	78.73	95.83	100	100	100
%Formaldehyde (S)	0.49	0.50	0.62	0.54	0.46	0.46	0.41
%Propionaldehyde (S)	0	0	26.58	32.62	36.45	36.54	38.63
%Propylene (S)	98.83	97.94	67.32	60.53	52.22	52.37	50.00
%Carbondioxide (S)	0	0.47	1.55	6.22	10.06	9.85	10.79
%Propylene (Y)	8.22	41.39	53.00	58.01	52.22	52.37	50.00

D3 The data of propylene oxidation reaction test

Table D13 Data of figure 5.29

Component	Temperature (°C)						
	200	250	300	350	400	450	500
%Propylene (C)	0	0	5.03	8.12	14.83	15.92	22.00
%Propionaldehyde (S)	0	0	50.24	60.58	65.88	70.65	27.52
%Carbondioxide (S)	0	0	49.53	38.72	33.61	28.64	27.05

Table D14 Data of figure 5.30

Component	Temperature (°C)						
	200	250	300	350	400	450	500
%Propylene (C)	0	0	4.12	6.78	12.65	14.96	20.12
%Propionaldehyde (S)	0	0	48.47	51.26	55.79	58.63	60.45
%Carbondioxide (S)	0	0	50.68	48.72	43.01	40.64	39.08

D4 The data of 1-propanol oxidation reaction test [Kittikerdkulchai (1999)]

Table D15 Data of figure 5.31

Component	Temperature (°C)						
	200	250	300	350	400	450	500
%1-Propanol (C)	1.78	5.73	28.07	59.93	73.80	75.26	76.39
%Formaldehyde (S)	0	3.18	3.83	4.51	4.01	3.69	3.59
%Propionaldehyde (S)	91.19	89.85	87.13	77.59	71.98	69.01	68.25
%Methane (S)	0.09	0.03	0.02	0.04	0.10	0.27	0.26
%Ethylene (S)	1.24	0.64	0.27	0.60	1.32	1.23	1.42
%Propylene (S)	1.26	0.74	1.67	2.10	2.32	2.39	1.27
%Carbondioxide (S)	7.17	4.26	5.60	13.02	18.00	18.57	20.07
%Propionaldehyde (Y)	1.63	5.14	24.46	46.50	53.12	51.94	52.14

APPENDIX E
BLANK TEST OF OXIDATION REACTION

The oxidation reaction of 1-propanol and 2-propanol at the same reaction condition but have no catalyst (blank test) are shown as follow:
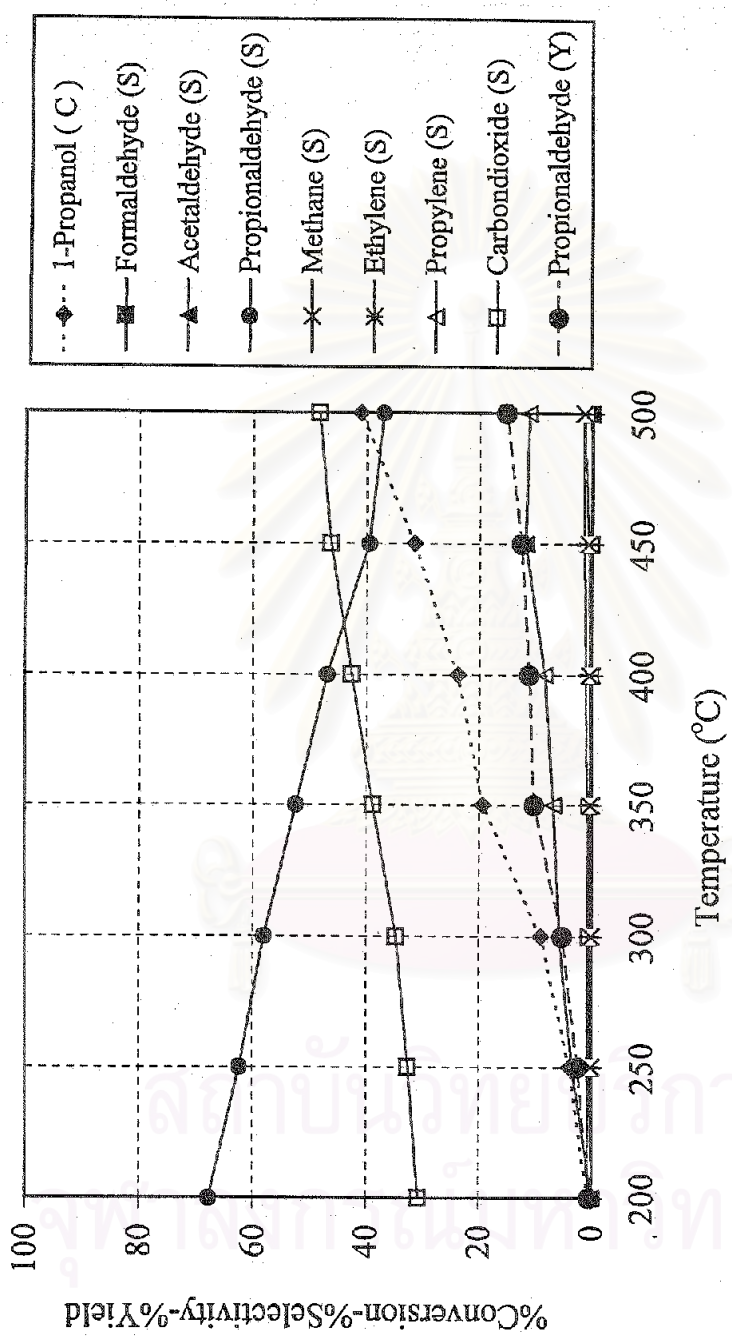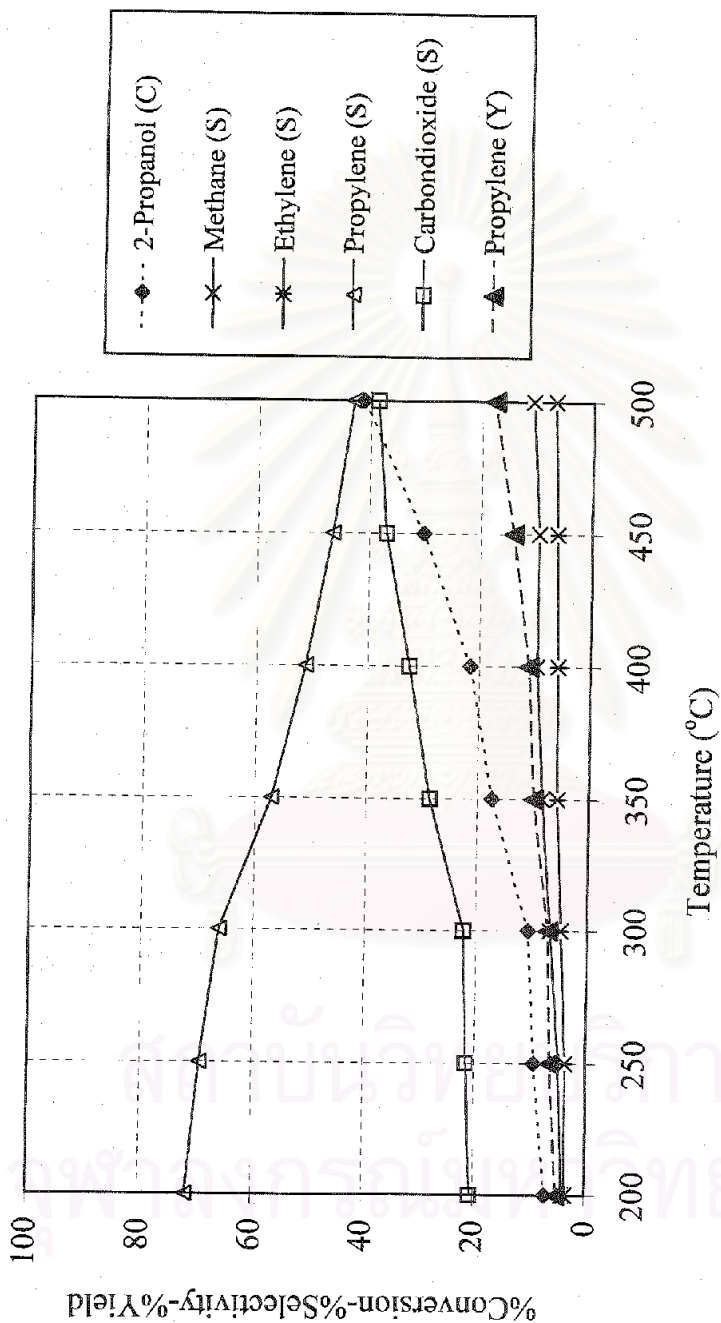
C – Conversion, S – Selectivity, Y – Yield

Figure E1 Catalytic property in the 1-propanol oxidation

Figure E2 Catalytic property in the 2-propanol oxidation

C - Conversion, S - Selectivity, Y - Yield

VITA

Miss. Nungruetai Chaiyasit was born on Febuary 13, 1978 in Bangkok, Thailand. She received the Bachelor Degree of Chemical Engineering from Faculty of Engineering, King's Mongkut Institute of Technology Ladkrabang in 1999. She continued her Master's Study at Chulalongkorn University in June, 1999.